Experimental analysis, modeling and simulation of drop breakage in agitated turbulent liquid/liquid-dispersions

vorgelegt von
Diplom-Ingenieur
Sebastian Maaß
aus Neustrelitz

von der Fakultät III - Prozesswissenschaften
der Technischen Universität Berlin
zur Erlangung des akademischen Grades
Doktor der Ingenieurwissenschaften
-Dr.-Ing.-

genehmigte Dissertation

Promotionsausschuss:
Vorsitzende: Prof. Dr. rer. nat. habil. Sabine Enders
Berichter: Prof. Dr.-Ing. Matthias Kraume
Berichter: Prof. D.Sc. F.R.Eng. Alvin W. Nienow

Tag der wissenschaftlichen Aussprache: 22.08.2011

Berlin 2011

D 83

What we know is a drop, what we don't know is an ocean."
- Sir Isaac Newton (*1643 - †1727)

Acknowledgements

This work was carried out during my time as a research and teaching assistant at the Technische Universität Berlin, Germany at the Chair of Chemical & Process Engineering. This work was partly supported by the Vinnolit GmbH and the Max-Buchner-Forschungsstiftung.

First of all, I would like to express my gratitude to my advisor Prof. Matthias Kraume for his help, support and insights on the problems throughout my PhD project. I am very grateful for the freedom and trust I received from him to develop own ideas. At the same time his thoughtful guidance kept me not to get lost in an overwhelming broad field of research. I very much appreciated the numerous opportunities to attend several international conferences, symposiums and workshops. It helped to direct research as well as to get in touch with other researchers and methodologies from around the world.

I would also like to thank Prof. Alwin W. Nienow to take the time and energy to judge my thesis together with an additional trip to Berlin. I am grateful for Prof. Sabine Enders who took the responsibility to lead the examination board.

The work would not have been possible without the support of a number of people. At foremost I would like to thank Dr. Ansor Gäbler, who inspired me for drop related research.

Dr. Mirco Wegener was not only a colleague but an example as a research engineer and a light in difficult and dark times.

Dr. Stefan Wollny was always a help with the discussions about breaking drops. The cooperation with him was outstanding, his personal commitment made a big difference on my project and several publication used for this thesis.

I would like to thank all my colleagues in the department for the great atmosphere, their always helpful, constructive, honest advices and feed-back on my work. I would like to thank especially Stephanie Herrmann, Thomas Eppinger, Friedemann Gaitzsch and Jochen Grünig for the support and spirit of cooperation in our research group.

Our project partner from the Vinnolit GmbH Dr. Torsten Rehm supported my work with his strong personal commitment to this project.

I'd like to thank all my students especially Florian Metz, Elodie Lutz, Georg Brösigke and Melanie Zillmer for the valuable research support and hard work they invested into our projects.

The automated drop detection would not be existent without the hard work of Jürgen Rojahn, who became one of my best friends over the last five years of shared research. I was often encouraged by the great and cheerful heart of So-Jin Kim.

Many new experiments had to be performed; many set-ups had to be build. The people always serving in the back to support my research are Andrea Hasselmann, Christine Kloth, Rainer Schwarz and Werner Alborn.

Family support is most important even though it is from distance. My parents, Regina and Hans-Peter Maaß, have been a great help and encouragement. They supported my decisions throughout my life, gave valuable directions and left enough space for own decisions.

I greatly acknowledge the tremendous support by my parents in law Dr. phil. habil. Ingrid Thienel-Saage and Prof. Dr. phil. habil. Richard Saage. They are always an inspiration to see the value of science. Especially the support from my mother in law with my loved daughters Luise and Antonia made an immeasurable difference for my project and our family.

I want to thank my wife for her unconditional love and support throughout this project.

Thanks to the LORD JESUS CHRIST, for he is good and His love endures for ever. (Ps 136)

This work is dedicated to my wife.

Table of contents

Nomenclature

I. Symbols

1. *Latin symbols*

a_f	total interfacial area per total volume [1/m]
$B_{br,coa}$	birth rate for breakage or coalescence [m^3/s]
c	empirical, numerical and proportionality constants [various]
c	concentration [mg/g]
d	drop diameter [m]
d_{32}	Sauter mean diameter [m]
D	stirrer diameter [m]
$D_{br,coa}$	death rate for breakage or coalescence [m^3/s]
f	daughter to mother drop volume ratio [-]
F	coalescence rate [m^3/s]
g	breakage rate [various]
h	collision frequency [various]
h	stirrer bottom clearance [m]
h_{St}	stirrer height [m]
H	liquid level [m]
l	length [m]
l_B	length of immersed baffle [m]
L	tolerance limit for the Gaussian distribution (the used value in this thesis is 2.5)
n	relative number of events [-]
n	stirrer speed [rpm]
N	number of drops [-]
P	example position of a single fluid element [-]
s	stirrer - stirrer distance [m]
t	time [min]
T	vessel diameter [m]
V	volume [m^3]
V	variance [various]
w	velocity [m/s]
Y	example variable [undefined]

2. *Greek symbols*

β	daughter drops size distribution [various]
γ	interfacial tension [mN/m]
ε	energy dissipation rate [m^2/s^3]
$\dot{\varepsilon}$	elongation rate [1/s]
η	dynamic viscosity [mPa·s]
λ	coalescence efficiency [-]
λ_κ	Kolmogoroff scale [m]
μ	expectation value of a Gaussian distribution [m]
ν	kinematic viscosity [m^2/s]
ν	number of daughter drops [-]
Ξ	global shear strain tensor
ρ	density [kg/m^3]
σ	standard deviation [various]
φ_d	dispersed phase fraction [-]

II. Subscripts

av	average
br	brekage
c	continuous
ch	chord
coa	coalescence
crit	critical
d	dispersed
imp	impeller region
in	initial
max	maximum
M	mother drop (in the work of Tcholakova et al. (2007) displayed only in Figure 38)
P	particle
tot	total amount
Tip	tip of the stirrer blade
V	volume based distribution (in the work of Tcholakova et al. (2007) displayed only in Figure 38)
x,y,z	the three dimensions

III. Dimensionless numbers

Ca	capillary number ($Ca = \eta w/\gamma$)
Ne	Newton number ($Ne = P/\rho n^3 D^5$)
Re	Reynolds number ($Re = nD^2/\nu$)
We	Weber number ($We = \rho_c n^2 D^3/\gamma$)

IV. Abbreviations

2D	2 dimensional
3D	3 dimensional
CCD	charge-coupled device
CFD	computational fluid dynamics
CLD	chord length distribution
CMC	critical micelle concentration
C&T (1977)	Coulaloglou and Tavlarides (1977)
DDSD	daughter drop size distribution
DSD	drop size distribution
exp	experiment
FBRM	focus beam reflectance measurement
fps	frames per second
IPP	inline particle probe
l/l	liquid/liquid
LDA	laser Doppler anemometry
LED	light-emitting diode
nn	normal gradient [1/s])
nt	shear gradient [1/s]
NCC	normalized cross correlation
ORM	optical reflectance measurement
o/w	oil in water dispersion
PARSIVAL®	PARticle SIze eVALuation
PBE	population balance equation
PI	phase inversion
PIV	particle image velocimetry
PVA	polyvinyl alcohol
PVC	polyvinyl chloride
PVM	particle video microscope
QMOM	quadrature method of moments

RCI	retreat curve impeller
sim	simulation
SQMOM	sectional quadrature method of moments
sstrnr	shear strain rate [1/s]
tt	direction gradient [1/s]
w/o/w	water in oil in water dispersion

Abstract

Despite the extensive literature dealing with both the fluid dynamic and the interface science aspects, the dispersion of immiscible liquids remains one of the most difficult and least understood mixing problems. Minor changes in the chemical composition of the system drastically affect the performance of such systems. Therefore, an improved understanding of the evolution of liquid/liquid dispersions is a key factor in operation, control and optimization of these processes. This becomes even more complex with the increasing geometrical diversity of agitated reactors. Growing markets and economies demand higher production rates. Limits in space and transportation have changed the outfit of the used mixing vessels. The height (H) of a reactor is increasing with constant tank diameter (T). H/T ratios of 2.0 or 3.0 are common today and ratios over 4.0 are expected.

The aim of this study is to develop and validate a model which will be able to predict system changes and intensification possibilities of stirred liquid/liquid breakage dominated processes. The dominance of breakage is achieved by the use of high surfactant concentrations clearly above the critical micelle concentration.

As a means of process intensification, dispersed phase fraction and reactor volume is increased in order to enhance productivity while the used power is decreased. Moreover, this is done exemplary for four different organic solvents. Based on simulation results of the used population balance equation (PBE), the process volume was increased by increasing the H/T ratio from 1.0 to 5.0 and the dispersed phase fraction from 25 to 45%. Additionally the used power was decreased by 20%. For the power decrease the impeller was changed from a single stage retreat curve impeller into a multi stage flat blade impeller. That lead to an overall process intensification in terms of an increase of the power related product by a factor of six.

All simulation results have been evaluated with lab-scale experiments, using a photo optical in-situ method, to size the drops. Selected experiments have been repeated at pilot plant scale to evaluate also the scale-up capacity of the used model. The detailed flow field was investigated using computational fluid dynamics to obtain circulation flow streams and energy dissipation rates throughout the reactors.

Furthermore, fundamental research was carried out on breaking single drops. These insights lead to a new model of a breakage rate, which is a sub-model within the PBE framework. This new model is able to predict the process intensification in terms of increasing reactor volume and reducing power input by using different impellers for the four investigated phases. The prediction of process changes by changing the dispersed phase fraction is possible until catastrophic phase inversion occurred. The model is not able to predict this dramatic process failure at the critical value of the dispersed phase fraction.

To overcome such failures a dynamic tracking of the evolving drop size distribution has been developed. The used endoscope probe allows real time recording of two dimensional images of the drops. A measurement of drop size distribution in the size range of 5 to 5000 μm is provided fully automated with computation times below 3 min per data point. Manual evaluation of the drops on the images was used to quantify the accuracy of the image algorithm software. The results showed a very good agreement between manually and automatically determined values, as long as the particle shapes stay spherical. Even the high concentrations of 45% can be investigated with the method. If the particle shape is irregular in comparison to spheres, the automated recognitions failed to measure the real particle size.

Keywords: liquid/liquid dispersion, drop size distribution, single drop breakage, population balance equation, breakage modeling, flow field analysis, drop size measurements, process intensification

Zusammenfassung

Aufgrund der beständig wachsenden Anforderungen an Wirtschaftlichkeit und Umweltverträglichkeit von Prozessen und industriellen Technologien wird auch in Zukunft die exakte Vorhersage bei Auslegung und Optimierung von Verfahren eine weiterhin wesentliche Rolle spielen. Im Rahmen von wachsender Konkurrenz durch Globalisierung und sinkender Rohstoffverfügbarkeit wird dies bei möglichst geringem personellem und experimentellem Aufwand zu vollziehen sein.

Eine entscheidende Rolle in dieser fortbestehenden Dynamik wird der Simulation von einzelnen Verfahrensschritten oder sogar gesamten Prozessen zukommen. Um eben diese Simulationen vertrauensvoll anzuwenden, bedarf es physikalisch basierter, exakter Modelle, welche experimentell ausreichend validiert wurden.

Im Rahmen dieser Arbeit wurden Modelle zur Simulation von turbulenten Flüssig/flüssig Systemen angewandt, evaluiert und weiter entwickelt. Im Fokus der Arbeiten standen gerührte Apparate. Ihre industrielle Verbreitung lässt sie noch immer zu den wichtigsten Anwendungen nicht nur in der chemischen Industrie zählen. Ein kurzer Überblick im ersten Kapitel dieser Arbeit zeigt daher die vorhandene Anwendungsbreite.

Da es sich im Laufe der letzten zwei Dekaden durchgesetzt hat, Flüssig/flüssig - Dispersionen und deren zeitliche Entwicklung sowie räumliche Verteilung mit Hilfe von Populationsbilanzgleichungen zu beschreiben, wird auch in dieser Arbeit auf eben jenes Werkzeug zurückgegriffen.

Die experimentelle Auswertung basiert auf photooptischer Messtechnik mit Bildverarbeitung. Diese, wenn manuell ausgeführt, sehr zeitaufwendige Prozedur wurde mit Bildverarbeitungsalgorithmen voll automatisiert.

Die Vielzahl von existierenden Modellen sowie die Herausforderungen bei der eindeutigen Lösung dieser gekoppelten Integral- und partiellen Differentialgleichungen werden in der Literatur breit diskutiert. Im Rahmen dieser Arbeit wurde diese Diskussion hauptsächlich am Beispiel des Modells von Coulaloglou und Tavlarides (1977) geführt. Doch auch hier wird deutlich, dass die entgegengesetzten physikalischen Phänomene des Tropfenbruchs und der Tropfenkoaleszenz zu uneindeutigen Aussagen bei der Modellanalyse führen. Eine Separation beider Phänomene zur eindeutigen Analyse ist daher in den vorliegenden experimentellen Arbeiten vorgenommen worden um sich auf Tropfenbruchanalysen fokussieren zu können.

Zum einen wurden die Untersuchungen in Rührkesseln unter hohen Polyvinylalkoholkonzentrationen durchgeführt. Da die eingesetzte Menge dieses wasserlöslichen Polymers deutlich oberhalb der kritischen Mizellbildungskonzentration verwendet wurde, konnte die Koaleszenz in den untersuchten Systemen vollständig unterdrückt werden. Dies ermöglichte die gezielte Analyse des Tropfenbruchs im Tropfenschwarm bei breiter Variation von Geometrie- und Betriebsparametern sowie Stoffeigenschaften der dispersen Phase.

Zum anderen wurden gezielte Tropfenzerfallsanalysen an Einzeltropfen durchgeführt. Diese halfen den Einfluss der Strömungsgeschwindigkeit der kontinuierlichen Phase sowie der Viskosität der dispersen Phase und der Grenzflächenspannung zwischen den beiden Phasen auf den turbulenten Tropfenzerfall zu quantifizieren.

Die experimentellen Ergebnisse beider Analysemethoden (der Tropfenschwarmanalyse sowie der Einzeltropfenanalyse) wurden zur Validierung bestehender Populationsbilanzmodelle herangezogen. Hierbei lag der Fokus nur auf den Sub-modellen der Bruchterme. Diese sind die Bruchrate, die Anzahl der Tochtertropfen sowie die Tochtertropfengrößenverteilung.

Vor allem die Einzeltropfenuntersuchungen gaben Aufschluss über das Verhalten dieser Sub-modelle. So konnte zum einen die gängige, weil unkomplizierte Annahme einer normal verteilten Tochtertropfenverteilung als Resultat einzelner Bruchereignisse widerlegt werden. Ein ungleichmäßiger Bruch in einen kleinen und einen großen Tochtertropfen ist deutlich wahrscheinlicher beim binären Bruch.

Doch auch der binäre Bruch, die häufigste Annahme für die Anzahl der Tochtertropfen in der Literatur, muss als algemeingültige Aussage hinterfragt werden. Mit zunehmendem Muttertropfendurchmesser steigt auch die Anzahl der entstehenden Tochtertropfen rapide an. So wurden für einen 3 mm Toluoltropfen bis zu 212 Tochtertropfen als Konsequenz einer gesamten Bruchsequenz gezählt. Zwar ließen sich diese multiplen Brüche durch hohe zeitliche Diskretisierung mit der verwendeten Hochgeschwindigkeitskamera häufig in eine Kaskade binärer Brüche zerlegen, jedoch diese einzelnen Brüche als losgelöst von einander zu werten, scheint eine fatale Simplifizierung des Tropfenbruches zu sein. Es ist daher sinnvoll, nicht nur die Initiierung eines Tropfenbruches zu bewerten sondern den ganzen Vorgang.

Die gemessene Bruchwahrscheinlichkeit der Einzeltropfenanalyse bleibt von dieser Diskussion unberührt, da die Aussage, ob ein Tropfen bricht, losgelöst ist von der Frage in wie viele Bruchstücke er zerfällt. Die Bruchwahrscheinlichkeit stellt einen von zwei Faktoren der Bruchrate dar. Wird sie mit der inversen Bruchzeit multipliziert, ergibt dies die Bruchrate.

Verschiedene Modelle der Literatur konnten sehr gut mit den experimentellen Daten der Bruchwahrscheinlichkeit aus den Einzeltropfenanalysen korreliert werden. Auch ein Wechsel des dispersen Stoffsystems von Petroleum zu Toluol war ohne zusätzliche Parameteranpassung durch die Modelle beschreibbar. Die erzielten Werte für die Anpassungsparameter in den Modellen der Bruchwahrscheinlichkeit konnten weiterhin mit akzeptablem Erfolg für die Simulation von Tropfenschwärmen in einem gerührten System eingesetzt werden.

Dies war nicht der Fall für die Bruchzeit. Diese Zeit, welche diese Arbeit als die Spanne vom Eintritt des Tropfens in den Rührernahbereich, dessen Verformung und ersten Aufbruch beschreibt, ist deutlich kürzer als die verwendeten charakteristischen Zeiten in gängigen Bruchmodellen. Dem gegenüber stimmen sie sehr gut mit experimentell ermittelten Bruchzeiten anderer Arbeitsgruppen überein.

Diese Unstimmigkeit führte zu der Schlussfolgerung, nicht von einer Tropfenbruchzeit eines einzelnen Tropfens zu reden, sondern vielmehr von einer charakteristischen Verweilzeit des Tropfens in bruchrelevanten Volumina im Apparat. Eine mögliche Anpassung der bestehenden Modelle in diese Richtung wurde gezeigt.

Die weiterhin notwendige Einbeziehung anderer Bruchmechanismen als nur der turbulenten Fluktuationen ist durch Einbeziehung der Tropfen-Kapillar-Zahl möglich. Ein neu entwickeltes Bruchmodell berücksichtigt zusätzlich zu den turbulenten Bruchmechanismen auch die durch Beschleunigung der kontinuierlichen Phase im Rührernahbereich entstehende Dehnung. Die präzisere Beschreibung von Tropfenbrüchen anhand dieses Modells wurde erfolgreich an Einzeltropfenbeispielen sowie durch Simulationen im Rührbehälter gezeigt.

Die Versuche im Rührbehälter zeigen deutlich, dass eine Reproduktion der experimentellen Daten mit Hilfe der Populationsbilanz nach einmaliger Parameteranpassung auch durch klassische Modelle vollzogen werden kann. Es ist sogar möglich, eine Vielzahl an Geometrie- und Betriebsparametern (z.B. Drehfrequenz, Reaktorgröße oder Rührertyp) zu variieren, ohne dafür die Anpassungsparameter in den Modellen neu wählen zu müssen. Selbst extreme Veränderungen, wie der Wechsel von einem einstufigen zu einem 4-fachen Rührsystem mit entsprechend höherem Füllstand bei konstantem Reaktordurchmesser, konnten mit Abweichungen kleiner 10% vorhergesagt werden.

Der entscheidende Vorteil des neu entwickelten Modells liegt vor allem darin, einen Wechsel des Stoffsystems mit höherer Vorhersagepräzision zu beherrschen. So konnten mit einmaliger Parameteranpassung für das System Toluol/Wasser auch die Systeme Anisol/Wasser sowie N-Butylchlorid/Wasser mit Abweichungen unter 5% des transienten Sauterdurchmessers beschrieben werden.

Ein weiterer wesentlicher Parameter im Betrieb von gerührten Flüssig/flüssig Systemen ist der Phasenanteil. Eine Vorhersage des Einflusses des Phasenanteils in den untersuchten koaleszenzstabilisierten Systemen war möglich, wenn die Turbulenzdämpfung durch die Variation der Menge der dispersen Phase berücksichtigt wurde. Hierfür wurde auf gängige Annahmen aus der Literatur zurückgegriffen.

List of own publications used for the cumulative thesis

This thesis is based on the following publications, which are reprinted in Appendix A3 - Own publications used for the cumulative thesis (full text) and which are referred to in the text by their roman number, author and year of publication. The order is chronological. The complete list of publications can be found in the references section.

I. Maaß, S., Gäbler, A., Zaccone, A., Paschedag, A.R. and Kraume, M., **2007**. Experimental investigations and modelling of breakage phenomena in stirred liquid/liquid systems. Chemical Engineering Research and Design, 85(A5): 703-709.

II. Zaccone, A., Gäbler, A., Maaß, S., Marchisio, D. and Kraume, M., **2007**. Drop breakage in liquid-liquid stirred dispersions: Modelling of single drop breakage. Chemical Engineering Science, 62(22): 6297-6307.

III. Maaß, S., Wollny, S., Sperling, R. and Kraume, M., **2009**. Numerical and experimental analysis of particle strain and breakage in turbulent dispersions. Chemical Engineering Research and Design, 87(4): 565–572.

IV. Maaß, S., Metz, F., Rehm, T. and Kraume, M., **2010**. Prediction of drop sizes for liquid-liquid systems in stirred slim reactors - Part I: Single stage impellers. Chemical Engineering Journal, 162(2): 792-801.

V. Maaß, S., Wollny, S., Voigt, A. and Kraume, M., **2011a**. Experimental comparison of measurement techniques for drop size distributions in liquid/liquid dispersions. Experiments in Fluids, 50(2): 259-269.

VI. Maaß, S., Rehm, T. and Kraume, M., **2011b**. Prediction of drop sizes for liquid-liquid systems in stirred slim reactors - Part II: Multiple stage impellers. Chemical Engineering Journal, 168(2): 827–838.

VII. Maaß, S. and Kraume, M., **2011**. Determination of breakage rates with single drop experiments. Chemical Engineering Science (DOI: 10.1016/j.ces.2011.08.027): pp. 20.

VIII. Maaß, S., Eppinger, T., Altwasser, S., Rehm, T. and Kraume, M., **2011c**. Flow field analysis of stirred liquid-liquid systems in slim reactors. Chemical Engineering Technology, 34(8): 1215–1227.

IX. Maaß, S., Buscher, S. and Kraume, M., **2011d**. Analysis of particle strain in stirred bioreactors by drop breakage investigations. Biotechnology Journal, 6(8): 979–992.

X. Maaß, S., Paul, N. and Kraume, M., **2011e**. Influence of the dispersed phase fraction on experimental and predicted drop size distributions in breakage dominated stirred liquid-liquid systems. Chemical Engineering Science (submitted): pp. 12.

XI. Maaß, S., Rojahn, J., Hänsch, R. and Kraume, M., **2011f**. Automated drop detection using image analysis for online particle size monitoring in multiphase systems. Computers and Chemical Engineering (submitted): pp. 10.

Introduction

Breakage of particulate matter into smaller fragments is encountered in many natural phenomena and technological processes. For instance at the geological time scale, a fragmentation process is apparently responsible for the distribution of particulate material on the earth surface. Technological aspects of fragmentation concern mineral processing, polymer degradation and break-up of liquid droplets or air bubbles [Kostoglou and Karabelas 1997].

This work deals with the break-up of fluid particles in dispersions with the major focus on drop breakage.

I. Industrial application examples

In industrial practice at present the trend is going away from standardized towards individual solutions. This is also true for dispersion processes. There, all functional components including the mixing equipment are analyzed in their interacting performance with each other. Therefore, searching only for an optimum impeller is not considered any longer as the solution for optimizing these processes. In fact, searching for an overall optimal mixing system which is lowering production and investment costs or as just recently shown in literature for an increase in yield is expected as the solution [Himmelsbach 2009].

Parallel to this, the size of production plants is increasing to benefit from the economy of scale. A large plant is in terms of investment costs and fixed operation expenses almost always advantageous compared to a sum of smaller plants with the same production capacity. This has increased the challenges on process engineering, especially in terms of scale-up, as little or no experience is available at these scales.

Furthermore, a system analysis and development is not only beneficial for the bulk products, but also for the specialty products which are produced in smaller amounts [Himmelsbach 2009].

The following paragraphs will present only a section from the broad variety of liquid/liquid (l/l) dispersions in industrial applications. Although all have a long history in chemical engineering, they all have huge potential in further process understanding, optimization and intensification. It is even stated in literature, that the challenges of the 21st century in terms of shrinking availability of nonrenewable feedstock, rising energy prices and a broad spectrum of environmental and safety issues will force chemical engineering into a "drastic improvement of equipment and process efficiency" [Van Gerven and Stankiewicz 2009].

Therefore, a systematic analysis of such processes is crucial and promising.

1. Extraction processes

Drumm et al. (2011) describe solvent extraction processes as a separation operation. These processes are also known also as liquid–liquid extraction processes, which are based on the different distribution of the components to be separated between two liquid phases. The process is used primarily when distillation is impractical or too intensive in terms of costs [Drumm et al. 2011]. Different types of countercurrent extraction columns are used in these processes. One major type are rotating disc columns [Drumm et al. 2008]. One compartment of such a column can also be modeled by a continuous stirred tank because fluid dynamics, droplet movement, droplet interaction (breakage and coalescence) and their interconnection to physical and process parameters are described by the same models.

In the mining industry an extraction process is normally carried out in a series of mixer-settlers, which operate in a countercurrent mode [Ruiz and Padilla 2004]. The purification and concentration of metals like copper from solutions produced by leaching of ores and concentrates are the major tasks in these processes. Up to now solvent extraction technologies continue to be an attractive option for metal producers (see an example plant in Figure 1).

The major objective for process engineering in an extraction process independent from the used equipment is the creation of a dispersion which provides large specific interfacial area between the phases across which a valuable component is preferentially extracted from one phase to the other. The specific interfacial area between the phases should neither be too small nor too large. If the interfacial area is too small the extraction will be poor, if the interfacial area is too large, owing to drop sizes being fine, the settling vessel required for mechanical phase separation following the mixing will be large. A large settling vessel will lock in large inventory of the expensive solvents thereby tending to make the process uneconomical [Singh et al. 2009].

Therefore, a precise understanding and predictability of the drop breakage and coalescence phenomena in such processes is indispensable.

Figure 1 – Typical copper mixer settler (located in Arizona, USA)[i].

2. Two-liquid-phase biocatalytical processes

Deziél et al. (1999) describe two-liquid-phase culture systems as processes which involve the addition of a water-immiscible, biocompatible and non biodegradable solvent to enhance a biocatalytical process. They show in their study that two-liquid-phase bioreactors have been used since the mid-seventies[ii] for the microbial and enzymatic bioconversion of hydrophobic/toxic substrates into products of commercial interest. The increasing popularity of bioremediation technologies suggests a new area of application for this type of bioreactor. Two-liquid-phase bioreactors have the potential to resolve both limitations of biotreatment technologies by the enhancement of the mass transfer rate of compounds with low bioavailability and by the controlled delivery of nonpolar toxic compounds. This technology can also be useful in accelerating the enrichment of microorganisms degrading problematic pollutants [Deziél et al. 1999].

To date there has been little investigation into the design of large scale biotransformation processes using two-liquid-phase systems. The major problem is the poor understanding of many interfacial effects including stable emulsion formation as a result of biosurfactant production by the micro organisms [Cull et al. 2001]. Knowledge of the drop size distribution, in particular, is critical for the estimation of the interfacial area and hence the rates of solute transfer between the phases. Furthermore, the maintenance of constant interfacial area per unit volume is a key parameter for the successful scale-up of two-liquid-phase bioconversion processes [Cull et al. 2002]. Therefore, a detailed understanding of the evolution of drop sizes is of major importance for the use of such processes. As most of the processes are coalescence hindered, the breakage phenomena are dominant. Drop breakage modeling and prediction are the critical parameters for the successful scale-up, design and operation of agitated two-liquid-phase bioconversion processes.

3. Food engineering and technology

Since consumers' interest in the health-enhancing role of specific foods and in physiologically active food components have increased, the interest in so-called functional foods is receiving much attention [Hentschel et al. 2008]. Due to the various beneficial health effects of carotenoids, with lycopene as one example, these species are used as valuable ingredients in the construction of such new food products. Carotenoids are not water soluble and only slightly oil soluble. Therefore, their bioavailability is low. It is assumed that only a minor part from a natural fruit or a vegetable is absorbed by a human [Ribeiro et al. 2003]. In contrast, if these

[i] www.platinummetalsreview.com (2011.04.12).

[ii] See Deziél et al. (1999) for a detailed literature review on this field. Furthermore, the work of Galindo et al. (2000) is recommended as an introduction in this field

products are dissolved in vegetable oil they show a high bioavailability [Gramdorf et al. 2008]. Therefore, an emulsification of the carotenoids is necessary.

Due to the lack of suitable models in food industry, emulsified products are currently developed by combining a broad knowledge of the previous product formulations with empirical scientific experimentation to create new formulations with desired properties. Because this approach is intuitive and experimental, the progression of a formulation is generally unpredictable and a new product will often go through hundreds of prototype formulations in a laboratory or pilot plant before commercialization. Due to the very large number of possible formulations and processing combinations that need to be explored, the traditional trial-and-error approach requires significant time and resources. The lack of suitable models has impeded the development of systematic methodologies for designing emulsified products. Such methodologies will not eliminate the need for laboratory experimentation, but rather they will serve to guide and focus product experimentation on quantifying key physicochemical properties instead of attempting to directly identify new product formulations [Raikar et al. 2009].

4. Polymerization

Emulsion and suspension polymerization are both types of radical polymerizations that usually start with monomer emulsion, stabilized by a surface active agent. The most common type of these emulsions is an oil-in-water (o/w) emulsion, in which droplets of monomer are mechanically dispersed and chemically stabilized in a continuous phase of water.

Suitable conditions of mechanical agitation are maintained while the monomer droplets are slowly converted from a highly mobile liquid state, through a sticky syrup-like dispersion, to hard solid polymer particles. The stabilizer hinders the coalescence of the monomer drops first and later stabilizes the polymer beads whose tendency to agglomerate may become critical when the polymerization has advanced to the point where the polymer beads become sticky [Yuan et al. 1991].

The most important issue in the practical operation of suspension polymerization is the control of the final particle size distribution as it affects the polymer's handling, storage, processing and application characteristics. Suspension polymer particle diameters range usually between 50 and 2000 µm. The exact size depending on the monomer type, the concentration of stabilizer and the agitation conditions in the reactor have been widely investigated[iii]. However, the measurement and the control of polymerization reactions is still very challenging due to the complexity of the physical mechanisms [Frauendorfer et al. 2010; Richards and Congalidis 2006].

Since many polymerization reactions exhibit strong nonlinear dynamic behavior, advanced process control techniques are necessary such as model control. Various approaches have been developed by the academic process control community[iv]. It is very important for the development of control models to understand the process. This is typically achieved in a dynamic simulation using experimentally validated models. The quantitative calculation of the evolution of the particle size distribution presupposes a good knowledge of the droplet and particle breakage as coalescence mechanisms [Saliakas et al. 2008]. As most of the discussed reactions are taking place in strongly coalescence hindered processes, the understanding of breakage phenomena is of first order, while the understanding of coalescence is only of second order.

II. Analysis and modeling of agitated liquid/liquid dispersions

The properties of liquid/liquid dispersions have been an active field of scientific studies since the 1950s [Yuan et al. 1991]. Many excellent reviews are available [Angle and Hamza 2006; Leng and Calabrese 2004; Pacek et al. 1998; Singh et al. 2008; Yuan et al. 1991; Zerfa and Brooks 1996]. These summarize the experimental work that was carried out to determine and to understand the influence parameters on the drop size distribution and mostly on the Sauter mean diameter ($d_{32} = \Sigma\, d_i^3/\Sigma d_i^2$). This diameter is the ratio from the third and the second moment of the distribution and is directly related to the dispersed phase fraction φ_d and the total interfacial area per total volume a_f in the system ($d_{32} = 6\varphi_d/a_f$).

In most of the reviewed cases, the experimental data has been correlated using a functional form based on the turbulence theory [Kolmogoroff 1941] developed by Hinze (1955). Hinze postulated that a drop would break up at a critical Weber number ($We = \rho_c n^2 D^3/\gamma$). The Weber number is the ratio between external defor-

[iii] See Yuan et al. (1991) for a detailed literature review on this field.

[iv] See Richards and Congalidis (2006) and also Qin and Badgwell (2003) for a detailed literature review on this field.

mation forces provided by the stirrer (n - stirrer speed, D - impeller diameter) and the drop restoring forces associated with the interfacial tension γ. With the knowledge of this critical Weber number the drop size is predictable ($d_{32} \sim We^{-0.6}$).

Several extensions and further developments to that theory in the form of correlations have been published as this can be seen in the named references above. However, most of the studies have focused on the analysis of the steady state drop diameter and not on transient analysis. The steady state diameter is the diameter where the opposed phenomena of drop breakage and drop coalescence are equal throughout the vessel. Therefore, the drop size is constant at this state over time.

A complete description of the transient drop size distribution occurring in most industrial applications cannot be achieved with such correlations. A further drawback is a huge variety of correlation constants reported in literature (see also the named review references for a parameter overview). The complexity of these correlations and therewith their dependency on physical parameters has increased over the last decades. Unfortunately, the number of fitting parameters in those equations and the variance of reported values have increased too. Therefore, literature states caution in the use and extrapolation of these correlations [Leng and Calabrese 2004].

For the analysis of the time evolution of a drop size distribution, population balance equations (PBE) are mostly applied. Population balances may be regarded either as an old subject that has its origin in the Boltzmann equation more than a century ago, or as a newer one in the light of growing variety of applications in which engineers have put it to practice. The methodology of population balances is indispensable for a rational treatment of dispersed phase processes in engineering. It is the capacity of population balances to address the evolutionary aspects of a dispersion [Ramkrishna 2000].

The PBE in l/l systems define how populations of separate drops develop in the specific properties over time. They are analogous to material balances, but instead of applying them to each chemical species, they are applied to drop size class comprising the entire drop size distribution (DSD). Therefore, sink and source terms are referred to as birth and death rates by breakage and coalescence for a drop of a specific size [Leng and Calabrese 2004].

As the fluid dynamics and therewith the energy dissipation rates ε of the system strongly influence the drop sizes, detailed analysis of the flow field in the investigated apparatus is necessary. The technology of computational fluid dynamics (CFD) shows excellent results analyzing single phase flows. This was shown by many researchers which were just recently reviewed by Joshi et al. (2011). The local resolution of the fluid dynamic allows a precise description of the fluid dynamics within the PBE.

The opportunities and challenges using population balances are described in detail in the following chapter 2. The general scheme and a brief introduction about solution methods of population balances can also be found there.

III. Scope and outline of the thesis

As explained in the previous sections, dispersed l/l systems are of major importance in chemical, pharmaceutical, mining, petroleum, food industries and biotechnology. The efficient operation, design and scale-up of reactors usually require expensive experimental investigations.

Complete models describing the timely evolution of the drop size distribution considering all major influence parameters could already be established using PBE in combination with CFD. But as just recently stated the modeling of multiphase dispersion processes (including liquid/liquid processes) is not state of the art in industry practice [Rohn and Keller 2011]. Only qualitative predictions are possible with market available technologies. Although computational fluid dynamics and population balance models have made much progress in recent years, the strong variations of industrial equipment are overstraining these technologies. Especially the broad variety of mixing equipment, installation of multiple impeller systems and the change in reactor design for example to higher aspect ratios (ratio between liquid level H and vessel diameter T - see also Figure 2) in industrial practice create new boundaries for the actual modeling approaches [Bey and Dienes 2010; Joshi et al. 2011].

The aim of this thesis is to evaluate already existing and to further develop model approaches which will help to overcome the gap between industrial process practice and detailed process understanding. Therefore, various experiments have been carried out, analyzing the flow field and the drop size as a function of geomet-

ric factors, operating parameters and physical characteristics of the l/l dispersion. A list[v] of the parameters analyzed in this work can be found in the following paragraph. Figure 2 displays one overview of the geometrical factors of an exemplary stirred tank used for this thesis.

Geometric factors:
- reactor size T
- reactor aspect ratio H/T
- stirrer type (Ruston turbine, retreat curve impeller, flat blade impeller)
- stirrer height h_{St}
- stirrer - bottom clearance h
- number of stirrers n in multiple impeller systems
- stirrer - stirrer distance s in multiple impeller systems
- baffle type (cylindrical or planar)
- immersion depth of baffles l_B

Operating parameters:
- stirrer speed n
- dispersed phase fraction φ_d
- stabilizer concentration c

Physical characteristics:
- interfacial tension between the immiscible liquids γ
- density of the dispersed phase ρ_d
- viscosity of the dispersed phase η_d

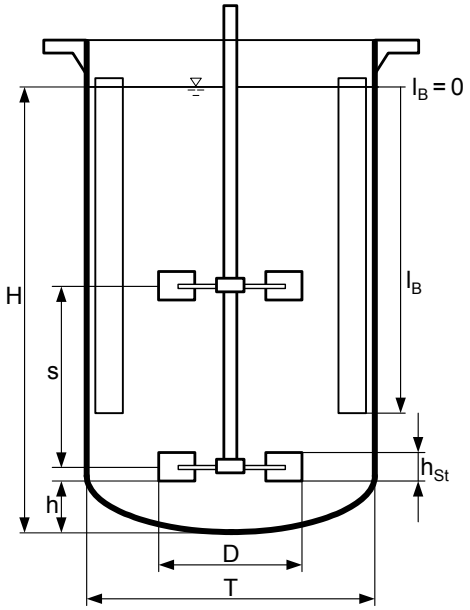

Figure 2 – Example geometry of used stirred tanks.

The prediction of the timely evolving drop size distribution for this broad variety of investigated parameters will be carried out using population balances. To solve the PBE, the breakage and coalescence functions must be specified. The determination of these functions from experimental drop size distributions obtained either at steady state or at transient state is difficult mainly because both rate processes occur simultaneously. Primary information on drop breakage can be obtained by reducing the coalescence between drops to a negligible value. Under this condition, breakage events would be essentially responsible for the evolution of the drop size distribution, particularly in the early stages when the system is far from equilibrium. As this work focuses

[v] This list follows the one, given by Yuan et al. (1991), who listed the main influence parameters on suspension polymerizations. It does not have the aim to be a complete listing of influential parameters on drop size distributions, although it covers most of them.

on the analysis of the drop breakage phenomena, two different ways have been used to investigate breakage separately from coalescence.
The first method is to use dispersions with very low dispersed phase fractions, which will reduce interactions between drops to a minimum due to the low number of drops [Ruiz and Padilla 2004]. The second method is to add surfactants to immobilize the droplet surface and thereby to suppress coalescence [Kumar et al. 1991].

The work followed both ideas, to gain new insights from the complex phenomena of drop breakage (see Figure 3). On one hand the l/l system was diluted and at the end transferred into a new experimental set-up where the breakage of single drops is investigated. On the other hand the complete dispersion was stabilized. Under stabilized conditions, breakage events are essentially responsible for the evolution of the drop size distribution, particularly in the early stages of the process.

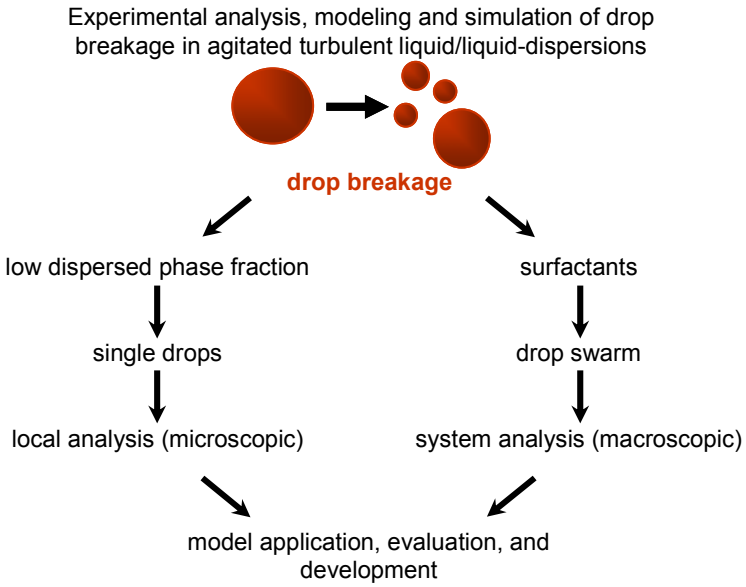

Figure 3 – Outline of the thesis: procedural method.

The resulting DSD in an agitated vessel is the sum of complex phenomena occurring on a single particle level. Local analysis (left wing in Figure 3) on a microscopic scale allows observation on those single individuals. The influence of parameters like the fluid dynamics or physical properties of the continuous or dispersed phase on individual drops can be determined with this procedure. Below, this procedure is always named single drop analysis.

As drops interact with each other and thereby influence each other, the same parameter studies have to be carried out with a drop swarm to gain insights on the weighting of the collective. Therefore, the whole system is analyzed (right wing in Figure 3) on a macroscopic level. Below, this procedure is always named drop swarm analysis.

The results from both procedures will be used to evaluate and to further develop breakage models for the population balance equation. Furthermore, the models and the increased dispersion process understanding will be used to analyze industrial applications. Different processes will be simulated and thereby explained in detail.

This dual procedural method can also be found in the publications used for this thesis. All eleven papers have been classified belonging to one or the other procedure. An overview is given in Figure 4.

A further subdivision can be seen there. The publications not only belong to either the single drop or drop swarm analysis, they can also be subdivided in fundamental work and model based work. The following paragraph describes the structure of the single drop analysis.

The experiments in publication I - Maaß et al. (2007) aim at representing a breakage of a single drop close to a stirrer blade in an agitated vessel using a drop breakage cell. The general method using single drops as base for breakage analysis is explained and already partly verified there. A more detailed analysis of the flow field in the vicinity of a stirrer and a detailed comparison with the fluid dynamics in the single drop breakage cell is carried out in publication III - Maaß et al. (2009). The transferability of drop breakage in an agitated vessel to the used single drop breakage cell is proven.

The results from the breaking single drops are used for PBE breakage model evaluation and development in publications II - Zaccone et al. (2007) and VII - Maaß and Kraume (2011). The experimental data of the resulting daughter drop size distribution functions are compared with various models from literature in II - Zaccone et al. (2007). Furthermore, an own developed model approach for the daughter drop size distribution is proposed in II - Zaccone et al. (2007).

The durations of the individual breakage events and the overall breakage probabilities for different drop sizes are compared with model results from literature in publication VII - Maaß and Kraume (2011). Since the influence of the physical properties, like viscosity or interfacial tension, was only poorly reflected in the available models of the breakage time, an improved model which takes into account different breakage mechanisms and the influence of viscosity and interfacial tension was derived.

The application of PBE simulations evaluating mechanical stress in bio reactors as the application of single drop results on simulations of a breakage dominated l/l system is carried out in publication IX - Maaß et al. (2011d).

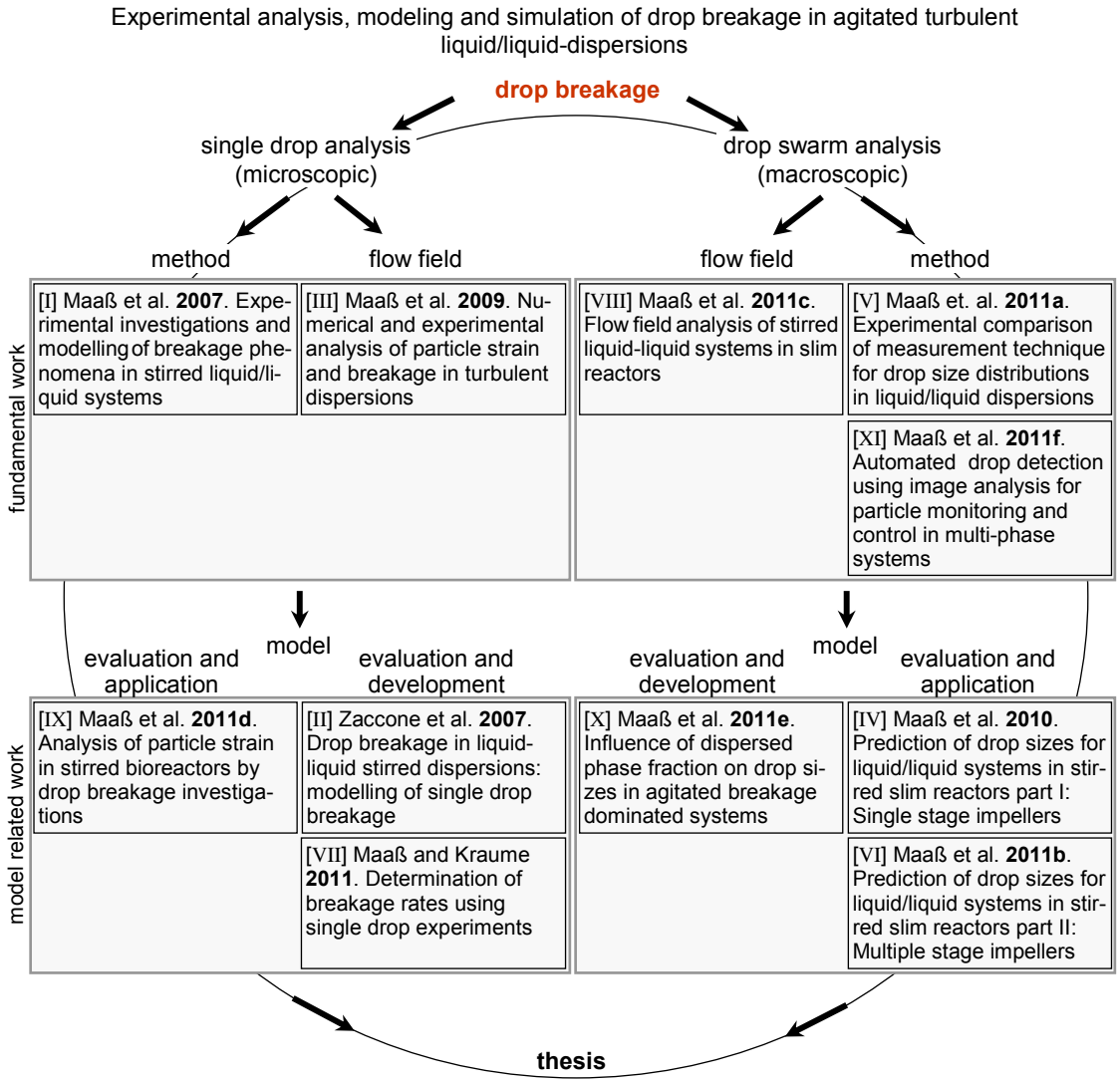

Figure 4 – Structure of the thesis.

The validation of the experimental methods used to measure the size of drops within an agitated vessel are reported in publication V - Maaß et al. (2011a) and XI - Maaß et al. (2011f). The comparison of different measurement techniques in publication V - Maaß et al. (2011a) revealed that the exterior smooth surface of the drops investigated in this project is leading to strong errors in the measurement of the size of the drops if photo optical methods are not used.

To overcome the drawback of time consuming manual quantification using photo optical methods with image analysis, a full automation based on MATLAB® was implemented and put into practice. The software employs a normalized cross correlation procedure (NCC) algorithm, which is explained in detail along with the pre-filtering which was employed. Additionally, it avoids human generated bias by different observers, also shown in publication XI - Maaß et al. (2011f).

As it was already mentioned above, the fluid dynamics inside the agitated vessel strongly affect the drop size in the system. Unfortunately, knowledge about the flow field in vessels differing from the standard geometry in textbooks is rare or even not existent. Therefore, experiments and CFD simulations are carried out in industrial relevant reactor configurations with aspect ratios H/T up to 5 at lab and pilot plant scale to determine the flow field of single and multiple stage impeller systems. The results are given in publication VIII - Maaß et al. (2011c).

With secure knowledge of the fluid dynamics in slim vessels, model evaluation and model development became possible. One standard population balance model (the one from Coulaloglou and Tavlarides (1977) - see the following chapter for the model details) was used in publication IV - Maaß et al. (2010) and VI - Maaß et al. (2011b) to simulate transient drop size distributions of various geometric factors and operation parameters that all have been successfully validated with experiments. Mainly the influence of the dispersed phase fraction on the drop sizes in breakage dominated systems was investigated and then estimated with different PBE model approaches in publication X - Maaß et al. (2011e). The experimental and simulation results were used to develop a new model, taking physical characteristics and the dispersed phase fraction better into account. The new developed model is based on a model from literature.

The content of the following chapters will contain short summaries of the associated publications from this thesis. Moreover, it will also provide an additional literature review to classify own work within the state of the art. Supplementary data which have not been published yet will also be provided. This combination of published and new information is used to come to an overall discussion and conclusion which proclaims to be more than just the sum of the individual publications[vi]. The structure of the thesis follows basically Figure 4.

Chapter 2 briefly develops the general framework and focuses straight on the closure terms for breakage and coalescence which have been used for this thesis. Additionally, an overview of solution methods is given there, while the one used in this study is described more detailed. Limitations and challenges dealing with the PBE will round up the given picture of this valuable engineering tool.

The third chapter deals with the experimental analysis methods and is represented by the two method sections in Figure 4. An overview and evaluation for drop size measurements in drop swarm experiments based on publication V - Maaß et al. (2011a) is given. Additionally, the measurement technique and the set-up for the single drop analysis as some general motivations behind single drop analysis are presented there.

Image analysis is the major tool for both experimental works, the single and drop swarm analysis. The working procedures based on publication I - Maaß et al. (2007) and XI - Maaß et al. (2011f) are briefly described.

Chapter 4 deals with the flow field in the single drop breakage cell and the stirred vessel. This has the aim to lay a fundamental understanding of the fluid dynamics in the used experimental set-ups. This chapter is represented by the two flow field section in Figure 4.

The following two result chapters 5 and 6 are equally structured. They start with an overview of the measurement program, followed by the section model application and than the section model development. This structure is equal to the one presented in Figure 4.

Chapter 5 gives some further material about the breakage time and the number of daughter drops of breaking single drops. These unpublished additional materials are integrated in the named structure of model application and model development.

Chapter 6 shows supplementary experimental and computational results of drop swarms in an agitated vessel. The influence of surfactant concentration and the occurrence of phase inversion during the experiments are shown. Together with the supplementary material from chapter 4 to 6 the results are discussed and interpreted. Based on this discussion, unpublished ideas are proposed for the modeling of breakage in agitated vessels.

Conclusions as further necessary works are given in the last chapter.

[vi] "The whole is more than the sum of its parts" Aristoteles (*384 BC - †322 BC).

The procedure of this thesis, analyzing drop breakage separate from drop coalescence in single drop and drop swarm experiments, will provide necessary information to evaluate and derive physical based breakage models.

Furthermore, the detailed flow analysis which will be correlated with the simulations will provide a secure base to take the fluid dynamics in a meaningful matter into account.

These insights will be used to simulate and predict agitated liquid/liquid systems under a broad industrial relevant variation of geometric factors, operating parameters and physical characteristics. This will provide a trustful base for process and reactor design, scale-up and optimization.

2. Population balances

The integro-differential nature of the equations describing population balance models has inspired many researchers in the last five decades to establish mathematical tractability and solutions of the model equations. Up to today already commercial solvers are available so the variety of applications where PBE are used has intensively grown. The focus of this following chapter is only on population balances applied to turbulent liquid/liquid dispersions. Therefore, the general framework and the closure terms for drop breakage and coalescence under such conditions are briefly discussed. Different solution possibilities are shown, the one used in this work is described in more detail. At the end of this chapter the challenges and limitation of this tool are discussed.

Population balances have been originally introduced in the chemical engineering community for crystallization processes by Hulburt und Katz (1964). The first who applied the PBE to l/l dispersions were Valentas and Amundson (1966). They described the transient behavior of a continuously fed, agitated vessel and an agitated batch reactor. Below only batch systems will be discussed. The complete equations for further cases and their derivation are given by Ramkrishna (2000).

I. General framework

The most general form of a population balance equation, applicable for a batch system, can be written as follows. It only considers size change of the individuals:

$$\frac{\partial f(V_P)}{\partial t} = B_{br}(V_P,t) - D_{br}(V_P,t) + B_{coa}(V_P,t) - D_{coa}(V_P,t) \tag{1}$$

Since this form only describes the size change over time, it is called a one dimensional PBE. In equation (1) B_{br}, D_{br}, B_{coa} and D_{coa} are the birth rate by breakage, death rate by breakage, birth rate by coalescence and death rate by coalescence, respectively. Each of these terms is a single kernel which contains further sub-models. The complete description of the breakage and coalescence terms following Coulaloglou and Tavlarides (1977) is given by:

$$\begin{aligned}\frac{\partial f(V_P)}{\partial t} = & \int_{V_p}^{V_{P,max}} \nu(V_P')\beta(V_P,V_P')g(V_P')f(V_P',t)dV_P - g(V_P)f(V_P,t) \\ & + \frac{1}{2}\int_{V_p}^{V_P} F(V_P',V_P'')f(V_P',t)\,f(V_P'',t)dV_P' - \int_{0}^{V_{P,max}-V_P} F(V_p,V_P')f(V_p',t)dV_P'\end{aligned} \tag{2}$$

Where the breakage kernel contains $\nu(V_p')$ the number of dispersed fluid entities formed upon breakage of a particle, $\beta(V_p, V_p')$ which is the size distribution of daughter fragments formed from the breakage of a particle V_p and the breakage frequency also called breakage rate $g(V_p)$. The coalescence kernel contains the coalescence rate $F(V_p', V_p'')$ which is assumed to be a two step process involving drop collision and film drainage of the continuous fluid. Thus it can be expressed as the product of the collision frequency $h(V_p', V_p'')$ and the coalescence efficiency $\lambda(V_p', V_p'')$.

II. Closure terms describing the breakage processes

The breakage of drops in turbulent dispersions is influenced by the continuous phase fluid dynamics and interfacial interactions. Generally, the breakage mechanism can be expressed as a balance between external stresses from the continuous phase, which attempt to destroy the fluid particle and the surface stress of the particle [Liao and Lucas 2009]. Some model approaches also include the viscous stress of the fluid inside it, which restores the drops. These are the major ideas behind most of the available phenomenological models.

As the breakage of particles occurs independently of each other, the breakage function of a drop d_p at time t in an environment Y can be represented also by pure probabilistic functions. However, for both descriptions, the breakage rate $g(d_p)$, the number of daughter drops $\nu(d_p')$ and the daughter drop size distribution (DDSD) $\beta(d_p, d_p')$ have to be formulated.

Each of these functions will be discussed in a separated paragraph below.

1. Breakage rate

The literature on efforts to determine breakage rate functions over the past 50 years is very large. Two papers have more or less recently reviewed the numerous research reports [Lasheras et al. 2002; Liao and Lucas 2009]. Among the several ways proposed for obtaining the breakage functions, i.e. "inverse" problem solution (by employing experimental data), purely algorithmic functions, probabilistic and phenomenological models, the latter seems to be the most promising one. The main advantage of phenomenological models is their explicit dependence on the system physiochemical parameters [Kostoglou and Karabelas 2005].
The number of phenomenological models for breakage functions in the literature is large. Some contradicting ideas among those kinds of models have been discussed in publication VII - Maaß and Kraume (2011).

The most widely used and quoted[i] model for the drop breakage rate is the approach of Coulaloglou and Tavlarides (1977). It was also most often used in the publications associated with this thesis. Therefore, only this model is explained in detail here. For further details on other model approaches the work of Liao and Lucas (2009) and also publication VII - Maaß and Kraume (2011) are recommended.

The mechanistic model for $g(d_p)$ proposed by Coulaloglou and Tavlarides (1977) is based on the assumption that $g(d_p)$ is a product of the fraction of the total number of breaking drops and the reciprocal time needed for the drop breakage to occur:

$$g(d_P) = \left(\frac{1}{\text{breakage time}}\right) \cdot \left(\frac{\text{fraction of}}{\text{breaking drops}}\right) = \frac{1}{t_{br}} \cdot \frac{N_{br}}{N_{tot}} \tag{3}$$

The fraction of breaking drops is assumed to be proportional to the fraction of turbulent eddies colliding with the drops that have a turbulent kinetic energy greater than the drop surface energy. The drop breakage time t_b is estimated by assuming that it is approximately equal to the characteristic time for drop deformation. It is derived from Batchelor's equation for the motion of two lumps in the turbulent field [Batchelor 1952]

For equally sized daughter drops after a binary breakage, the distance between both daughter particles is equal to their diameter d_p', which is equal to d_p''. This assumption is a valid simplification, since possible distance variation is low. The appearance of unequally sized breakage events at all is not neglected by this assumption, since it is determined by the daughter drop size distribution $\beta(d_p, d_p')$ explained in the following section. With this assumption and an introduced proportionality constant c, the breakage time can be calculated with the following equation:

$$t_{br} = c \cdot \frac{d_P^{2/3}}{(1+\varphi_d)\varepsilon^{1/3}} = \frac{1}{c_{1,br}} \cdot \frac{d_P^{2/3}}{(1+\varphi_d)\varepsilon^{1/3}} \tag{4}$$

The overall breakage rate by Coulaloglou and Tavlarides (1977) is written as follows:

$$g(d_p) = c_{1,br} \frac{\varepsilon^{1/3}}{(1+\varphi_d) d_P^{2/3}} \exp\left(-c_{2,br} \frac{\gamma(1+\varphi_d)^2}{\rho \varepsilon^{2/3} d_P^{5/3}}\right) \tag{5}$$

and has an absolute maximum for a certain critical particle diameter. This has been generally criticized by several authors [Bapat et al. 1983; Chen et al. 1998; Tsouris and Tavlarides 1994]. The intention of Coulaloglou and Tavlarides (1977) is to use the breakage time in order to determine the breakage rate. The mentioned maximum with increasing mother drop diameter occurs because the duration of breakage increases with rising diameter. Therefore, once the diameter has reached a certain size the breakage rate is mainly affected by the breakage time and decreases because the breakage probability is not increasing any further.

A more detailed discussion about the breakage time and its influence on the breakage rate can be found in publication VII - Maaß and Kraume (2011) and in chapter 6 (see page 63f). Simulation results achieved with the model of Coulaloglou and Tavlarides (1977) are described in the publications IV - Maaß et al. (2010), VI - Maaß et al. (2011b), IX - Maaß et al. (2011d) and X - Maaß et al. (2011e). Especially the last work of the named ones is recommended to review this model approach, as it compares simulations using different breakage rates.

---

[i] The paper from Coulaloglou and Tavlarides (1977) had 384 citations in ISI Web of Science (http://apps.isiknowledge.com; 2011.04.15) and 322 citations in scopus (www.scopus.com; 2011.04.15). In this ranking the model of Luo and Svendson (1996) follows with 204 citations in ISI Web of Science (http://apps.isiknowledge.com; 2011.04.15). The number of citations is almost equal to Tsouris and Tavlarides (1994) with 196 citations in ISI Web of Science (http://apps.isiknowledge.com; 2011.04.15).

2. Daughter drop size distributions

As described in equation (2) for the calculation of the transient drop size distribution, in addition to the breakage rate, the size of the drops that are formed during the breakage process, the DDSD, has to be known. According to Liao and Lucas (2009), who just recently reviewed this research field, models used for the description of daughter drop size distributions can be classified as statistical or phenomenological.

Liao and Lucas (2009) also distinguished the distributions regarding their shapes for the assumption of binary breakage: Bell-shaped distributions assume a maximum probability density for daughter drops of equal size. Contrarily, U-shaped and M-shaped distributions predict a minimum probability density for the same event. However, bell-shaped and M-shaped distributions have in common a zero probability density for infinitively small daughter drops, while U-shaped distributions predict these daughter drops most probable.

The most widely used models are statistical ones. They consider that the size distribution of the daughter drops is the combined result of a large number of independent random events. The early assumption was, that the daughter drop size distribution was a normal distribution [Coulaloglou and Tavlarides 1977; Valentas et al. 1966]. Such a density function gives a maximum probability for equally sized daughter drops. This kind of distribution was used by many authors[ii] and is therewith the most spread one. It is described for binary breakage in the following paragraph.

The expectation value of one daughter drop is $\mu = V_p/\nu$ with $\nu = 2$, if a maximum probability density for equally sized daughter drops is postulated. The standard deviation is expressed as $\sigma = \mu/L$, assuming that L is a single value equal to 2.5. This value was chosen to get a truncated distribution which conserves at least 99.98% of the mass of the distribution (see Kostoglou et al. (1997) for more details). The dimensionless representation is given with the daughter to mother drop volume ratio $f = V'_P/V_P$ as follows:

$$\beta(f,1) = \frac{L\nu}{\sqrt{2\pi}} \exp\left(-\frac{(\nu f - 1)^2 L^2}{2} \right) \tag{6}$$

A further stochastically approach is the beta distribution for the daughter drop size distribution. Both the beta and the normal distributions are bell-shaped functions with higher probability density in the middle of the distribution. However, the beta distribution has the advantage over the normal distribution in that the density function always reduces to zero at a daughter drop size $d'_P = 0$ and a daughter drop size d'_P equal the mother drop size d_P [Ruiz and Padilla 2004]. The normal distribution is truncated and needs for comparable results very small standard deviations (see Kostoglou et al. (1997) for a detailed discussion and presentation of this topic).

Phenomenological models vary strongly in complexity and underlying theory as no general theory describing such phenomena has yet been discovered.

A detailed discussion about necessary characteristics that a DDSD of drops should have based on the constraints of surface energy and capillary pressure is carried out by Wang et al. (2003). These characteristics for the daughter drop size distribution include: existence of a local minimum at exactly equal breakup; dependence on the mother drop size and energy dissipation rate. The model should go to zero when the breakage probability tends to zero. The model should not have a singularity point nor parameters that are difficult to determine [Wang et al. 2003]. However, for this approach, the implementation in numerical and simulation codes is made cumbersome by the mathematical complexity of its formulation that requires the solution of a three-dimensional integral.

The influence of different DDSD on the simulated timely evolution of the drop size distribution is discussed in detail in publication IX - Maaß et al. (2011d). The results show clearly a strong dependency of the simulated drop size distribution on the used daughter drop size distribution. It seems possible to reproduce every kind of DSD shape with the right DDSD. Therefore, a physically rooted model for the DDSD is needed. A simple approach for describing the daughter drop size distribution suitable for population balance is described in publication II - Zaccone et al. (2007). It displays a first step establishing phenomenological models also for the daughter drop size distribution.

3. Number of daughter drops

Most population balance equation models applied to l/l systems are based on the assumption of binary breakage ($\nu = 2$). Only a few works report about PBE models accounting for multiple breakage [Chatzi and Lee

[ii] See Ruiz and Padilla (2004) for a more detailed literature review on this field.

1987; Hill and Ng 1996; Raikar et al. 2010; Tcholakova et al. 2007]. These works were mostly dedicated to the development of a new DDSD. Therefore, they have to be treated with great care, as the number of daughter drops used in the associated work was the fitting parameter to provide best agreement with experimentally achieved drop size distributions in different l/l applications. It seems that just a mathematical solution was found but the physical interpretation is uncertain (see also section V - Challenges and limitations in this chapter).

However, experimental results show clearly a possibility for multiple drop breakage. A review of experimental work, analyzing the number of daughter drops, can be found in publication IX - Maaß et al. (2011d).

Some of the results have been correlated as by Bahmanyar and Slater (1991) in equation (7). They determined minimum energy dissipation rates at which drops of a given size do not break. The mean number of daughter drops ν produced by breakage was correlated as a simple function of the drop diameter based on the critical diameter. There, the critical diameter is the smallest unstable diameter which does break first under the given conditions. Agreement was found with data from other types of agitated systems:

$$\nu = 2 + 0.9\left[\left(d_P / d_{P,crit}\right) - 1\right] \tag{7}$$

Additionally, own experimental results on this theme are given in publication IX - Maaß et al. (2011d) and I - Maaß et al. (2007) based on single drop experiments. The results show a clear tendency on the position of the observer. If the observer follows the drop in a Lagrangian perspective, every multiple breakage can be discretized into a cascade of binary breakage events. If the observer follows the drop in an Eulerian perspective, the time discretization is relevant for the evaluation of the breakage. Low time resolution always leads to higher number of breakage particles formed during the investigated breakage event.

Therefore, the discussion of the number of daughter drops should not be excluded from the discussion of the other parts of the breakage kernel. The kind of the timely discretization of the breakage rates and the physical description of the used daughter drop size distributions determine the interpretation of the number of daughter drops. This discussion was started in publication IX - Maaß et al. (2011d) and is continued in chapter 6 (see page 67ff).

III. Closure terms describing the coalescence processes

For modeling coalescence the frequently quoted model from Coulaloglou and Tavlarides (1977) is employed for the coalescence kernels. The coalescence rate $F(d'_p, d''_p)$ is assumed to be a two step process involving drop collision and film drainage of the continuous fluid. Thus it can be expressed as the product of the collision frequency $h(d'_p, d''_p)$ and the coalescence efficiency $\lambda(d'_p, d''_p)$. The collision frequency from Coulaloglou and Tavlarides (1977) has found broad acceptance in the scientific community and is formulated as follows:

$$h(d'_p, d''_p) = c_{1,coa} \frac{\varepsilon^{1/3}}{1+\varphi_d} (d'_p + d''_p)^2 (d'^{2/3}_p + d''^{2/3}_p)^{1/2} \tag{8}$$

Liao and Lucas (2010) give a broad and updated overview of research in the field of coalescence efficiencies. They differentiate between three model approaches which have been used for the calculation of coalescence efficiency: the energy model, critical approach velocity model and film drainage model. Although the validity of the film drainage model has been criticized, it remains the most popular approach and forms the starting point of almost all subsequent models, including that developed by Coulaloglou and Tavlarides (1977), given in equation (9).

$$\lambda(d'_p, d''_p) = \exp\left(- c_{2,coa} \frac{\eta_c \rho_c \varepsilon}{\gamma^2 (1+\varphi_d)^3} \left(\frac{d'_p \cdot d''_p}{d'_p + d''_p} \right)^4 \right) \tag{9}$$

Their entire coalescence rate $F(d'_p, d''_p)$ gives low values for the contact of two small or two large drops and high values for the contact of a small and a large drop. The influence of surfactants in this coalescence model is only expressed by the surface tension within the coalescence efficiency (see equation (8) and (9)). This overlooks the fact that contaminants such as surfactants are modifying the drop surfaces and hence reducing the film drainage. Moreover, the concept of a concentration threshold above which coalescence is drastically reduced is already well established in empirical models and remains central when modeling the effect of DSD in l/l systems [Martín et al. 2009].

Although the number of published models is extremely high, only one just recently published approach for the PBE model takes this interrelation into account. The surfactant adsorption is assumed to be proportional to

the amount of free surface. A similar assumption is done in the coalescence efficiency modeling [Hakansson et al. 2009]. This model is only valid for collision based emulsifier dynamics with no clear concentration gradient at the surface. Also the described macromolecular surfactant is assumed to have a low surface viscosity. The influence of surfactants on the simulation results of population balances is discussed in publication VII - Maaß et al. (2011b) and X - Maaß et al. (2011e). The results show clearly that if coalescence is completely hindered, the simulations are able to reproduce the system behavior after a parameter adaptation. Additional analysis is presented in chapter 6 (see page 52ff).

IV. Solution methods

The focus of this section is the description of the solution for PBE stand alone models. The recently largely increased number of coupled CFD-PBE approaches will be discussed in the following section V - Challenges and limitations.

Analytical solutions of the PBE exist only for unreasonably simplistic assumptions [Leng and Calabrese 2004]. Because numerical methods have grown in reliability and flexibility they are the technique commonly used by many investigators to solve the PBE (see Azizi and Al Taweel (2010) for an overview). This is either done by direct numerical integrations or by statistical simulations, such as a Monte Carlo technique (see Ramkrishna (2000) for details). However, little is published about the factors affecting the accuracy and stability of numerical solutions, as well as the computational demands associated with this approach.

The occurring problems are intensively discussed by Azizi and Taweel (2010) and have been generally summarized by them as follows: One of the problems associated with the use of the numerical solution approach is the fact that no prior knowledge about the time at which steady state conditions are approached is available to the user. This is a very important point since significant errors and/or solution instabilities may be introduced if the numerical solution is extended beyond the point where the evolution of drop-size distribution practically ceases.

In general the numerical approach for solving the one dimensional PBE is based on describing continuously changing variables by discretized functions. This discretization takes place in both the time and the drop size domains and introduces a multitude of errors. The magnitude of these errors depends on the discretization technique used.

Another error, the round off error, arises from the finite nature of the computing machine (which cannot deal with infinitely represented numbers); nevertheless it is used to simulate a number system which uses infinitely long representations. The round off error accumulates as the number of calculations increases [Azizi and Al Taweel 2010].

As already mentioned, the discretization of the drop size domain needs to be applied carefully. Significant errors can be introduced through the use of classes and inappropriate selection of the average value representing a class [Calabrese et al. 1995]. Up to 200 classes are necessary in order to achieve stable and accurate numerical solutions [Azizi and Al Taweel 2010].

Highly accurate and rapid numerical solutions could be obtained at lower computational effort when the DSD is described as a continuous function that is sampled at regular intervals in conjunction with the use of a moving grid approach such as the adaptive Galerkin h-p method [Wulkow et al. 2001]. The Galerkin discretization could even treated more efficiently by Koch et al. (2006). They used operators based on the idea of H-matrices.

Many other numerical solution methods are described in literature [Drumm et al. 2010; Kiparissides et al. 2004; O'Rourke and MacLoughlin 2010]. However, a commercial solver for the PBE is PARSIVAL® (PARticle SIze eVALuation). It uses the aforementioned Galerkin h-p method, which is based on a generalized finite-element scheme with self-adaptive grid and order construction. The mathematical details are given by Wulkow et al. (2001). PARSIVAL® is used as the PBE solver for all simulations associated with this thesis.

V. Challenges and limitations

Despite the fact that the PBE technology has been used by the chemical engineering community since the 1960s and that commercial software to solve the equation are available (see above section), little practical industrial use has been made of it for l/l dispersions. Part of this is due to the difficulty in obtaining quality drop size data which is suitable for quantitative model evaluation.

A further challenge is that the quantities in the model are flow dependent. Therefore, various efforts have been made to couple PBE with CFD, which has proven to be valuable in characterizing the local flow fields in

stirred applications. However, the computational demands for the calculations of a full 3 dimensional (3D) geometry are too expensive for most industrial relevant scales.

A limitation is that the breakage and coalescence kernels tend to be specific to the equipment and scale used to acquire the evaluation data. It is reported in literature that PBE simulations are highly scale dependent. Once information is obtained using PBE, it cannot be used, with confidence, for scale-up [Leng and Calabrese 2004].

As already mentioned above, not every influence parameter of the drop size found its application already in the existing models. The concentration of surfactants or other surface active agents is the most obvious example. Generally, an additive or unintended 'impurity' can have a profound impact on the drop size. This influence is most often applied by the variation of the model parameters, which led to a broad variety of parameters reported in literature. This limitation leads to intense challenges in interpreting the different PBE simulation results. The challenges and limitations discussed in detail in this study are listed below. They represent also the following subsections:

Accurate drop size measurements for model evaluation
Appropriate consideration of fluid dynamics in the simulation results
Influence of reactor scale
Parameter estimation and analysis

1. Accurate drop size measurements for model evaluation

The measurement of drop sizes in l/l dispersion is a major challenge in process engineering. For accurate modeling, control and optimization of these systems exact knowledge about the drop size distribution and its transient behavior under changes of energy input, temperature or composition is of major importance. This challenge is discussed in publication V - Maaß et al. (2011a) and in the following third chapter (sees page 23ff).

2. Appropriate consideration of fluid dynamics in the simulation results

It is generally assumed that the drop size distribution in turbulent dispersions is directly dependent on the energy dissipation rates in the continuous phase. The turbulent energy dissipation rates determine the distribution of eddy sizes and corresponding eddy energy. The energy associated with the eddy represents turbulent velocity (pressure) fluctuations [Srilatha et al. 2010b]. These velocity fluctuations determine the breakage and the coalescence frequency (see equation (5), (8) and (9) for details).

In agitated vessels the energy dissipation rates are highest near the impeller (impeller region) and very low in the rest of the vessel (bulk region). The local values can sometimes vary as much as a factor of 100 or 1000 [Bakker and Oshinowo 2004; Delafosse et al. 2009; Zadghaffari et al. 2010].

The impeller creates a pumping flow throughout the vessel. The drops are following this flow and circulating through the impeller region as the bulk region and thus they experience a wide variation of energy dissipation rates. This creates a wide variation in breakage and coalescence frequencies throughout the reactor. Therefore, the drop size distribution of an agitated system should not be calculated based on a single average value.

CFD has been used with great success for the prediction of detailed fluid dynamics and turbulence characteristics using real industrial equipment. The implementation of PBE in CFD allows the local calculation of the drop sizes based on the local fluid dynamics. Vice versa with the knowledge of the local drop size distribution the local fluid dynamics can be recalculated as both influence each other. However, this leads in an infinite number of additional partial differential equations due to the continuous variation of the drop size (as already discussed in the previous section). This dramatic increase in the computational load was faced with the development of several solution methods to achieve reasonable computational time.

Reviews of the various methods are available in several[iii] literature sources [Attarakih et al. 2009; Drumm et al. 2010; Marchisio et al. 2003].

To summarize, many attempts have been made to improve the accuracy of simulated l/l dispersion via a coupled CFD-PBE approach at the price of a higher computation time. One can choose between various methods that guarantee a high accuracy for the fluid dynamics and the information about the distribution. Drumm et al.

[iii] The work of Drumm et al. (2010) is recommended for the most compact review.

(2010) come to the conclusion that the most efficient method at the moment seems to be the quadrature method of moments (QMOM[iv]).

However, this or comparable methods are still limited in their applicability due to the still expensive computational costs. Therefore, often only 2 dimensional (2D) assumptions or symmetry assumptions for a 3D geometry are made or only systems at small scale are analyzed. This is in contradiction to the industrial need. Gaining insights into the overall equipment behavior for various operating parameters using species with various physical characteristics encounter in industrial practice. Unfortunately, because of the tremendous computational load, parameter fitting is hardly feasible at any scale analyzed with a coupled CFD-PBE approach [Drumm et al. 2010; Laakkonen et al. 2007].

Some recent attempts have been made to reduce these costs by the sectional quadrature method of moments (SQMOM), introduced by Attarakih et al. (2009). It has shown in first studies to be able to decrease the computational time by a factor of two compared to QMOM. It also has to be mentioned that this method can only be considered if the distribution itself is not of engineering interest [Drumm et al. 2010].

However, the assumption of an ideally mixed tank, which means that the dependency on space is neglected and therefore computational friendly, is a too restrictive simplification. For an appropriate description of the processes in a stirred tank, the spatial inhomogeneities have to be taken into account. Thus, it is reasonable to find a compromise between detailed modeling and savings in computational time.

A simplification can be achieved by solving the flow equation on a fine grid followed by solution of population balance equations on a very coarse grid [Singh et al. 2008]. Coarse means a zonal approach with down to only two zones, where one zone stands for the impeller region and one for the bulk region in the vessel. Some studies using this simplified approach with varying number of zones have been reported and were just recently reviewed by Srilatha et al. (2010b).

The challenges which are occurring with the intense inhomogeneities in stirred vessels are discussed in publication IV - Maaß et al. (2010). The solution of using a two-zone approach is the base for all other simulations carried out for this thesis. The results of the detailed analysis of the flow fields in the simulated vessels are given in publication VIII - Maaß et al. (2011c). These findings are also discussed in chapter 4 (see page 34).

3. Influence of reactor scale

The complex interaction of the various mechanisms involved in l/l mixing processes makes it very difficult to scale-up such processes. The experimental and simulation work on that field have been shortly reviewed by Srilatha et al. (2010a). They show that various authors have carried out investigations under completely different conditions. Therefore, the scale-up conclusions resulting from these studies differ from one another.

Srilatha et al. (2010a) carried out CFD studies to test the validity and rational behind different scale-up rules on the fluid dynamics. Furthermore, they carried out experiments for high dispersed phase fractions and reproduced them with PBE simulations. A network of zones model was developed for solving the PBE to predict the spatially varying drop size distributions in their system. Zones were constructed with the help of CFD modeling [Srilatha et al. 2010a]. Equal power input per unit volume and geometric similarity was found to result in almost similar drop size at various scales. The same result is reported in publication VI - Maaß et al. (2011b) for single stage impeller systems but this scale-up rule did not work for multiple impeller systems in slim reactors. The limitation occurring for the scale-up of liquid/liquid systems and a broad change in geometry factors is analyzed in detail in the publications IV - Maaß et al. (2010) and VI - Maaß et al. (2011b).

4. Parameter estimation and analysis

A general solution of equation (2) does not exist, or only for unreasonably simplistic assumptions. For practical relevant cases different numerical solutions are possible. The verification of the possibility of reaching different computational optima is discussed in Figure 5.

Simulated Sauter mean diameters for $\varphi_d = 0.1$ at three different stirrer speeds (400, 550 and 700 rpm) are plotted in comparison to experimental data. The experimental data are from the studies by Gäbler et al. (2006). The experiments were conducted in a baffled-glass vessel with a diameter T of 150 mm equipped with a Rushton turbine of D/T = 0.33. Toluene was used as dispersed phase and water as continuous phase. The

[iv] See McGraw (1997), who established that method in chemical engineering and Marchisio et al. (2003) for detailed analysis of that method.

coalescence was decreased but not completely hindered by increasing the pH to 13. At increasing pH values coalescence is lowered due to the increasing electro-chemical double layer around the droplets. At the organic droplet surface, negative hydroxide ions are adsorbed specifically and spontaneously [Marinova et al. 1996].

The simulation data are reproductions from Gäbler et al. (2006) and own studies using the equations from Coulaloglou and Tavlarides (1977). These model equations for the breakage and coalescence kernels have been given above. The used parameters for the associated simulations are listed in Table 1. The description of the simulations ((a) to (d)) follows the description in Figure 5.

Table 1 – Parameter listing for the simulation results presented in Figure 5.

simulation	$c_{1,br}$ [-]	$c_{2,br}$ [-]	$c_{1,coa}$ [-]	$c_{2,coa}$ [m^2]	$c_{1,br}$ / $c_{1,coa}$ [-]	scource
(a)	$6.14 \cdot 10^{-4}$	$5.70 \cdot 10^{-2}$	$1.50 \cdot 10^{-4}$	$2.56 \cdot 10^{12}$	$4.1 \cdot 10^{0}$	Gäbler et al. (2006)
(b)	$2.33 \cdot 10^{-3}$	$3.08 \cdot 10^{-2}$	$5.68 \cdot 10^{-4}$	$7.11 \cdot 10^{12}$	$4.1 \cdot 10^{0}$	this study
(c)	various, see Figure 5	$3.08 \cdot 10^{-2}$	$c_{1,br} \cdot 4.1^{-1}$	$7.11 \cdot 10^{12}$	$4.1 \cdot 10^{0}$	this study
(d)	$5.31 \cdot 10^{-3}$	$4.50 \cdot 10^{-2}$	$2.18 \cdot 10^{2}$	$8.53 \cdot 10^{14}$	$2.4 \cdot 10^{-5}$	this study

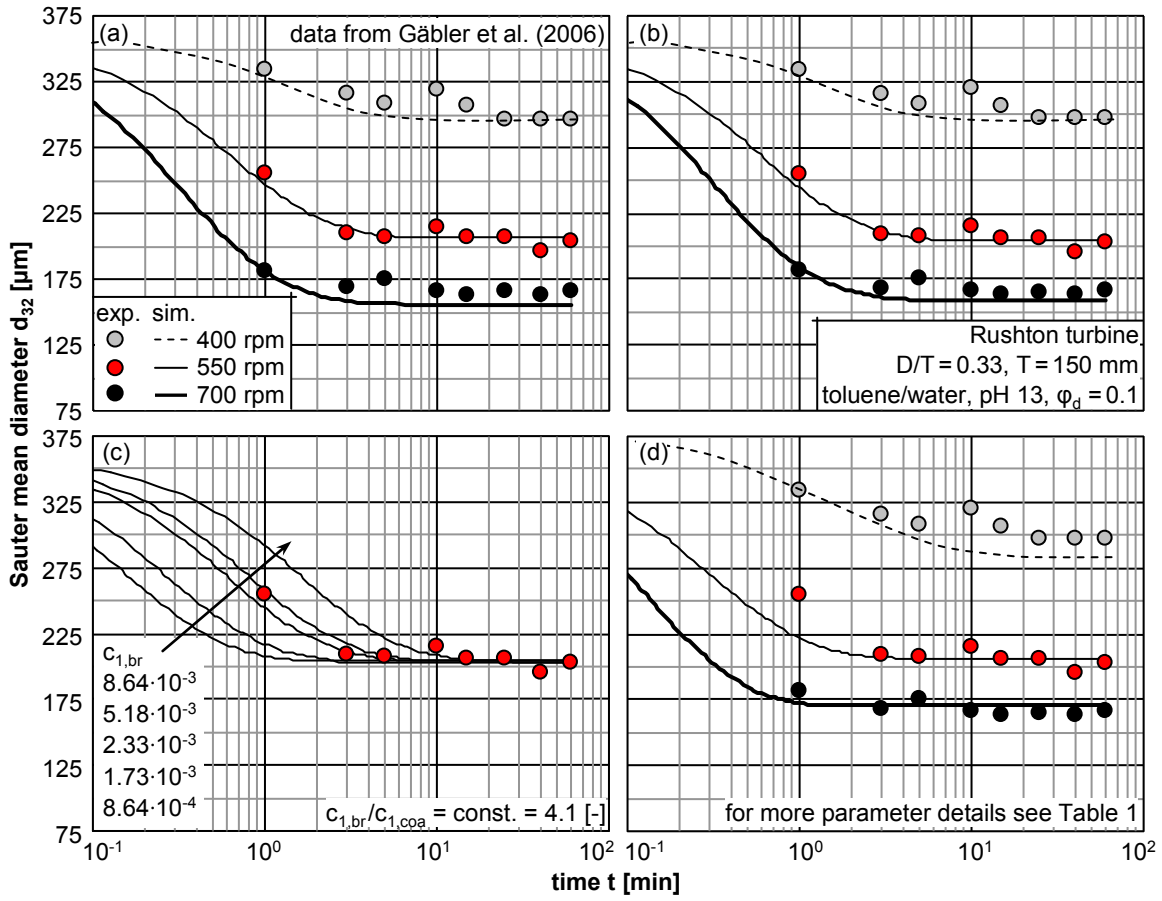

Figure 5 – Comparison of one set of experimental data (symbols) from Gäbler et al. (2006) and various simulations with different model parameter (lines): (a) - simulations using the parameters from Gäbler et al. (2006), (b) - simulations using own optimized parameters achieving the same accuracy as Gäbler et al. (2006), (c) - simulations varying $c_{1,br}$ for a constant ratio between $c_{1,br}/c_{1,coa}$ using the parameters from simulation (b) as initial values for the variation, (d) - simulations using a third parameter combination with strong differences compared to the used values in (a) and (b).

Four different simulation results are compared to one set of experimental data in Figure 5 (a) - (d). The simulations, which are all aiming to reflect the experimental measurements, were carried out using the complete model of Coulaloglou and Tavlarides (1977) for a well mixed assumption as in the work of Gäbler et al.

Simulation (a) is reproducing the results from Gäbler et al. (2006). The same prediction accuracy is achieved with a completely different set of parameters with simulation (b). It has to be mentioned, that both parameter sets are in the same order of magnitude (see absolute values in Table 1 for (a) and (b)).

Opposed are the results for the parameters of simulation (d). The coalescence parameters are two orders larger and $c_{1,br}$ is one order larger than in the two other parameter sets. The simulation results are in a comparable range of prediction quality although the results for the lower stirrer speed are less satisfying. This may be a widely familiar result of the fortuitous fall of the solution in different local optima.

The results shown in Figure 5 (c) may additionally uncover some correlations between the parameters. The ratio between $c_{1,br}$ and $c_{1,coa}$ was kept constant at the same value resulting from the parameter values by Gäbler et al. (2006). As it can be seen from Figure 5 (c) the strong variation of $c_{1,br}$ (by a factor of 10) is not influencing the steady state result of d_{32} if the ratio between $c_{1,br}$ and $c_{1,coa}$ was kept constant. This is in excellent agreement with the results by Ribeiro et al. (2011) who found the same dependency and reported a value of around 4.7 for the ratio between these parameters, which supports a physically interpretable interdependence between the kinetics of the breakage and coalescence processes [Ribeiro et al. 2011].

They explain that behavior by the fact that steady state batch conditions imply a virtually infinite residence time, which means that it is impossible to set a definite time scale. This is only true, if only the steady state results are interpreted as done by Ribeiro et al. (2011). The results here show a significant influence on the time to achieve the same steady state value for d_{32}. As larger the value of $c_{1,br}$ is as faster reaches the simulation the steady state. That shows for the selected example, that the breakage kinetic (employed by $c_{1,br}$) is of higher impact than the coalescence one.

This interconnection between the different parameters together with the influence of the broad variance of the parameter sets are shown in the following paragraphs.

Many parameters differing in several orders of magnitude are used in literature to adapt the models to experimental results. As mentioned above, breakage and coalescence terms influence each other and therefore different mathematical solutions are possible to display the same set of experiments.

A detailed parameter review was carried out in this study for the model of Coulaloglou and Tavlarides (1977). Only values used for the simulation of l/l system have been taken into account. The results are displayed in Table 2.

Table 2 – Parameter listing from literature for the empirical constants in the drop breakage and drop coalescence rate function of Coulaloglou and Tavlarides (1977).

	$c_{1,br}$ [10^{-1}]	$c_{2,br}$ [10^{-1}]	$c_{1,coa}$ [10^{-1}]	$c_{2,coa}$ [m^2]
Coulaloglou and Tavlarides 1977	3.360	1.06	0.0022	$2.28 \cdot 10^{13}$
Ross et al. 1978	0.049	0.8	0.0022	$3.00 \cdot 10^{12}$
Hsia and Tavlarides 1983	0.103	0.635	0.0045	$1.89 \cdot 10^{13}$
Bapat et al. 1983	0.049	0.551	0.0022	$2.00 \cdot 10^{9}$
Bapat and Tavlarides 1985	0.049	0.8	0.019	$2.00 \cdot 10^{12}$
Ribeiro et al. 1995	0.049	0.558	0.017	$4.74 \cdot 10^{12}$
Ribeiro et al. 2011	0.021	0.318	0.0045	$6.41 \cdot 10^{12}$
Ribeiro et al. 2011	0.047	0.318	0.01	$5.45 \cdot 10^{12}$
Chen et al. 1998	0.06	0.011	-	-
Gäbler et al. 2006	0.006	0.57	0.0015	$2.56 \cdot 10^{12}$
Maaß et al. 2010 (1-Zone)	0.034	0.756	2.91	$3.58 \cdot 10^{17}$
Maaß et al. 2010 (2-Zone)	0.14	3.33	2.91	$3.58 \cdot 10^{17}$
Maaß et al. 2011b	0.39	3.33	2.91	$4.64 \cdot 10^{18}$
Maaß et al. 2011d	0.119	2.75	-	-
Azizi and Al Taweel 2010	10.0	41.0	1.0	$1.00 \cdot 10^{9}$
Azizi and Al Taweel 2011	8.6	41.0	0.4	$1.00 \cdot 10^{10}$
this study - simulation (b	0.023	0.308	0.0057	$7.11 \cdot 10^{12}$
this study - simulation (d	0.053	0.45	2180.0	$8.53 \cdot 10^{14}$
average value	1.29	5.47	137.0	$3.35 \cdot 10^{17}$
variance $V(c_i)$	0.91	16.8	29600.0	$1.33 \cdot 10^{36}$
minimum value	0.006	0.011	0.0022	$1.00 \cdot 10^{9}$
maximum value	10.0	41.0	2180.0	$4.64 \cdot 10^{18}$

The values scatter dramatically, only the variance of the values for $c_{1,br}$ is smaller as their average value. This results are disturbing because only the influence of the coalescence parameter $c_{2,coa}$ is known as almost uninfluencial on the drop size compared to the other parameters.

The interconnection between the different parameters is discussed in Figure 6. All literature values are plotted as a function of the breakage parameter $c_{1,br}$. Although the single values scatter a lot, some tendencies can be postulated.

The values of the breakage parameter used in literature show a vague tendency to a linear correlation ($c_{2,br} = 3 \cdot c_{1,br}$). That means with increasing breakage kinetic (equal to decreasing breakage times in this model), employed via $c_{1,br}$, e breakage probability is decreasing (employed as $\exp(-c_{2,br})$ - see equation (5)). This means, that the values used in literature for the breakage parameter partly balance each other. A fast kinetic is damped by a low probability and vice versa.

The same is true if the tendencies between $c_{1,br}$ and the coalescence parameters is analyzed. The increase of the breakage kinetic leads to an increase of the coalescence kinetic. Although the ratio between both parameters is scattering a lot, the tendency between them can be estimated by a linear correlation too ($c_{1,coa} = 0.7 \cdot c_{1,br}$).

An increase in $c_{2,coa}$ leads to a decrease in the coalescence efficiency (see equation (9)) the increase of $c_{1,br}$ leads to a decrease of $c_{2,coa}$. Again the opposed phenomena of drop breakage and drop coalescence partly balance each other. Of course these tendencies are qualitative. The proposed correlations are not suitable to predict single parameter values as a function of the other one. However, the results support the assumption, that several local optima are possible for the same application. That is the major reason, why it is hard to analyze the pure physics behind the model approaches. The mathematical background needs always be reflected.

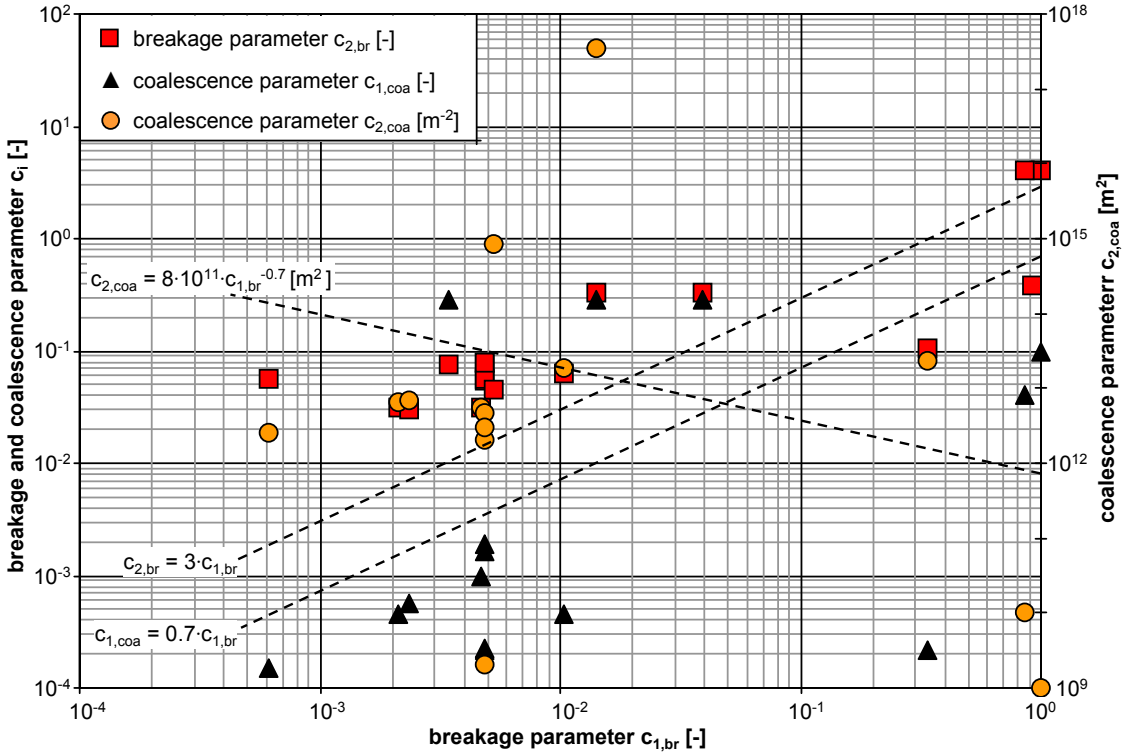

Figure 6 – Dependency of literature values of the parameters $c_{2,br}$, $c_{1,coa}$ and $c_{2,coa}$ from the model of Coulaloglou and Tavlarides (1977) on the breakage parameter $c_{1,br}$.

A further aspect, the strong influence of the fluid dynamics on the absolute values of the parameters can be revealed by analyzing the parameter from Azizi and Al Taweel (2010) & (2011) in Table 2. These researchers have reported extreme values for $c_{1,br}$, $c_{2,br}$ and $c_{2,coa}$. The values for the breakage parameters are the largest as the coalescence parameter is the smallest value found in literature.

The used experimental set-up is a working section of several static mixers which alternate with the same number of rest zones. Each of these zones is modeled as a number of compartments with homogenous energy dissipation within these compartments. Note that the number of compartments used for the description of the

breakage and coalescence dominated zone is not presented by Azizi and Al Taweel (2010) & (2011). However, the development of the used energy dissipation rates in the different zones is presented by Azizi and Al Taweel (2011). The value ranges from $1 \cdot 10^{-1}$ to $1.4 \cdot 10^{4}$ m^2/s^3. The use of these local values implements a more detailed physical description of the process in the model. It is in contradiction to the commonly used well mixed simplification with only one average value for ε.

This postulation is in accordance with own achieved values. Two sets of parameters are reported in publication IV - Maaß et al. (2010). One was estimated for the well mixed condition, the other was estimated after a separation of the system into a stirrer and a bulk region, following the multi zone approach by Alopaeus et al. (1999). The differences between experimental data and PBE simulations have been minimized for both approaches, the values for the 2-zone model are four times higher than the values for the 1-zone model (see also the parameter values of line 11 and 12 in Table 2, as they present the parameter values from publication IV - Maaß et al. (2010)).

VI. Concluding remarks on PBE

Population balances have become a powerful tool in chemical engineering over the last decades. Developing computer technologies have facilitated robust numerical solution methods which can be coupled with CFD to base the calculations on precise description of the fluid dynamics.

Nevertheless, the increasing number of contradicting models, reported values of model parameters and the lack of evaluated experimental data from the broad variety of industrial applications limit the use of PBE in industrial practice.

To avoid a local optimum, simultaneous fitting of the different parameters, the use of different initial vales and a broad variation of the physical system are necessary but still no guarantee for an accurate description. Transient measurements should be given a high weight in the fitting process in order to identify especially the breakage parameters properly. Still the fitting of PBE parameters is a major challenge

Furthermore, the reported missing of objective solutions of the PBE interferes with the precise determination of coalescence and breakage models. However, this is the key challenge to be able to formulate trustful predictive PBE models [Raikar et al. 2009]. The proposed procedure of this thesis, analyzing drop breakage separate from drop coalescence in single drop and drop swarm experiments, will provide necessary information to evaluate and derive physical based breakage models.

Furthermore, the detailed flow analysis which will be correlated with the simulations will provide a secure base to take the fluid dynamics in a meaningful matter into account.

3. Drop size and single drop breakage measurements

The aim of this chapter is to introduce the experimental measurement techniques and procedural methods used for this thesis. As every publication contains a description of the used methods on a detailed level to provide reproduction opportunities for other researchers, it is done briefly here to avoid unnecessary repeating. The focus is to classify the used methods in the broad range of possible procedures used in literature.

The first part of the chapter deals with the analysis methods usable for drop swarm experiments. The second part describes the measurement techniques and procedures employed for the single drop analysis. Image analysis is used as fundamental tool to collect in the single drop and drop swarm experiments. Therefore, the third part of the paper describes the used image analysis procedures.

I. Overview of drop size measurement techniques

Drop size analysis is a broad area that covers a wide range of techniques. Barth and Flippen (1995) have given a review that includes all techniques which were available and most of them are still in use. The difficulty in applying such methods to stirred vessels is connected to the turbulence. It is not very well characterized since it is not only inhomogeneous throughout the vessel, but it is highly anisotropic consisting of high shear regions on the surface of the impeller [Martínez-Bazán et al. 1999]. Therefore, the possibility for local analysis is needed.

Today many different techniques for sizing transient drop behavior in such vessels are available. Often only samples are withdrawn over time [Bae and Tavlarides 1989; Bürkholz and Polke 1984; Desnoyer et al. 2003; Singh et al. 2008; Srilatha et al. 2010a], which are later diluted or stabilized, prior to their measurements. These sampling techniques neither guarantee that the drop sizes are frozen, nor that they are preserved during the sampling and have been criticized by many authors [Martínez-Bazán et al. 1999; Niknafs et al. 2011; Pacek et al. 1994]. Especially for technical applications with fast reactions such as polymerizations these measurements are not suitable. Even for sampling times less than one second, the drastic change in the flow condition during sampling results in significant measurement errors.

It is possible to use the none-intrusive measurement method of Phase Doppler Particle Analyzer locally which is presented in detail by Zhou and Kresta (1998). On one hand the data acquisition speed allows online investigations. On the other hand this technique needs total transparency of the liquid/liquid system. So it is limited to an industrial irrelevant dispersed phase fraction of less than one percent [Brown et al. 2004; Wille et al. 2001; Zhou and Kresta 1998]. With this limitation it is not suitable for this study.

The analysis of the effective l/l interfacial area using a chemical method was first applied by Nanda and Shama (1966) and has also spread in the chemical engineering community. The interfacial area of the system is obtained by quantifying the amount of a reactant A from the organic dispersed phase that is extracted to the aqueous phase, where it reacts very fast with reactant B [Quadros and Baptista 2003]. As this techniques uses mass transfer for the quantification of the interfacial area and therewith the d_{32} it is limited to such physical systems. Furthermore, the composition of the organic and aqueous phases has to be carefully chosen. An updated introduction into the strengths and limitations of this method is given by Quadros and Baptista (2003). Due to the named limitations, this technique is not considered for this study.

Niknafs et al. (2011) have presented a new reflectance technique to measure the drop size evolution in real time. They assume that the reflectance behavior can be directly correlated with the drop size. A chroma-meter is used to measure the reflectance of emulsions. A huge series of calibration measurements were designed and performed. As a small change in the used materials can have a significant impact on the optical properties of an emulsion, it is more than questionable to use such a technique in real industrial practice.

In the following work the focus is on inline measurement techniques, meaning the drop size distributions are measured directly inside the vessel as a function of position. These can be divided into four main types (see Figure 7):

1. Sound techniques working with ultrasound,
2. Laser techniques,
3. Coulter counter and
4. Photo based methods working with digital images and image recognition.

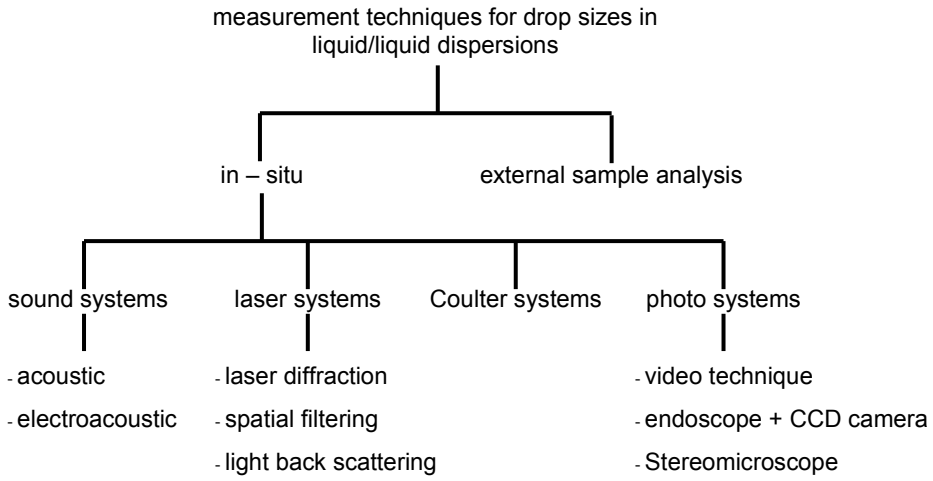

Figure 7 – Overview of measurement techniques for drop size distributions in liquid/liquid systems.

1. Sound systems

Many attempts to determine particle sizes in industrial application by means of ultrasound have been reported in the past. An overview and the theoretical background is given in Riebel and Löffler (1989). The method can be subdivided into acoustic and electroacoustic spectroscopy analysis. Dukin and Goetz (2001) are describing both very detailed. They summarize that acoustic spectroscopy deals only with the acoustic properties of the dispersion such as sound speed and attenuation while electro-acoustic spectroscopy is related to the coupling between the acoustic and electric properties of the system. This measurement technique is limited to concentrations of $\varphi_d \leq 0.1$ [Riebel and Löffler 1989]. Other authors have reported limitations at five percent [Cents et al. 2004]. However, the main drawbacks of these techniques are the need for determination, prior to performing any experiment a number of material properties which are often difficult to measure. Furthermore, the lack of a predictive model for sound behavior in concentrated systems that can be used to determine drop sizes makes that technique not suitable for industry relevant applications [Niknafs et al. 2011].

2. Laser systems

The laser methods should be subdivided into three main groups based on their specific operation principle (see Figure 7). The first one is the application of Fraunhofer diffraction [Simmons et al. 2000]. The beam of a low-power laser is expanded. While drops are passing through the beam they scatter light which is detected by concentric annular detectors placed at the focal point of a Fourier transform lens. So each detector picks up light scattered at a specific angle and independent of the position of the drops. Some problems occur by transforming the energy intensity distribution into a DSD.

The Inline Particle Size Probe IPP 30 [Petrak 2002] allows the measurement of the transient drop size distributions online. This technique is a method of determining the velocity and the size of the investigated particles simultaneously. It uses the spatial filtering velocimetry and additionally the fibre-optical spot scanning. The basic principle of this technique is to observe the shadow of the particles moving through a small channel. This constriction of the flow influences the flow field and thereby the DSD. First results just recently published by Hermann et al. (2011) showed poor results of this probe obtained in l/l systems.

The last and most common method is the "simple" analysis of light back scattering. For example the FBR-Sensor (forward-backward-ratio sensor) uses the analysis of the spatial intensity pattern of light scattered into the forward and backward direction. This means spherical particles whose radius is below approximately one-tenth of the wavelength of the incident radiation can be measured [van de Hulst 1981]. With increasing diameter an increased asymmetry between forward and backward scattering can be observed due to the pronounced diffraction lobe. Depending on the sensor configuration and the type of light source, a size range from 50 nm to 200 µm can be detected [Sachweh et al. 1998].

More precisely are probes working with rotating laser beams, which are focused through a lens to produce a very small focal point of high intensity. The lens rotates at a known velocity to produce a circular scanning

beam. When the beam intercepts a drop, the laser light is backscattered to be recorded by a detector mounted behind the lens. As both the scanning velocity and the time delta between start and end of backscatter for a single particle are known, a characteristic length l_{ch} also called chord length can be determined. The probability of the beam hitting any part of the projected area of the drop is equal, so the resulting chord length distribution (CLD) needs to be transformed into a drop size distribution [Simmons et al. 2000].

For a spherical drop l_{ch} is generally shorter than d_p (see Figure 8) and so the chord length distribution is wider then the originally one. While the laser beam crosses each chord randomly, the number of times a given chord length is measured takes the form of a probability density function. The interpretation of CLD's has been discussed since more than a decade by many authors [Hu et al. 2006; Li and Wilkinson 2005; Worlitschek et al. 2005; Yu et al. 2008]. Stochastic models have been developed and published for transformation of CLD into DSD under the assumption of perfect spherical particles. For a broader overview especially the work of Hu et al. (2006) is recommended.

The most widely used laser probe using back scattering is the focus beam reflectance measurement (FBRM). A large community of users successfully applied FBRM technology for monitoring, fault detection and quality control of dynamic solid/liquid or gas/liquid processes. Greaves et al. (2008) applied it to emulsions and ice and clathrate hydrate formation processes. It was found that while the FBRM can successfully identify system changes, certain inaccuracies exist in the chord length distributions. Particularly, the FBRM was found to undersize droplets in an emulsion.

Cull et al. (2002) and Lovick et al. (2005) employed a 3D optical reflectance measurement (3D-ORM) technique, similar in operation to the FBRM and the 2D optical reflectance measurement (2D-ORM) in a liquid/liquid biocatalytic reactor successfully.

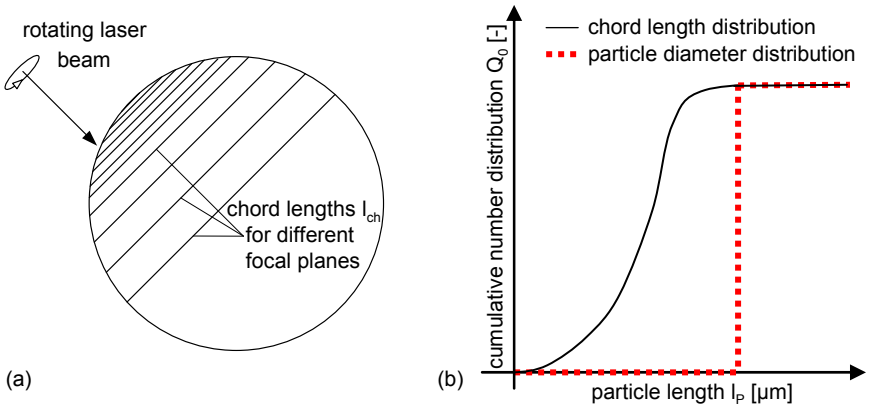

Figure 8 – Demonstration of chord length possibilities on a two-dimensional projection of a spherical particle (a) and comparison of a cumulative chord length and a cumulative particle size distribution resulting from mono disperse particles (b).

3. Coulter Counter

The Coulter principal can be used with an intrusive probe. This method of sizing and counting particles is based on measurable changes in electrical resistance produced by nonconductive particles dispersed in an electrolyte; therefore, the conductance has to be known precisely. This is assured in prepared solutions in laboratory so the method was used as external sampling [Wachtel and Lamer 1962]. Nowadays, the electrolyte concentration can be measured precisely online in almost every application. So it is possible to use the Coulter method as an intrusive probe. The working principle itself sets some boundaries for its use in industrial applications. The dispersion has to pass through an orifice with a certain diameter. This limits the maximum size of a measurable drop diameter. The major disadvantage of this technique is the limit to its measurable concentrations of $\varphi_d < 0.01$ [Mima and Kitamori 1966].

4. Photo systems working with image recognition

Three different methods are named in Figure 7 associated with photo optical systems: firstly, the use of a microscope combined with a video camera [Alban et al. 2004; Pacek and Nienow 1995; Ribeiro et al. 2004; Sæther 2001]. This technique combines the magnification power of a microscope with the image acquisition capability of a video camera. The work of Pacek and Nienow (1995) is described exemplary here, as it was

the foundation for many others. Pacek and Nienow (1995) used a conventional 700 line high quality video camera that took images through a stereo microscope from outside the vessel near the wall (8 mm at most) or inside the vessel through a light tube. Both methods are intrusive since lighting is provided always from behind the focal plane by a strobe light guided through a thick fibre optic tube. The light was edited to be synchronous to the camera. Pictures were taken at a frequency of 50 frames per second (fps) and scanned for non-overlapping drops by recognition software. This requires human intervention for correction and to categorize drops pictured inside of larger drops. The fast and continuous data acquisition and the flexible positioning of the light tube are of advantage. The intrusion of this tube and the fibre optic tube as well as the outdated hardware is of disadvantage. The technique was expanded to a digital video camera and improved image recognition.

Secondly, the use of a PVM probe (particle video microscope) as presented by O'Rourke and MacLoughlin (2005) is named in Figure 7. Light from six independent laser sources is focused using a hexagonal array of lenses to provide a fixed region of illumination within an area of 2.0 mm². A micrometer adjustment of the probe optics allows the positioning of this area relative to the probe window. Particles passing through the illuminated region scatter the incident light diffusely in all directions. A lenses system inside the probe collects light backscattered toward the probe window and relays it to a CCD array [O'Rourke and MacLoughlin 2005].

Thirdly, with the endoscope technique images are taken intrusively from inside the vessel by placing an endoscope in front of a CCD camera as a microscope lens [Ritter and Kraume 2000] is named in Figure 7. A market available example is the EnviroCamTM probe [Junker et al. 2007]. This system is based on a digital, high-speed, high resolution modular camera system, attached to a stainless steel shroud. An LED light source is integral with the shroud and the images are analyzed with commercial image analysis software and standard statistical methods.

5. Own results on drop size measurement techniques and conclusion.

Based on the literature survey, the laser and photo optical systems were the most promising techniques available. Both provide not only a mean value for the drop size but a complete distribution. Unquestioned the photo optical systems using image analysis are the standard in literature for precise measurements [Greaves et al. 2008; Hu et al. 2006; Pacek et al. 1994]. But as the image analysis is carried out manually this procedure is extremely time consuming and therefore not useable for online observation or control.

Therefore, laser probes seem to be an interesting alternative for online measurements of drop sizes. Three of them (FBRM, 2D-ORM and a fiber optical FBR-sensor) were tested and their results are compared with trustful image analysis results from an in-situ endoscope. The results achieved for a concentrated toluene/water system ($\varphi_d = 0.2$) are discussed and presented in publication V - Maaß et al. (2011a). It is clearly shown, that the measurement of drop sizes in liquid/liquid systems is a major challenge for all tested laser probes and none provides exact results for the tested system. Differencing the free laser probes, the worst results were observed from the FBR-sensor. It was not applicable at all to the investigated system.

The influence of ε on the DSD showed reasonable results for the FBRM and the 2D-ORM. The same proportionality of d_{32} over ε for the image analysis results and both probes were observed. They both gave unreasonable results over time for a constant stirrer speed and are thereby no online probes for such evolving liquid/liquid dispersions. While all three laser probes are based on back scattering, the general question of the usability of this principle for measuring drop size distributions in liquid/liquid systems is asked. The exterior smooth surface of droplets in such systems is leading to strong errors in the measurement of the size of the drops. That leads to widely divergent results. This effect of the kind of the surface was analyzed in detail by adding micro-particles to the system. The produced synthetic roughness of the drop surface is leading to much more reasonable results of the FBRM-probe. Still the absolute values were much smaller than the image analysis results. This is in absolute agreement with the results of Boxall et al. (2010). They analyzed water drop sizes in crude oil emulsions with a PVM and an FBRM. The DSD was shown to be dramatically undersized by the FBRM probe, even taking into account that it measures chord lengths rather than actual drop diameters.

Resulting from own studies and literature reports, the measurement of the drop size distributions in the drop swarm experiments was carried out with the trustful endoscope technique in combination with image analysis (see Figure 9 for different example images). Ritter and Kraume (2000) suggested a minimum number of 200 particles building one sample for one drop size distribution as a reliable number for statistical demands. This number was always excelled by a factor of two for all investigated cases.

Figure 9 shows clearly the broad applicability of the endoscope measurement technique for different particulate systems. It has to be mentioned that different endoscopes with different lenses which created different magnifications were used to take the different example images. The lens with the highest magnification was always used for the n-butyl chloride/water system. The smallest measurable drop diameter with this lens is around 10 µm. The largest screen size was achieved with the lens which was used for the presented air/water system (see Figure 9). The diameter of the image was 8000 µm.

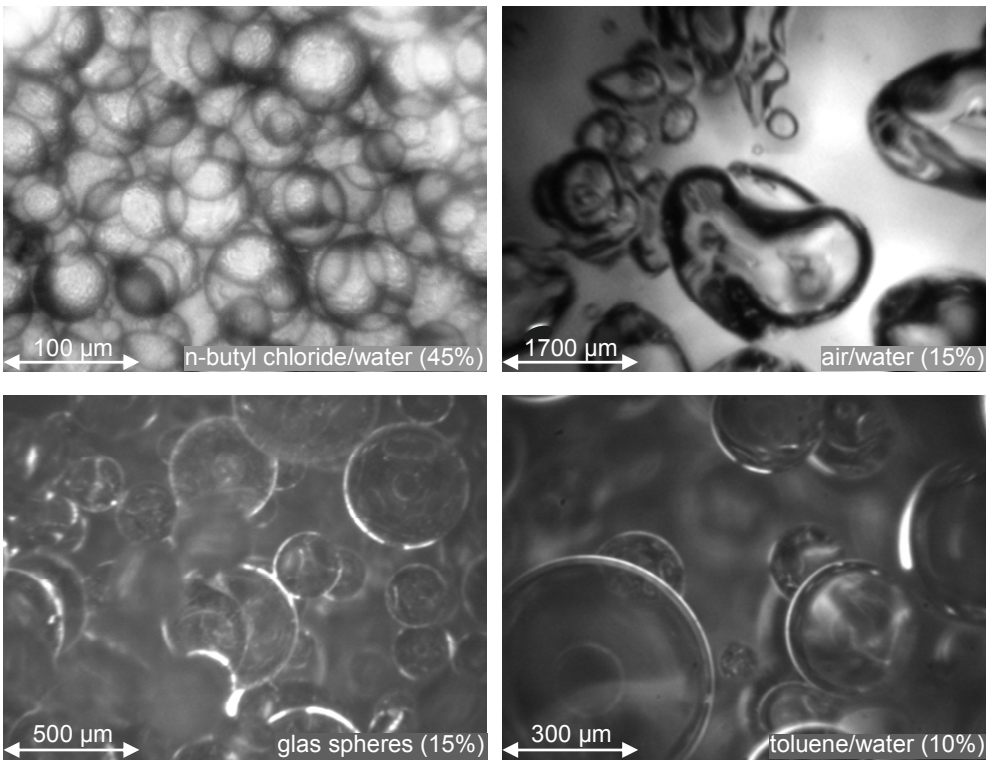

Figure 9 – Example image gallery: Representing samples taken with the endoscope technique using different lenses according to the expected particle size for different systems.

II. Single drop breakage measurements

The fundamental phenomena which are responsible for the occurring drop size distribution in l/l systems are taking place on a single drop level. There, drop breakage, coalescence and mass transfer are taking place. These phenomena are strongly influenced by the fluid dynamics occurring in the used industrial application. Although droplet swarms rather than single droplets occur in such apparatuses, the understanding of fluid dynamic behavior of single fluid particles is the basis for detailed process understanding and prediction. This is the major reason why single drop experiments have been carried out now for decades to analyze those phenomena precisely.

The first systematic analysis using single drop experiment reported are all dedicated to mass transfer in liquid/liquid extraction processes [Whewell et al. 1975]. The number of systematic studies increased over the years. Now also the other parameters like breakage [Cabassud et al. 1990; Gourdon et al. 1991] and coalescence [Henschke et al. 2002] are investigated systematically on the base of single drop experiments. Furthermore, the complete description of such systems with numerical models describing 3D processes became possible [Wegener et al. 2009]. This can not be the case for the drop swarm as the computational demands would be too expensive.

Experimental analysis of drop swarm experiments can also be very expensive due to the price and necessary amount of the used organics or the increased safety requirements handling toxic or flammable species [Bart et al. 2006].

The advantage of single drop experiments for systematic drop breakage analysis is the complete avoidance of coalescence. The influence of operating parameters and physical characteristics can be directly correlated to the drop breakage processes. The measurements are simple, reliable and automatic. Although thousands of

single drops were investigated for statistical reliability they consume only little product and reduce the costs in comparison to drop swarm experiments. The used set-up will be explained in the following paragraph.

A single blade representative of a section of a Rushton turbine is fixed in a rectangular channel (see Figure 10 - 3). This set-up reflects the flow field in the impeller region, where turbulent pressure fluctuation, shear flow in a thin layer at the impeller blade and the two-dimensional elongational flow field in front of the rotating blade are the major drop breakage reasons. All these phenomena were assumed to occur simultaneously (Kumar et al. 1998). The relative velocities between blade and liquid flow and the energy dissipation rates are varied by the volume flow of the continuous phase. A more detailed description of the breakage cell can be found in publication III - Maaß et al. (2009) and VII - Maaß and Kraume (2011).

The verification of the flow field using such a simplified approach as a model for a highly anisotropic agitated vessel and the description for the coordinate transformation of the rotating stirrer blade in a vessel into a fixed stirrer blade in the breakage channel is given in publication III - Maaß et al. (2009).

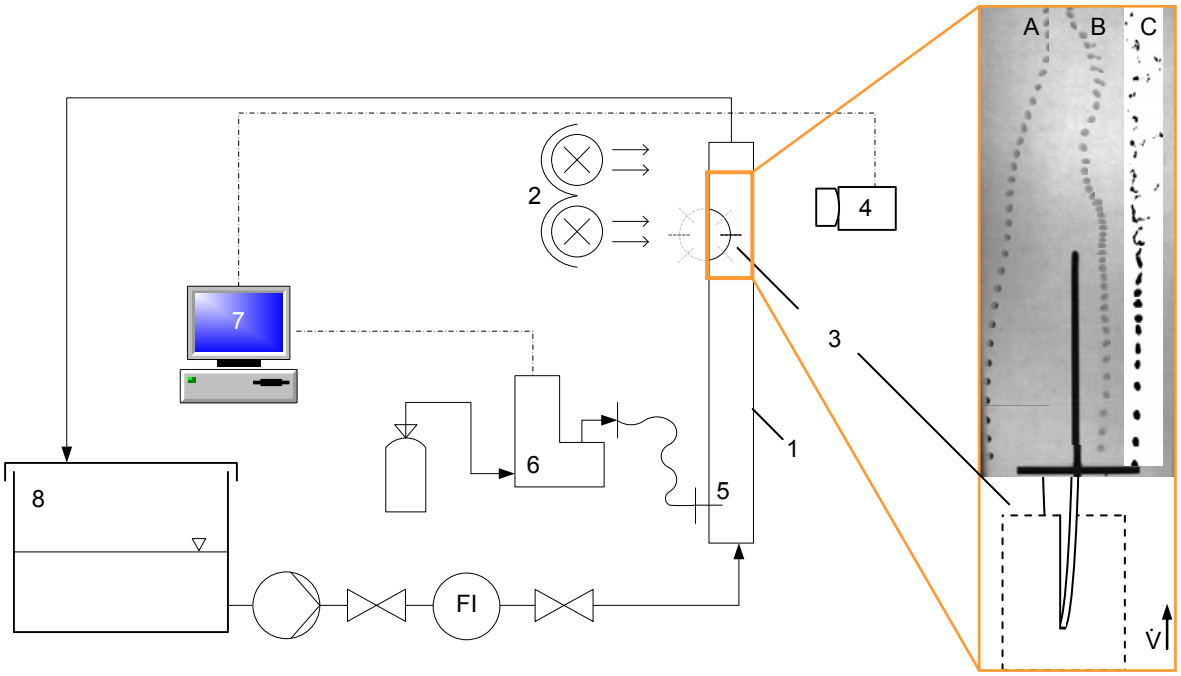

Figure 10 – Experimental set-up for single drop experiments: (1) breakage cell, (2) illumination, (3) section of a Rushton turbine, (4) highspeed camera; (5) nozzle for drop formation, (6) precision dosing pump, (7) computer control, (8) water storage tank - all left part of the figure - and three exemplary toluene drops (drop A and B – original images, drop C - after image processing) - all right part of the figure.

Pictures of the single drop breakage event and the resulting daughter drops are taken with a high-speed camera (Figure 10 - 4) using a frame rate of 822 fps. Automated image recognition delivers results for the breakage time, number and size of daughter drops. For constant operation parameters and physical characteristics at least 750 single drops have been investigated for statistically firm conclusions.

Examples of the high-speed images are shown at the right side of Figure 10. Three drops (A, B, C) and their paths through the impeller region are compared with each other. The drop swarm and the single drop experiments are using image analysis as fundamental tool for the data collection.

III. Image analysis

This section will briefly discuss the used methods and compare it with standards from literature. Various commercial software packages are now available that analyze images automatically and measure the size of the droplets. The qualities of the results from these packages differ and depend on a number of variables, including the quality of the initial images. Custom software can be written to incorporate previously validated image processing algorithms. Software is also available that allows the manual selection of droplets on images which are than measured by the computer. This process is extremely time consuming but generally considered essential for producing accurate results as well as checking the performance of automatic software [Brown et al. 2004].

1. Drop swarm applications

Considerable research attention is focused on the development of automated drop measurement on digitized images as photo optical analysis of DSD is seen as the most trustful method. But the process of manual counting is not only time consuming but it also introduces human bias. Boxall et al. (2010) showed the influence of human bias and variance on manually counted drop size distributions and additionally reported about the repeatability of drop measuring experiments. The repeatability and reproducibility of the measurements were found to be reasonable with an average difference of 8.4% of the mean diameter between the experiment repeats and an average difference of 5.1% between two different analyzers. Automated quantification would avoid bias by different observers.

The self chosen limitation in the dispersed phase fraction to values significantly lower than 5 % enabled several groups to develop automated drop detection software as at these concentrations only little overlapping of the drops occur [Khalil et al. 2010; Scherze et al. 2005]. Mickler et al. (2011) were able to increase this limitation of φ_d to 15 %, by using distance transformation and watershed segmentation algorithms to detect the drops. More promising are the works of Alban et al. (2004) and Brás et al. (2009). Both groups work with high concentrated dispersions in stirred vessels (φ_d up to 0.4) and developed their own software to evaluate such data. Both groups are using MATLAB® for their image recognition. Up to now, no commercial software for the analysis of highly concentrated dispersions is available but is needed for industrial relevant applications [Brás et al. 2009].

Based on these first promising results an own image analysis algorithm was implemented in MATLAB® to count and measure particles in multiphase systems fully automatic. The details of the analysis steps are described in publication XI - Maaß et al. (2011f). It has to be noticed that the software is limited in its detection to spherical particles

In order to ensure robust and accurate drop detection, a series of images is first pre-filtered to remove irrelevant and misleading image information. This is done with image subtraction using the integrated sequence as difference image (compare image (a) and (b) in Figure 11). The noise in the pictures is reduced by the self quotient image method [Gopalan and Jacobs 2010]. These operation norms the intensity of every local pixel based on the local environment. It is carried out by division of the processed image (image (b) in Figure 11) by a smoothed version of itself (see Figure 11 (c), smoothed image after convolution with a Gaussian matrix).

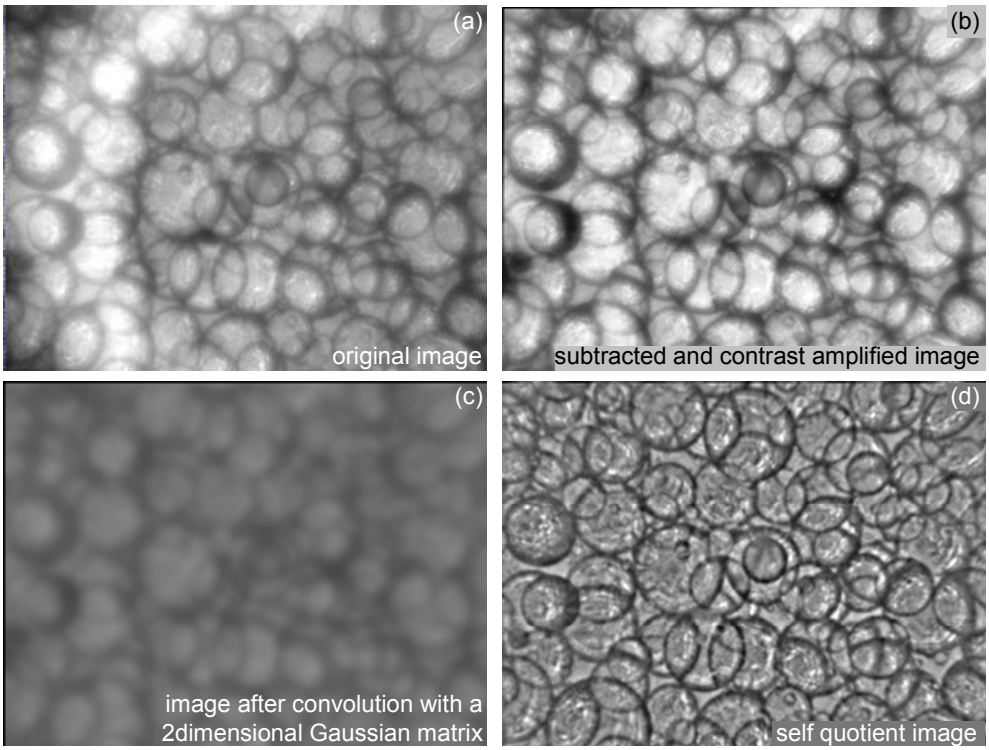

Figure 11 – Image processing steps to remove redundant information during and increase the ability to detect possible drop circles.

Figure 11 (d) shows the self quotient image which emphasizes the changes of the intensities from the original image. This results into an independency on any illumination or process variation.

Then the drop recognition follows. It consists of three steps: Pattern recognition by correlation of pre-filtered gradients with search samples, the pre-selection of plausible circle coordinates and the classification of each of those circles by an exact edge examination. The software employs a normalized cross correlation procedure [Lewis 1995] algorithm to evaluate possible drop matches (see publication XI - Maaß et al. (2011f) for more technical details and results).

The program has reached hit rates of 95 % with an error quotient under 1% and a detection of 250 particles per minute for visually simple images. For more difficult images, rates of 40% detection at a rate of 10 drops per minute are achievable.

In each of the processes, parameter optimization is necessary to save computing time and improve error quotient and hit rate. This is achieved by marking a few drops manually and letting the software extract their optical characteristics. These include the steepness and regularity of the particle border as general optical behavior. These values vary strongly from system to system but in one system solely depending on the drop radius.

The automatic drop recognition is most effective with high contrast backlight images with a high drop density. The high contrast ensures a good hit rate and low error quotient while the density ensures that the computation renders more drops recognized per minute. The software was proven to be very robust and able to compete with the human eye in complex images. The computation time is nearly proportional to the pixel-quantity being processed and is depending on the images twice to fifty times faster than manual counting. The user is able to define thresholds for the error quotient and the hit rate to force the program into further parameter optimization.

2. Single drop applications

The analysis of highspeed images from single drop experiments shows the same advantages as the drop size analysis in lean dispersions. As almost no overlapping occurs, the single individuals can easily be tracked within an image sequence (see Figure 10 - example drops).

To ensure optimum image analysis results the provided illumination needs to be free of fluctuations. The highspeed images need to be equally illuminated to reduce analysis errors during the following image recognition steps:

1. Image subtraction with a reference image.
2. Automated threshold determination based on the average value of the image.
3. Generation of binary images using the threshold in the subtracted image.
4. Object detection (number of objects, area and x, y - position of mass center of each particle on the image).

These general steps are always used to extract necessary information from every image sequence. The example drop C in Figure 10 shows the output of the binary images.

The method is described in publication I - Maaß et al. (2007). A commercial software was used - ImageProPlus 5.1®. This software with the described method has been successfully applied to several other applications [Gaitzsch et al. 2011; Grünig et al. 2011; Wegener et al. 2007]. However, the full automation of this procedure was achieved lately by using Matlab® for the automated threshold determination for every single sequences, as this was done manually in the past, using ImageProPlus®.

4. Flow field analysis

The fluid dynamics and therewith the energy dissipation rates of the used application strongly influence the drop sizes. Detailed analysis of the velocity field in single phase systems in the used apparatus was carried out using computational fluid dynamics to gain deeper insights.

I. Analysis of the flow field in the single drop breakage cell

The flow field of an agitated vessel equipped with a Rushton turbine belongs to the most studied fluid dynamics in the chemical engineering community [Baldi and Yianneskis 2004; Delafosse et al. 2009; Escudie et al. 2004; Höfken et al. 1996; Jahoda et al. 2007; Jaworski et al. 2000; Kukukova et al. 2005; Montante and Magelli 2004; Schäfer 2001; Stoots and Calabrese 1995; Zadghaffari et al. 2010]. These works have been carried out experimentally using laser Doppler anemometry and particle image velocimetry or numerically using CFD. A broad evaluation of own achieved data with results from literature is easy for Rushton turbine applications. Therefore, the single breakage cell was installed using a section of a Rushton turbine. The occurring flow conditions in this newly developed set-up have been intensively studied using CFD. The results and the technical details of the simulations are given in publication III - Maaß et al. (2009).

Exemplarily the velocity fields in two different section planes are shown in Figure 12. Image (a) is an example photo from the single drop breakage cell (front view). The perspective of the observer is the same in image (a) and (b). The presented section plane of the flow field in image (b) is shown as a black line in image (c). The perspective of the observer has rotated for 90° in image (c). The presented section plane of the flow field in image (c) is shown as a black line in image (b).

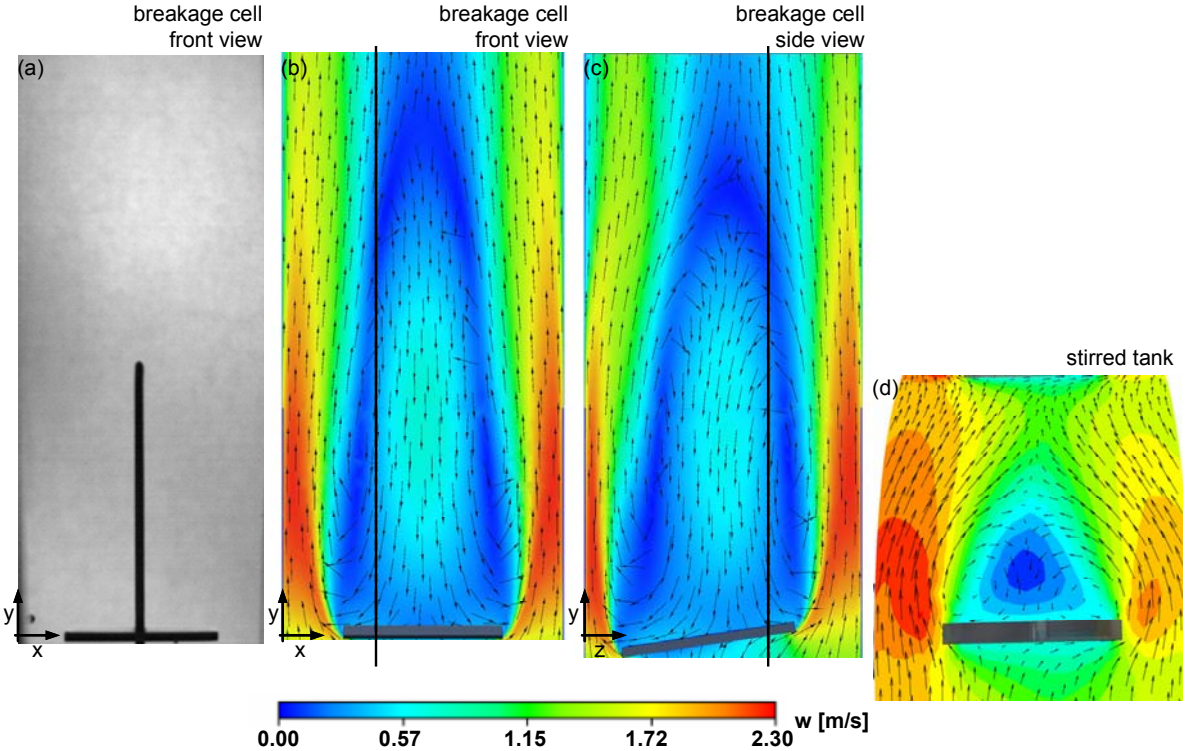

Figure 12 – Example image from the experimental single drop breakage cell and two section planes of the calculated flow field analyzed from two different perspectives (a - c). The flow field in the single drop breakage cell is further compared with the calculated flow field in an agitated vessel (d).

For validation purposes the flow pattern in the breakage cell was compared to the flow field in a stirred tank. Therefore, a 360 degree steady state simulation was carried out with a Rushton turbine installed in a baffled

tank (see image (d) in Figure 12). The CFD simulations were firstly validated with the experimental work of Schäfer (2001) and then used to compare the 3D flow field in an agitated vessel with the flow pattern in the single drop analysis set-up (see publication III - Maaß et al. (2009) for these results).

Considering Stoots and Calabrese (1995), the breakage cell represents a rotating frame of reference (that means fixed stirrer). So this specific flow is characterized by a wake behind the stirrer blade. This wake flow is characterized by two typical vortices behind the stirrer blade (see the results in publication III - Maaß et al. (2009) but also Stoots and Calabrese (1995) and Delafosse et al. (2009)[i]).

Usually in simulations stirred tanks are considered by a fixed frame of view (that means rotating stirrer). The transformation of the flow patterns in the breakage cell from a rotating to a fixed frame of view in the 3D agitated vessel are described in detail in publication III - Maaß et al. (2009).

The comparison showed in general a good agreement between breakage cell flow and flow pattern in stirred tanks. More detailed analysis revealed that the macro scale vortices behind the stirrer blade are smaller in the stirred tank than in the breakage cell. These disagreements result from the use of only one blade in the breakage cell. The following blade during the rotation compresses the macro scale fluid vortices in the stirred tank. The flow field is qualitatively the same in both applications, but it is more compact in the stirred tank than it is in the breakage cell. However, the absolute values for the simulated energy dissipation rate and the turbulence kinetic energy as the calculated values for the shear-gradients in the single drop analysis set-up as in the agitated vessel are in good agreements with each other and also with literature values [Höfken et al. 1996; Schäfer 2001; Stoots and Calabrese 1995].

These results are used as a proof for the transferability of the breakage analysis from the stirred tank to the single drop breakage cell in meaningful constraints.

Additionally, the CFD results have been used to analyze the influence of the flow field on drop breakage. Therefore, possible drop paths through the experimental set-up were investigated. These results gave first insights on the responsible breakage mechanisms close to the impeller. They are a result from the discussions of Wollny et al. (2008) (see the following paragraph) and have been used to interpret the results in publication III - Maaß et al. (2009).

The absolute velocity of an infinitesimal fluid element P in a flow is described by three velocity components for each of the three dimensions: w_x, w_y and w_z. Furthermore this element P has six neighbour elements. All velocity components have to be analysed in their change from P to the six neighbour points. According to this, all velocity changes can be expressed by the following tensor Ξ_{ij}:

$$\Xi_{ij} = \begin{pmatrix} \frac{\partial v_x}{\partial x} & \frac{1}{2}\left(\frac{\partial v_x}{\partial y} + \frac{\partial v_y}{\partial x}\right) & \frac{1}{2}\left(\frac{\partial v_x}{\partial z} + \frac{\partial v_z}{\partial x}\right) \\ \frac{1}{2}\left(\frac{\partial v_y}{\partial x} + \frac{\partial v_x}{\partial y}\right) & \frac{\partial v_y}{\partial y} & \frac{1}{2}\left(\frac{\partial v_y}{\partial z} + \frac{\partial v_z}{\partial y}\right) \\ \frac{1}{2}\left(\frac{\partial v_z}{\partial x} + \frac{\partial v_x}{\partial z}\right) & \frac{1}{2}\left(\frac{\partial v_z}{\partial y} + \frac{\partial v_y}{\partial z}\right) & \frac{\partial v_z}{\partial z} \end{pmatrix} \tag{10}$$

ANSYS CFX[ii] as the used commercial CFD - software, gives information about the so-called "shear strain rate" (sstrnr). The sstrnr is defined as the second invariant of the tensor from equation (9):

$$\text{sstrnr} = \sqrt{2\left(\frac{\partial v_x}{\partial x}\right)^2 + 2\left(\frac{\partial v_y}{\partial y}\right)^2 + 2\left(\frac{\partial v_z}{\partial z}\right)^2 + \left(\frac{\partial v_x}{\partial y} + \frac{\partial v_y}{\partial x}\right)^2 + \left(\frac{\partial v_x}{\partial z} + \frac{\partial v_z}{\partial x}\right)^2 + \left(\frac{\partial v_y}{\partial z} + \frac{\partial v_z}{\partial y}\right)^2} \tag{11}$$

On closer examination of the sstrnr it becomes evident that equation (11) is not describing the shear gradient but rather the overall velocity gradient including shear, acceleration and compressibility rates. Therefore, the invariant sstrnr is independent of the rotation of the coordinate system, whereas the single velocity gradients which are used for calculation of the sstrnr are not.

It is necessary to know the direction of the flow to define local normal and shear gradients. Therefore a local coordinate system is necessary which describes for example the flow direction parallel to its y-axis. So the global tensor Ξ_{ij} can be converted into a local tensor (see Wollny et al. (2007) and Wollny (2010) for details), which is dependent on the local flow direction and independent from the global coordinate system. With this transformation the sstrnr can now subdivided into one normal (nn), one shear (nt) and one direction gradient (tt):

---

[i] The work of Delafosse et al. (2009) is recommended as it contains a concise and updated review on this research topic.

[ii] ANSYS CFX software is a high-performance, general purpose fluid dynamics program that has been applied to solve wide-ranging fluid flow problems for over 20 years (http://www.ansys.com; 2011.07.01).

$$\text{sstrnr} = \sqrt{\left((\text{nn})^2 + (\text{nt})^2 + (\text{tt})^2\right)} \tag{12}$$

The normal gradient (nn) describes the change of the velocity in flow direction – acceleration and compressibility. The shear gradient (nt) describes the change of the normal components cross to the flow. The direction gradient (tt) gives information about points in the investigated system where the flow direction is different from their neighbors. This differentiation between these three gradients allows deeper insights into the responsible mechanisms for drop breakage.

In Figure 13 (a) seven different stream lines are describing exemplarily the sstrnr in different regions close to the stirrer. While a particle is changing its place to the stirrer blade, the breakage analysis has to follow such particle paths instead of analyzing different caption planes. The stream lines are demonstrating how the position and the sstrnr are changing along such a path. The highest values are close behind and in front of the stirrer blade.

Only the part of the sstrnr, which is related to the shear gradient nt (see equation (12)) is shown in Figure 13 (b). The values behind the stirrer blade are nearly the same for sstrnr and nt. Opposed are the values in front of the blade – the sstrnr reaches maximum values, the nt does not. This implies that mostly all of the stress behind the stirrer blade is caused by shear forces. Furthermore it becomes clear that no significant shear stress appeared in front of the blade.

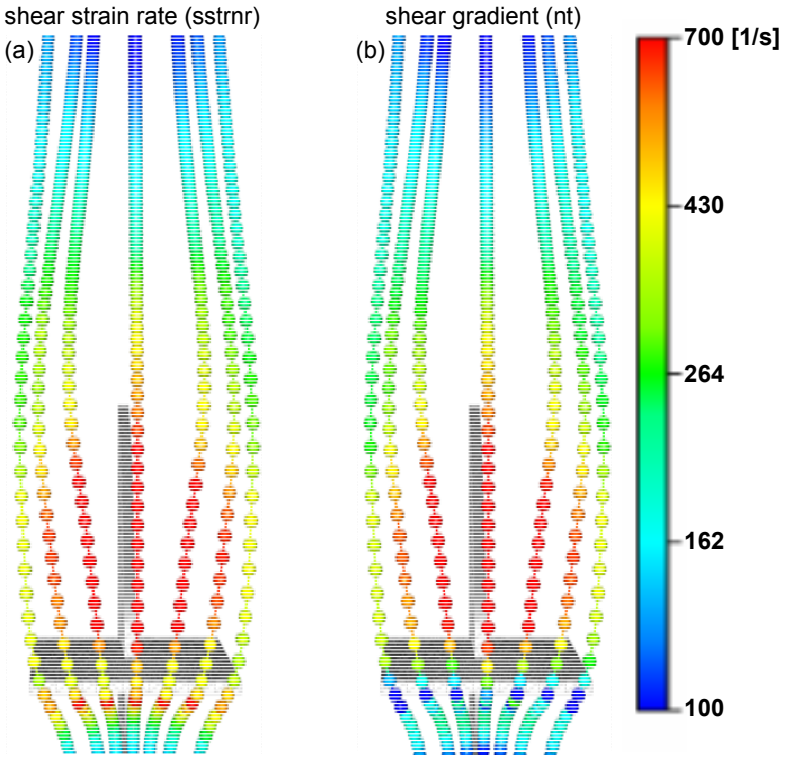

Figure 13 – Visualization of sstrnr for seven stream lines entering the stirrer region (a) compared with the same seven stream lines where only the nt part of the sstrnr is visualized.

Almost all recorded breakage events take place behind the stirrer blade and most of them in the closer region direct behind it (see publication III - Maaß et al. (2009) for details). This means that not the classic shear strain rate sstrnr but the shear gradient nt has to be taken into consideration as major reason for drop breakage.

The flow field simulations carried out in the single drop breakage cell gave valuable insights not only on the velocity fields to show comparability to an agitated vessel but also on the distribution of the different velocity gradients. The results propose, depending on the drop size, that not only the microscopic turbulent eddies but also macroscopic flow structures are responsible for drop breakage. This was already mentioned by Stoots and Calabrese (1995) who showed that intense deformation rates are formed out of the trailing vortices behind the stirrer blade.

II. Analysis of the flow field in stirred vessels

The turbulent flow field in the used agitated applications was intensively studied, as it is a crucial influence parameter on the drop size distribution. Experimental flow visualizations, particle image velocimetry (PIV) measurements and CFD simulations have been carried out to study the used geometries. The results are given in publication VIII - Maaß et al. (2011c). Additionally, the power numbers have been determined experimentally for each application.

A major focus was the analysis of industrial relevant slim reactors [Bey and Dienes 2010]. The advantages for an increase in reactor volume by increasing vessel height H at constant vessel diameter T are clear: the increased reactor surface compared to the reactor volume increasing heat transfer and the smaller footprint. They are accompanied with the disadvantages of the long distances for the flow over the reactor height. These dimensions favor local maxima or minima in temperature, concentration or the like. This is detrimental for an optimal process and therefore proper mixing is mandatory.

Figure 14 shows the mean velocity field of the turbulent flow in such a reactor (H/T = 2.3). CFD - simulations and PIV measurements are compared with each other. The results have been taken orthogonal and parallel to the two baffles, always in the centre section of the vessel through the rotation axis of the reactor. Two baffle immersion depths $l_B/H = 0.55$ (a) and 0.40 (b) are presented. The comparison between the CFD and the PIV results showed the same structure of the macroscopic flow. The primary circulation loop characteristic of a retreat curve impeller (RCI) is immediately evident. The impeller generates a strong axial flow in the downwards axial direction, which reaches its maximum magnitude at 0.5 stirrer tip speed ($w_{tip} = \pi nd$). As the jet reaches the vessel bottom, it changes direction and is deflected towards the wall. This behavior is only partially evident for the measured values, due to the optical falsification by the torospherical bottom. This region of redirection coincides with the strongest radial flow region [Unadkat et al. 2009]. The jet stream then flows up the vessel wall, where the axial velocities are around 0.1 w_{Tip}. Since this flow was fully turbulent (Reynolds number $Re = nD^2/\nu = 5 \cdot 10^4$ at the 400 rpm with $w_{tip} = 1.8$ m/s), this general flow pattern was found to be repeatedly measured for all investigated parameter variations of this stirrer.

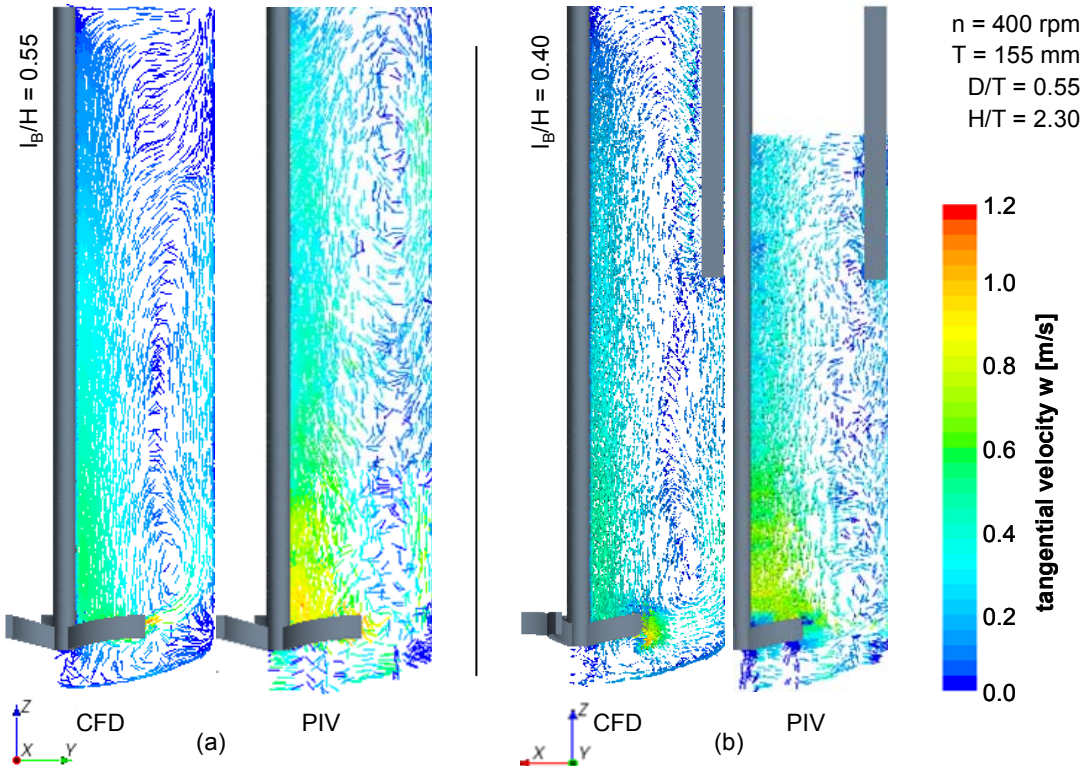

Figure 14 – Comparison of the 2D velocity field using CFD and PIV for a retreat curve impeller at a baffle immersion depth of $l_B/H = 0.55$, orthogonal to the baffle plane (a) and $l_B/H = 0.40$, parallel to the baffle plane (b).

The absolute values of the velocities are in very good agreement with those of Li et al. (2005), who analyzed the flow field of a RCI in an equally sized vessel (T = 148 mm, as T = 155 mm in this study) by CFD and

laser Doppler anemometry (LDA). The shape and magnitude of the flow and the vortex centers are satisfactorily predicted in this study as by Lee et al. (2005). The maximum prediction error of absolute 8% by Lee et al. (2005) could not be achieved. The deviations between PIV and CFD for the down coming flow are about 25% for the baffle length $l_B/H = 0.55$ (Figure 14 - (a)) and 20% for the baffle length of $l_B/H = 0.40$ (Figure 14 - (b)). The CFD underestimates the values of the measurements. However, the simulations were suitable to describe the flow field qualitatively. The deviations in the absolute values of the flow velocities are not as dominant as they could compromise the overall purpose of this study. That was to gain qualitative insights into the spatial distribution of the energy dissipation rate and the 3D flow field to construct different dissipation zones useable for PBE simulations.

The assumption of a well mixed condition, using a single value for the energy dissipation rate ε_{av} throughout the vessel is not to accommodate with the CFD simulations, which show intense velocity gradients and inhomogeneous flow structures in the impeller region and very low values for the energy dissipation rate at larger distances to the impeller. Although this is true for standard systems with H/T = 1.0, the inhomogeneities is even increased for the single stage high aspect ratio reactors.

The use of only one average value of the energy dissipation rate in PBE simulations for the complete vessel lead to poor prediction results of the drop sizes in slim reactors. Such an approach is also called 1-zone assumption; the results are presented in publication IV - Maaß et al. (2010). To overcome this failure, the vessel was always subdivided into two zones (one impeller and one bulk region) following the ideas of Alopaeus et al. (1999) & (2009). The outstanding success with this model improvement is shown in publication IV - Maaß et al. (2010) and also in chapter 6 (see page 55).

The values for the size of the zones as the interconnecting volume streams have been extracted from the CFD simulations. All results of the flow field used for the PBE simulations are listed in publication VI - Maaß et al. (2011b). The influence of the turbulence on the drop size as the necessity for a more detailed description of the spatial distribution of ε is discussed in Table 3 and Table 4.

Table 3 – Comparison between the experimentally achieved smallest drop size d_p with the calculated Kolmogoroff scale λ_κ for the assumption of the well mixed condition (1-Zone model).

study	stirrer diameter D [m]	Reynolds number Re [-]	power number Ne [-]	average energy dissipation rate ε_{av} [m^2/s^3]	Kolmogoroff scale λ_κ based on ε_{av} [µm]	smallest determined drop size $d_p(t = 60\ min)$ [µm]
IV - Maaß et al. (2010)	0.085	30 282	0.89	0.045	68.8	11
ibidem	0.085	48 450	0.89	0.183	48.4	20
ibidem	0.085	48 450	1.67	0.343	41.3	12
ibidem	0.085	84 788	0.89	0.979	31.8	11

Table 4 – Comparison between the experimentally achieved smallest drop size d_p with the calculated Kolmogoroff scale λ_κ for the assumption of a high energy dissipation rate in the impeller region ε_{imp} (2-Zone model).

study	stirrer diameter D [m]	Reynolds number Re [-]	power number Ne [-]	average energy dissipation rate ε_{imp} [m^2/s^3]	Kolmogoroff scale λ_κ based on ε_{imp} [µm]	smallest determined drop size $d_p(t = 60\ min)$ [µm]
IV - Maaß et al. (2010)	0.085	30 282	0.89	0.678	34.8	11
ibidem	0.085	48 450	0.89	1.420	29.0	20
ibidem	0.085	48 450	1.67	5.213	20.9	12
ibidem	0.085	84 788	0.89	7.610	19.0	11
VI - Maaß et al. (2011b)	0.093	59 102	0.39	3.355	23.4	11
ibidem	0.27	243 000	0.39	42.82	12.4	11

It is assumed that the final drop sizes of an agitated l/l system are small compared to the turbulence macro scale (presented in Figure 14) but large compared to the Kolmogoroff scale ($\lambda_\kappa = (\eta_c/\rho_c \cdot \varepsilon^{1/3})^{3/4}$ [Leng and

Calabrese 2004], the turbulent micro scale. A factor around 5 is usually expected between λ_κ and the smallest measured drop diameter.

The data in Table 3 and Table 4 show that all investigations were carried out under full turbulent condition, as the lowest stirrer speed was associated with a Reynolds number of 30,282. However, the smallest measured drop diameter was always smaller than the associated Kolmogoroff scale (note also the limitation of the drop size measurement technique, already discussed in chapter 3). Although satisfying results are already achieved with the 2-zone model, a further improvement of a more physical consideration of the fluid flow in the PBE models is still needed, as also the following result will show.

Surprising dispersion behavior in slim reactors was additionally found and reported in publication IV - Maaß et al. (2010). The influence of the immersion depth of two baffles on the transient drop size was studied. The values of d_{32} are clearly divided into two different regimes - under and above a certain baffle length l_B. The drop sizes for $l_B/H < 0.43$ are constant but two times larger than the constant drop size results for increasing $l_B/H > 0.43$. The parallel measured power input as the macroscopic flow field, determined with PIV and CFD showed a continuous increase for increasing baffle length.

Stream lines are used in Figure 15 to illustrate the 3 dimensional flow fields for increasing baffle lengths. For comparative purposes, all parameters of the stream lines are kept constant – space of origin, observed time and number of visualized stream lines. A significant change in stream line behavior is shown by changing the system from unbaffled to baffled with $l_B/H = 0.1$. There are low axial velocity-components in the unbaffled system, but instantaneously occur even with very low baffle lengths. The streamlines for l_B/H follow helicalcurves at the vessel wall to the surface and are pumped down at the impeller shaft in the middle of the reactor. The homogeneous, heli flow structure is disturbed and turns into a more random flow field by further increase of the baffle length. Inhomogeneities are created, the velocities are increased and thereby the tracked distances of every stream line in the observed interval.

All these results were not able to explain the drop size leap reported in publication IV - Maaß et al. (2010). A more detailed analysis with higher time and space resolution using finer grids seems to be necessary.

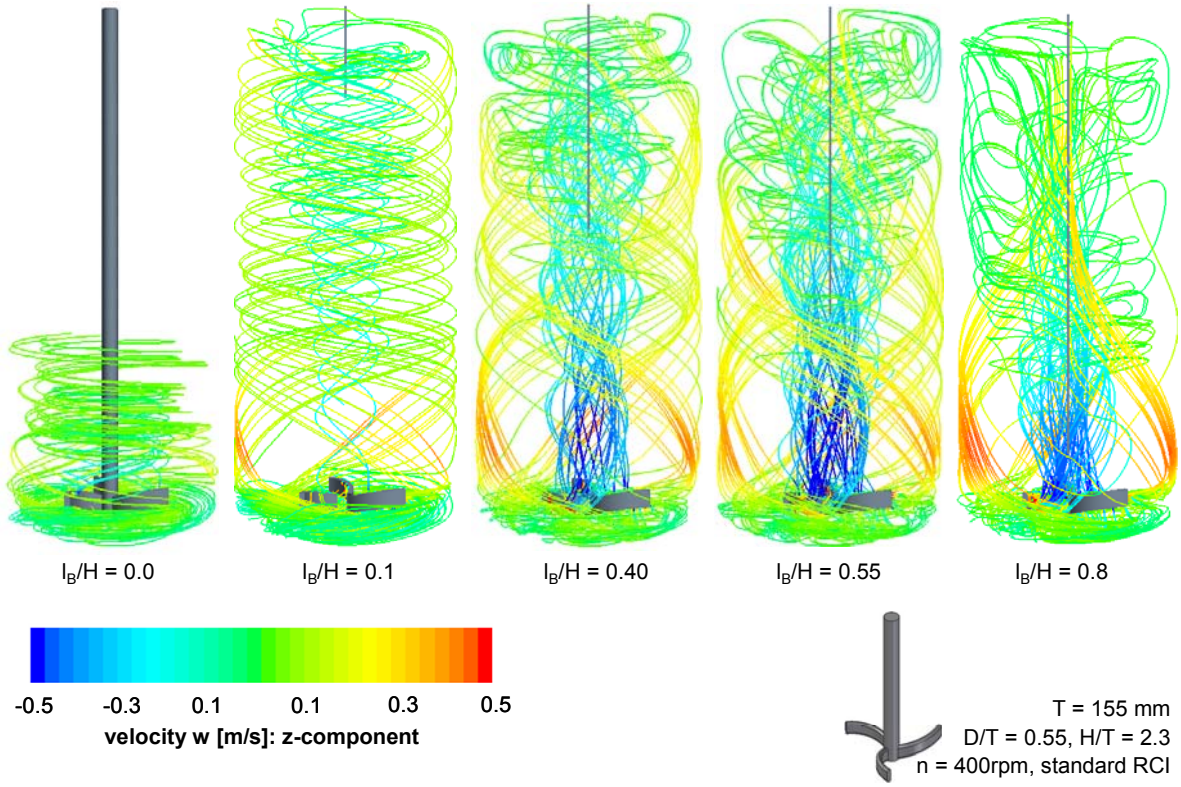

Figure 15 – Streamlines for unbaffled and baffled system with increasing baffle length $l_B/H = 0.1$ until 0.8

The current trends in CFD studies point towards an increasing application of more refined, grids such as in large eddy simulation, to capture turbulent structures at micro scales. This trend will further improve the quality of the simulation results for processes such as precipitation, in which micro mixing [Ochieng et al. 2009]

and breakage events are important. This should help to understand the dramatic change of d_{32} at an immersion depth of the baffles around 0.43 - a distinctive change in the flow pattern around this point should be expected on the micro scale.

5. Results of the single drop experiments

The mathematical description of agitated dispersions using population balances requires information about the number and sizes of daughter drops formed by break-up of a mother drop of a given size. It has usually been supposed (see chapter two for details) that only binary break-up occurs and that the resulting daughter drop size distribution can be approximated by a truncated normal or by a uniform distribution. Some authors describe the breakup process as a sequence of a number of binary breakages resulting in a specific daughter drop size distribution.

With regard to the lack of experimental data in this field, an attempt was made to find direct information from observation of the break-up of single drops. In the method used, a drop of known size was inserted in the continuous water phase. The drop was accelerated into a region with a part of a Rushton turbine miming the impeller region in an agitated vessel. The breakage time and probability of this mother drop and the number and sizes of the daughter drops resulting from its break-up were recorded using highspeed imaging (see chapter three for details).

As drop deformation and break-up in a turbulent flow field depends on the size of the drop, the physical characteristics (density and viscosity of the phases, interfacial tension) and the operation parameters (stirrer speed - meaning the continuous phase velocity), have been varied. With the presented method it was possible to gain direct information about the influence of the named parameters on breakage time and breakage probability and the number and sizes of the daughter drops resulting from its break-up. This information is needed for the mathematical description in the population balance equation.

The chapter is structured as follows: The first section gives an overview of the experimental working program, than followed by subsection II - model evaluation and closed with the subsection III - model development.

I. Working program

The two organic liquids used as dispersed phase for this investigation were toluene (99.98 % purity) and petroleum (99.9 % purity). Both were blended with a non-water soluble black dye, which decreases the interfacial tension between water and the organic liquid but increases the optical evaluation possibilities. The influence on the interfacial tension was quantified using the pendant drop method [Jon et al. 1986]. The physical properties for the used systems are listed in Table 5. It is important to mention, that petroleum is a mixture and not a pure liquid. It has different names; while it is called petroleum in German, it is called kerosene in American English and paraffin oil in British English. Due to the origin of the author the term petroleum will be used.

Table 5 – Properties of used chemicals.

	γ [mN/m]	γ [mN/m] with dye	ρ [kg/m³] at 20°C	η_d [mPa·s]
toluene	36	32	870	0.55
petroleum	42	38.5	790	0.65

The mother drop sizes have been set between 0.54 mm and 3.1 mm. An overview of the whole work program is given in Table 6. The influence of the flow velocity and therewith the energy dissipation rate was varied for a constant mother drop diameter of 1.0 mm for both systems. The dependency of the breakage rate on the mother drop diameter was investigated for a constant superficial velocity of 1.5 m/s. The influence of the chemical properties of the systems was shown by parallel investigations with the two used dispersed phases. The viscosity is almost equal to the viscosity of the continuous phase, for both chemicals. It can be assumed that the drop surfaces track the velocity of the continuous phase [Wichterle 1995].

Table 6 – Overview of the working program.

system	flow velocity w [m/s]	mother drop diameter d_p [mm]
toluene/ water	1.0	1.0
	1.5	0.65, 1.0, 2.0, 3.0
	2.0	1.0
petroleum/ water	1.0	1.0
	1.5	0.54, 0.7, 1.0, 1.3, 1.9, 3.1
	2.0	1.0

II. Model evaluation and application

The number and the size distributions of daughter fragments for single drops have been studied in publication IX - Maaß et al. (2011d). Following a Lagrangian perspective, the commonly used assumption of binary breakage was supported. The results for the daughter drop size distribution were used to evaluate models for the DDSD from literature. Based on these insights PBE simulations have been applied to an agitated liquid/liquid system to analyze the influence of the DDSD on the transient drop size distribution.

1. Number of daughter drops ν

The number of daughter drops occurring from the initial breakage of the breakage sequences was analyzed in publication IX - Maaß et al. (2011d). The used frame rate of 822 fps allowed a detailed timely resolution of the single breakage events. It was clearly shown that all multiple breakage events can be dissected into a sequence of binary breakages. Simultaneously breaking drops with $\nu > 2$ also occurred but these measurements were a function of the used frame rate. ν was decreasing for constant conditions with increasing frame rate. If the timely resolution is high enough, every single drop breakage event can be differentiated into a series of binary breakages.

These sequences of binary breakages happen extremely rapid and because they are strongly connected with each other, the interpretation can also be carried out with a different perspective. Every breakage is seen as a number of breakage events which is triggered by the first one. To count these absolute values of daughter drops, the maximum number of drops on one image throughout the sequence is counted. The results for toluene mother drops at a constant flow velocity of 1.5 m/s are shown in Figure 16. The distribution of the number of particles is much wider then the one presented in publication IX - Maaß et al. (2011d) analyzing only the initial breakage events.

As expected much higher numbers of daughter drops are achieved for all diameters compared to the results in publication IX - Maaß et al. (2011d). Additionally the maximum number of particles found n_{max} in all sequences is given as the average number n_{av} from the complete distribution. Both numbers are increasing with increasing drop diameter. The breakage sequence of a 3 mm toluene drop is shown in Figure 18.

The analysis of the sequence in Figure 18 supports the necessity of a different interpretation on the single drop breakage events as it is discussed in Figure 16. The drop was strongly deformed due to the intense influence of the stirrer blade on the flow field. The drop broke on image 3 in Figure 18 directly at the tip of the blade into two strongly deformed fragments. This is relatively seldom, however the first daughter drop broke by a sequence of binary breakages into numerous fragments (see image 5-17 in Figure 18). Then the second daughter drop was broken as it was also introduced into the turbulent region behind the stirrer blade (entrance of the second daughter drop starts on image 18 in Figure 18). Also this drop was destroyed by the turbulent flow.

The largest number of daughter drops on one image was 124, shown on image 37 in Figure 18. This is clearly above the average for this parameter combination. However, this single drop breakage example shows clearly the timely evolution of a sequence of breakages which are considered as one by some authors [Hancil and Rod 1988], while others would count it as a sequence of binary breakages [Konno et al. 1980].

The average numbers ν_{av} are clearly larger than two also for the smallest investigated mother drops. For example the 0.65 mm toluene mother drops broke to an average of 5.4 daughter drops.

The comparable results for petroleum mother drops at a constant flow velocity of 1.5 m/s are shown in Figure 17. The comparison with the toluene drops revealed, that the values are always smaller for the petroleum system but both follow the same trends. Therefore, the discussion carried out above for the toluene drops is also true for the petroleum drops.

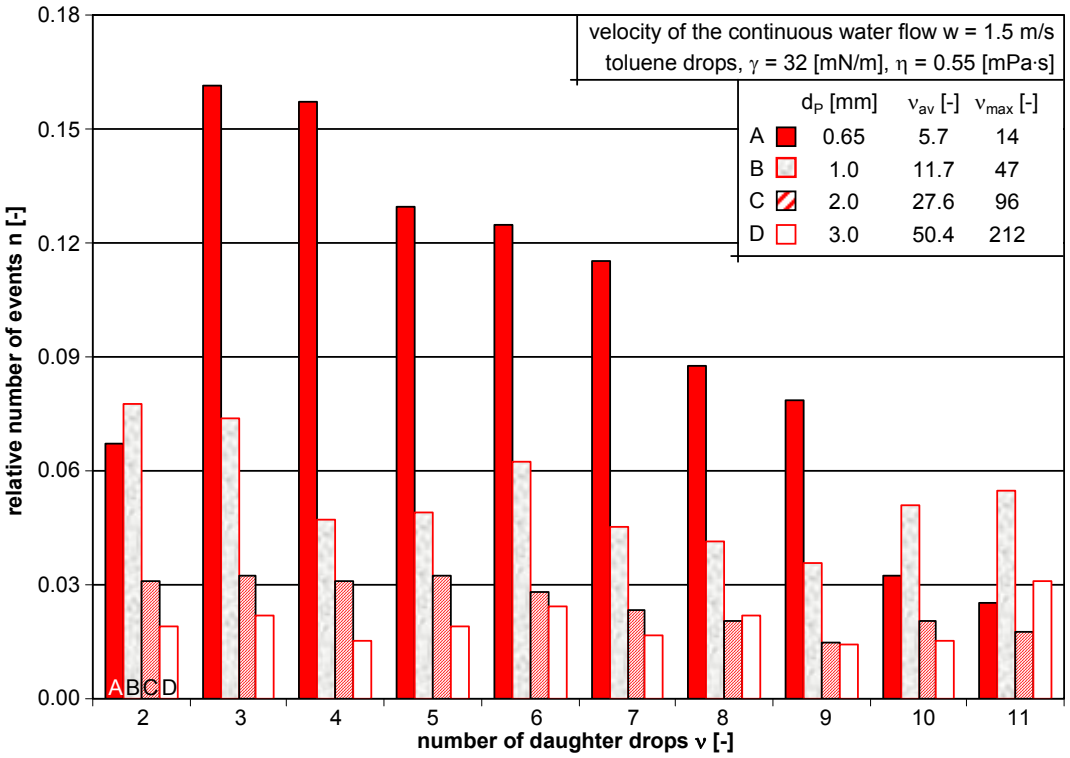

Figure 16 – Relative number distribution over the number of daughter drops measured at a constant flow velocity of 1.5 m/s, using toluene mother drops of four different sizes.

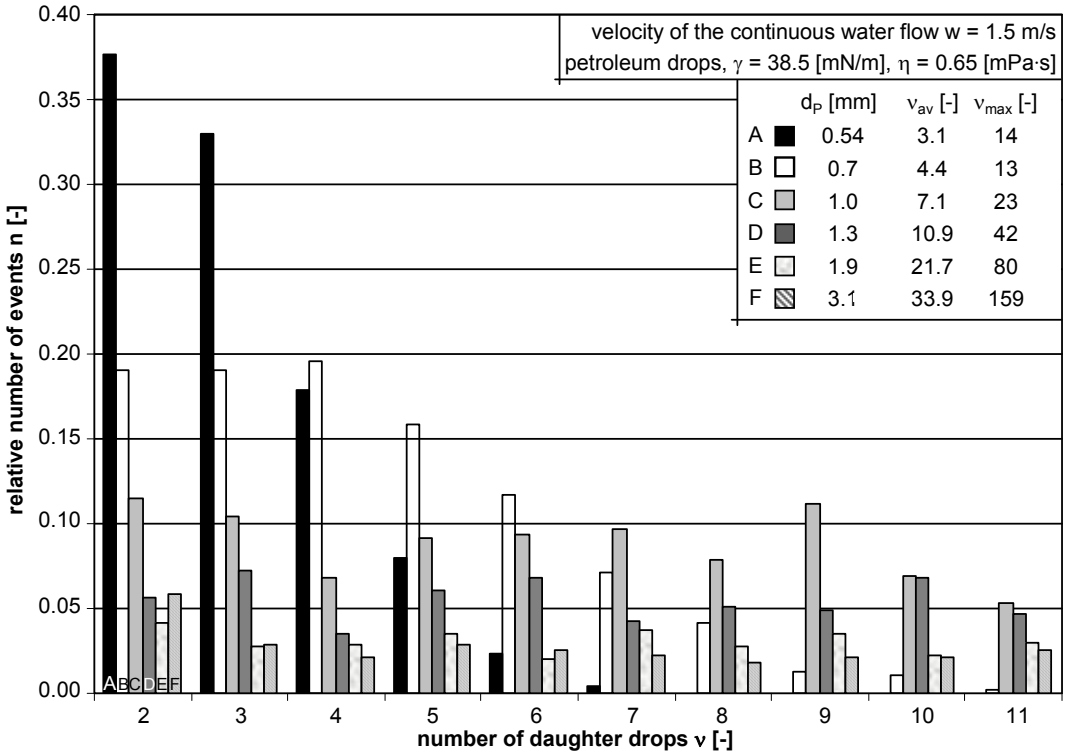

Figure 17 – Relative number distribution over the number of daughter drops measured at a constant flow velocity of 1.5 m/s, using petroleum mother drops of six different sizes.

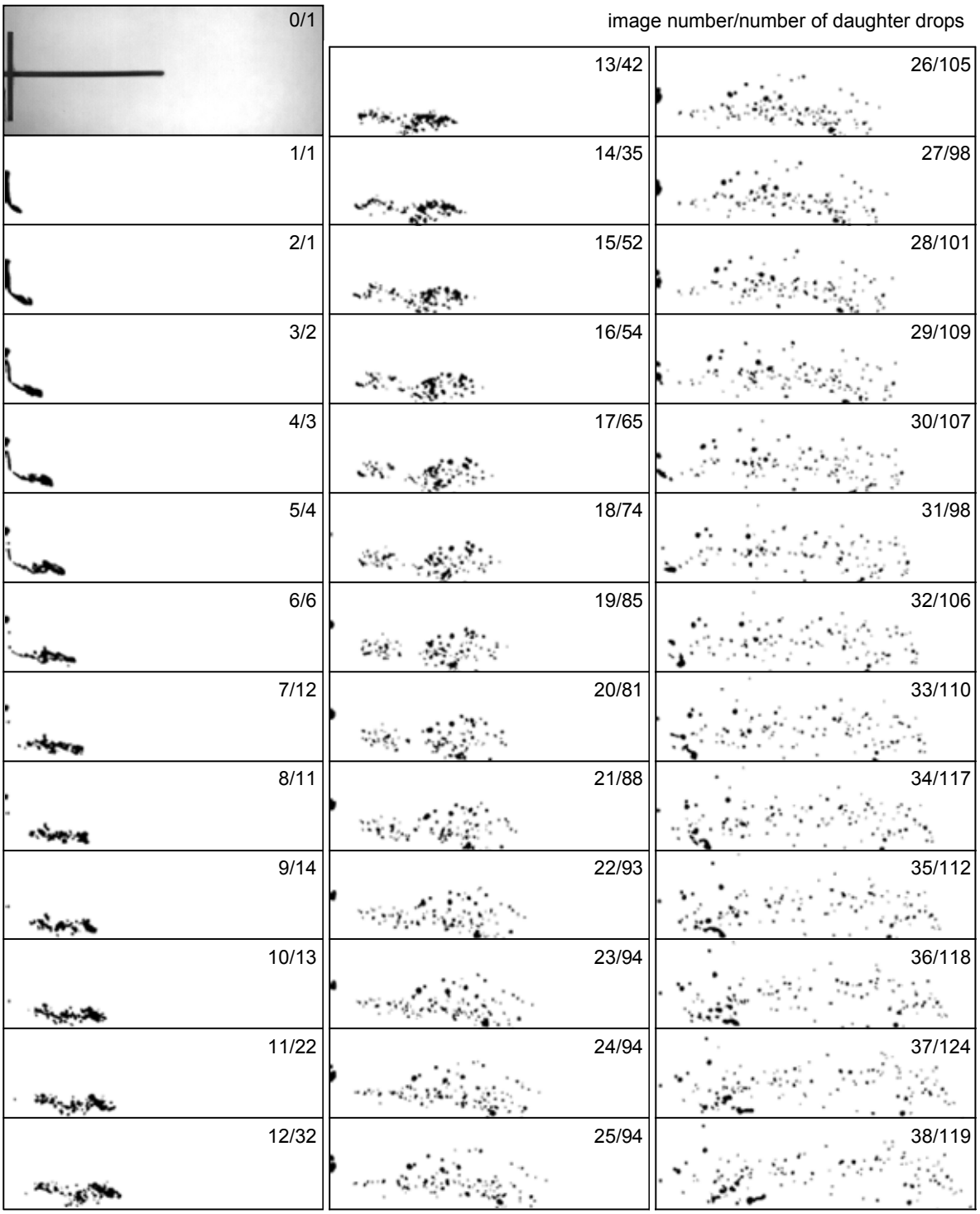

Figure 18 – Example sequence of a 3 mm toluene drop at a flow velocity of 1.5 m/s, which is a direct hit of the stirrer blade. The sequence was taken at a constant frame rate of 822 fps. The sequence shows in a impressive way how fast that many daughter drops can be created from one initial breakage event.

The average values of the maximum counted daughter drops from every set of experiment are shown as a function of the mother drop diameter in Figure 19. It was found that ν_{av} is an increasing function. This dependence was correlated using the function from Hancil and Rod (1988):

$$\nu_{av} = 2 + p\left[\left(d_P / d_{P,crit}\right) - 1\right]^q \qquad (13)$$

This correlation fulfills the requirement $\nu_{av} = 2$ for $d_P = d_{P,crit}$. The critical diameter $d_{p,crit}$ has to be determined either experimentally or calculated based on the turbulence theory. The two adjustable parameters p and q are sufficiently flexible to describe the behavior of any system. The values used for the results in Figure 19 are p = 0.47 and q = 1.5, just as originally proposed by Hancil and Rod (1988). They have been used for both systems, the petroleum and the toluene drops. The correlation was only adjusted by $d_{P,crit}$ This value was fitted to minimize the differences between the experimental and the correlation values. The values for $d_{P,crit}$ were fitted not only against one experiment but for all investigated mother drop diameters simultaneously. The sum of the error squares was minimized using the generalized gradient algorithm (Haggag 1981). The values achieved for the critical diameter are meaningful as they are in agreement to results from the stirred tank and to first experimental results of single drops, carried out in the breakage cell.

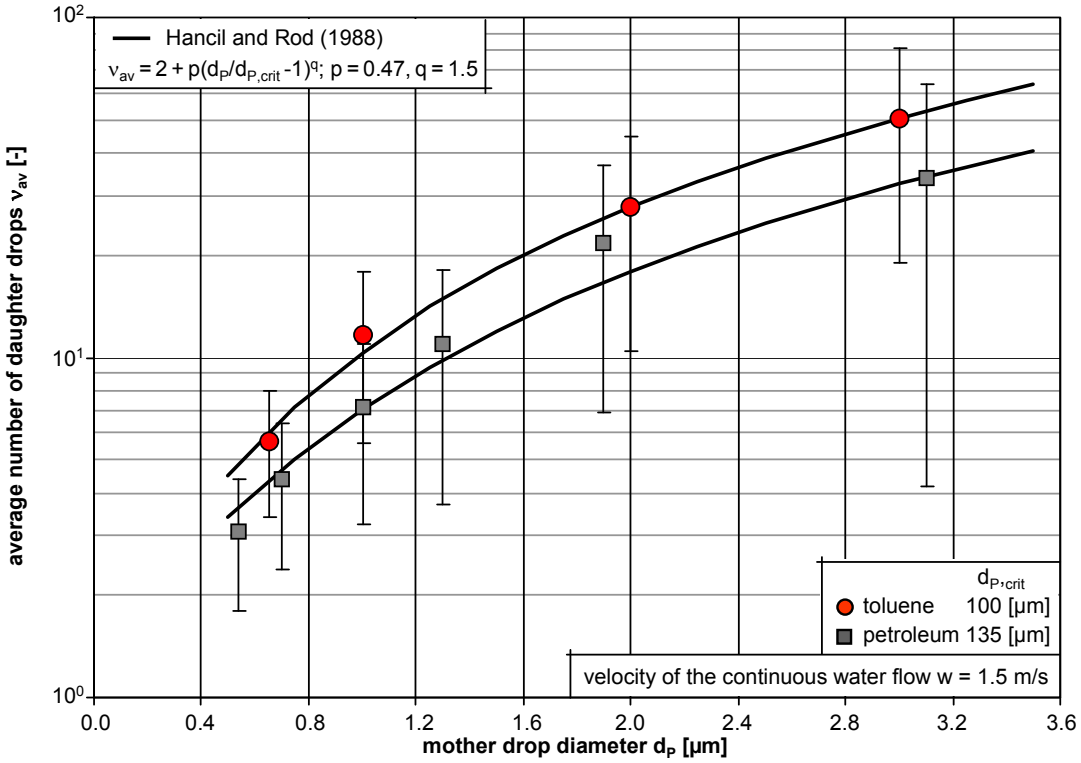

Figure 19 – Comparison of experimental results (symbols) with correlation results (lines) for the average number of daughter drops versus the mother drop diameter.

As already discussed, a wide distribution for the number of daughter drops was measured. That led into large values for the standard deviation (between 40 and 88%). Nevertheless, due to the large amount of investigated single drops these values are much smaller than comparable results in literature (see for example Hancil and Rod (1988)). The standard deviation for all data points is given in Figure 19.

The reliability of the complete data sets is analyzed in Figure 20. The standard deviation of the maximum average number of daughter drops is shown as a moving average value over the number of investigated drops. This is done for all investigated drop diameters and for both systems (toluene and petroleum). Additionally the moving standard deviation σ is given. The absolute values of σ are large, the variance of the moving values are small.

2. *Daughter drop size distribution β*

Determining the daughter drop size distribution based on single drop experiments has a long history and was firstly applied by Cabassud et al. (1990). They have determined DDSD in a Kühni column and proposed the use of β-distribution for the description of the DDSD in the PBE. Only a few experimental results are available for stirred tank applications.

Experimental determined DDSD of the initial breakages in the single drop breakage cell were presented in publication IX- Maaß et al. (2011d). The results showed clearly that the most quoted assumption in literature, a Gaussian distribution for the daughter drop size distribution, is misleading. The experimental values were

broadly distributed opposed to the theoretical model. Concretely, the breakage into a very small and a very large daughter drop was observed as most probable.

The resolution of the used highspeed camera did not allow a precise determination of the daughter drop sizes after the multiple breakage events. The tiny daughter drops resulting at the end of breakage sequence (see exemplarily Figure 18) were too small.

However, the simulations in publication IX - Maaß et al. (2011d) revealed a significant influence of the DDSD on the resulting DSD. There, the Gaussian distribution led always to too narrow distributions, opposed the u-shaped distributions proposed by Tsouris and Tavlarides (1994). The use of this DDSD lead to too wide simulated drop size distributions it they are compared to the experimental values. A β-distribution after Lee et al. (1987) and a bimodal distribution following the ideas of Kostoglou et al. (1997) gave the best agreements between simulated and experimentally determined DSD in the investigated agitated tank. The comparative results between experiments and PBE simulations of the cumulative number distribution are presented in Figure 21.

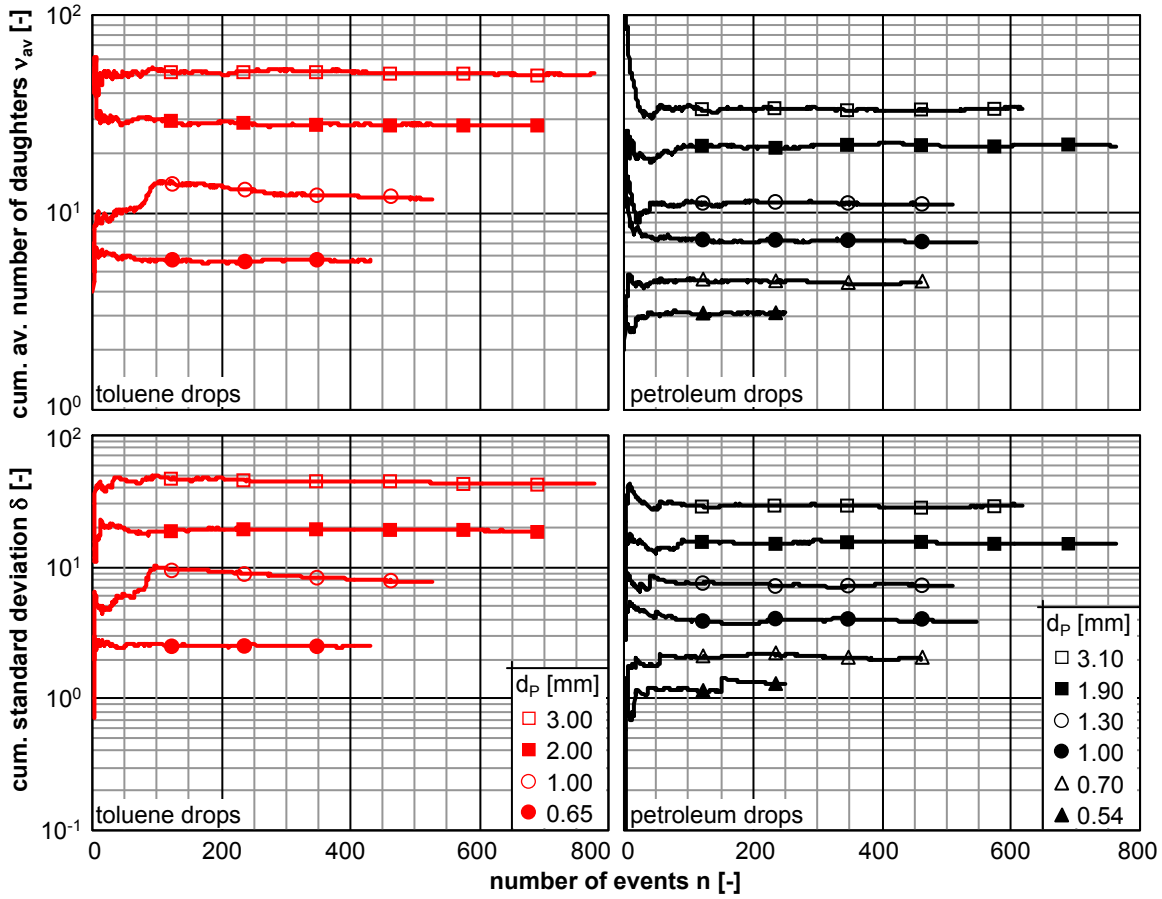

Figure 20 – Evaluation of the average number of daughter drops and the resulting standard deviation as a function of the sample size.

III. Model development

The results for the breakage probability experimentally determined in the single drop breakage cell were in good agreement to model results from literature. This comparative study was presented in publication VII - Maaß and Kraume (2011). Based on the experimental single drop results, the parameter in the PBE which is associated to the breakage probability ($c_{2,br}$ for the model of Coulaloglou and Tavlarides (1977) - see also equation (5)) in the models was determined and then used for simulations. The simulations are presented in publication IX - Maaß et al. (2011d).

The results for the breakage time are contrary in literature (see publication VII - Maaß and Kraume (2011) for details). The agreements between literature models and single drop breakage time were only in poor. These results are presented with more details in the following section.

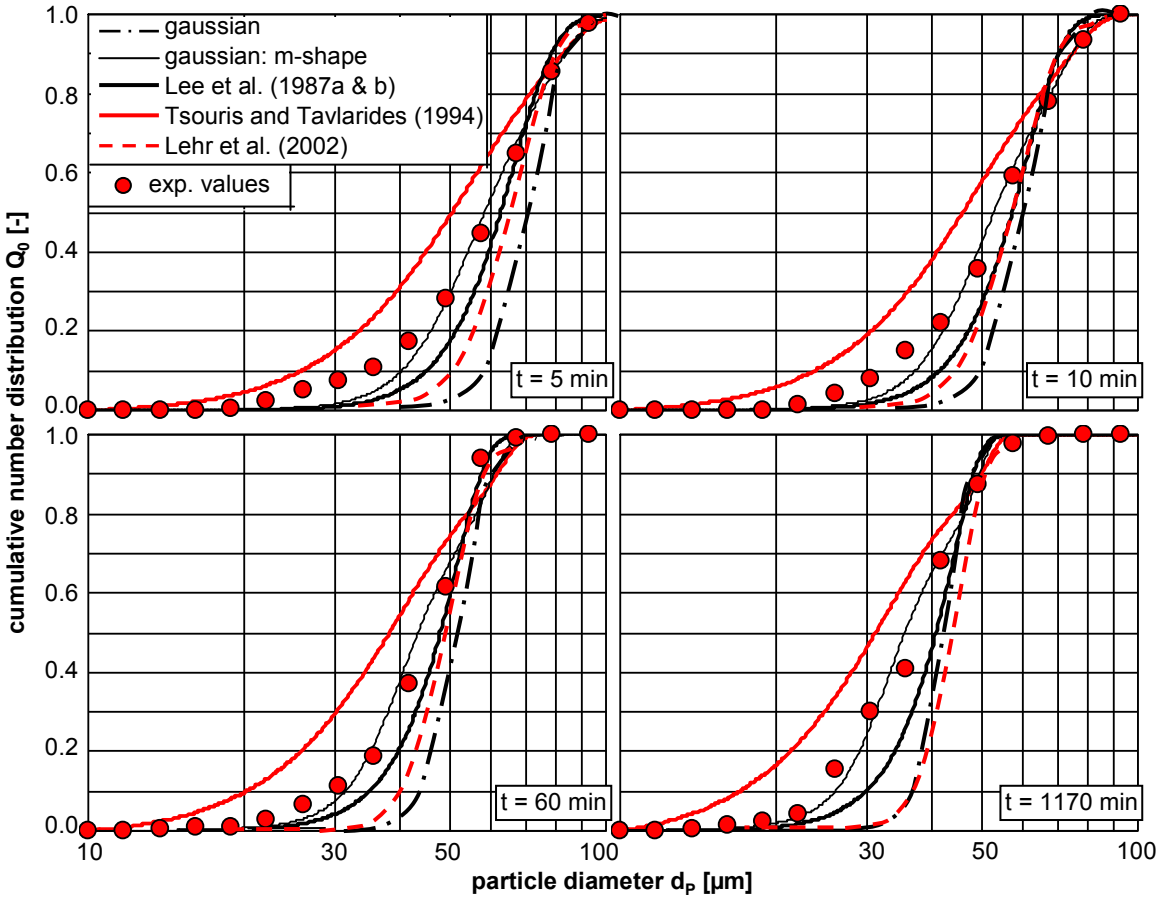

Figure 21 – Comparison of an experimental determined cumulative number density distribution and PBE simulations using several DDSD

1. Breakage time t_{br}

The time for breakage of individual drops in a fully turbulent flow field was measured. The results presented in publication VII - Maaß and Kraume (2011) determined the breakage time as follows: the time starts when the drop crosses the stirrer blade in the breakage cell (see also image 1 in Figure 18). As the number of objects on every image is tracked, the breakage time is stopped if more than one object is counted on one image in the sequence (see image 4 in Figure 18). This is the initial breakage time $t_{br,in}$, as it describes the necessary time to deform the drop until it broke for the first time.

However, the results of the initial breakage time distribution were correlated with a statistical model, the β-distribution. The peak values of the β-distribution $t_{br,in,\beta}$ were compared with each other. The experimental values showed an increase in $t_{br,in,\beta}$ with an increase in d_P. This was not true for the arithmetic average values of $t_{br,in,av}$ below a size of 1.0 mm for the toluene drops and 1.9 mm for the petroleum drops (see publication VII - Maaß and Kraume (2011) for details).

Figure 22 shows the relative number distribution of the breakage time for two different mother drop diameters. Opposed to the measurement procedure in publication VII - Maaß and Kraume (2011), the breakage time was stopped at that point of the breakage process where the maximum number of daughter drop particles result from the breakage (red curves in Figure 22). This can exemplary seen on image 37 in Figure 18.

The wideness of the distribution of the so called maximum breakage time in comparison to the results for the same mother drop diameter and the same flow velocity is decreasing for both investigated diameters. The standard deviations were smaller than the arithmetic average value, opposed to the results for the initial breakage time. The number distribution of the breakage time of the initial breakage events is given examplarily in Figure 22 (see the black circle symbols). The best fit to approximate this empirical data was a β-distribution, represented by the black line. A more profound discussion on that field is carried out in publication VII - Maaß and Kraume (2011).

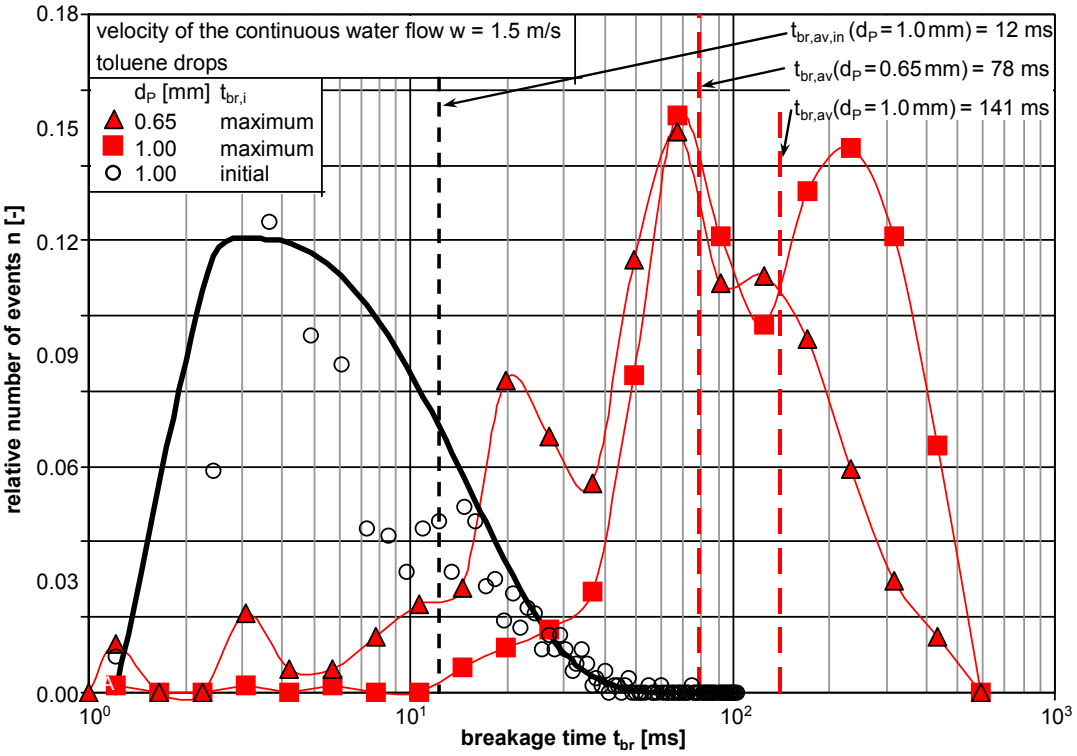

Figure 22 – Comparison of the relative number distribution of the maximum breakage time t_{br} for two different mother drops. The initial breakage time is compared with the maximum breakage time for the 1 mm mother drops. The initial breakage time was correlated using a β-distribution (black line).

The arithmetic average times are also given for all three distributions. All breakage time results are combined in Figure 23. This illustration also contains all data from publication VII - Maaß and Kraume (2011) together with the maximum breakage time results achieved in this study.

The comparison shows clearly, that the initial breakage time is two magnitudes smaller as the time from the first deformation until the maximum number of particles is achieved. But independent from the definition is used to analyze the breakage time, the duration of the breakage time from the petroleum drops are always longer than for the toluene drops. Already the physical properties (given in Table 5) revealed that the petroleum drops are more stable. The surface tension is higher and they are more viscous than the toluene drops. So it took more time to break the investigated samples. Note that the relevant drop sizes for stirred applications are most probable smaller than 1.0 mm. Therefore only these droplets have been analyzed concerning their maximum breakage time.

The results for the influence of the flow velocity on this specific consideration of the breakage time are given in Table 7. The increases in the flow velocity and turbulence led to a decrease in the breakage time. The dependency of t_{br} on $\varepsilon^{-1/3}$, derived from turbulence theory [Coulaloglou and Tavlarides 1977] is fulfilled in an acceptable experimental fluctuation.

Table 7 – Arithmetic average values of the maximum breakage time as a function of the flow velocity for petroleum and toluene mother drops with d_p = 1.0 mm.

	maximum breakage time $t_{br,av}$ [ms]	
flow velocity w [m/s]	petroleum	toluene
1.0	208	182
1.5	179	141
2.0	121	105

The influence of the flow velocity and therewith the energy dissipation rate is not discussed controversial in the literature. However, due to the lack of the influence of physical characteristics in the model of the t_{br} a new approach was derived and discussed in publication VII - Maaß and Kraume (2011).

Therefore, the interfacial tension as the dispersed viscosity are introduced into the breakage time modeling and additionally the use of the critical droplet Capillary number after Kumar et al. (1998).

Furthermore, the breakage times based on the turbulent pressure fluctuation were connected with those induced by the 2D elongational flow field in front of the rotating blade. It was considered that these mechanisms were operating simultaneously. The elongation of drops by accelerating rates $\dot{\varepsilon}$ [Stoots and Calabrese 1995] close to the blade are not considered in the description of common breakage time models. The experimental results show clearly, that drop elongation plays an essential role in the breakage processes. The new model equation is given as follows:

$$t_{br} = \frac{1}{c_{1,br}} \frac{n}{\dot{\varepsilon}} \ln\left(\frac{d_P \cdot \dot{\varepsilon} \cdot \eta_d}{\gamma \cdot Ca_{cr}}\right) \frac{d_P^{2/3}}{\varepsilon^{1/3}} \tag{14}$$

This correlation contains, like most PBE models, one fitting parameter $c_{1,br}$. The parameter was fitted only ones in the named study. After the fitting, the model was able to reflect the changes in the breakage time which occurred by switching from toluene to petroleum drops. The experimental results of the breakage time from publication VII - Maaß and Kraume (2011) are compared with the own developed model (see this publication also for the error analysis as for the parameter fitting procedure). The experimental results represent only the times for the initial breakage. As it was discussed in publication VII - Maaß and Kraume (2011), the peak values of a β-distribution are assumed to be more meaningful to characterize the breakage time distributions of the initial breakage event.

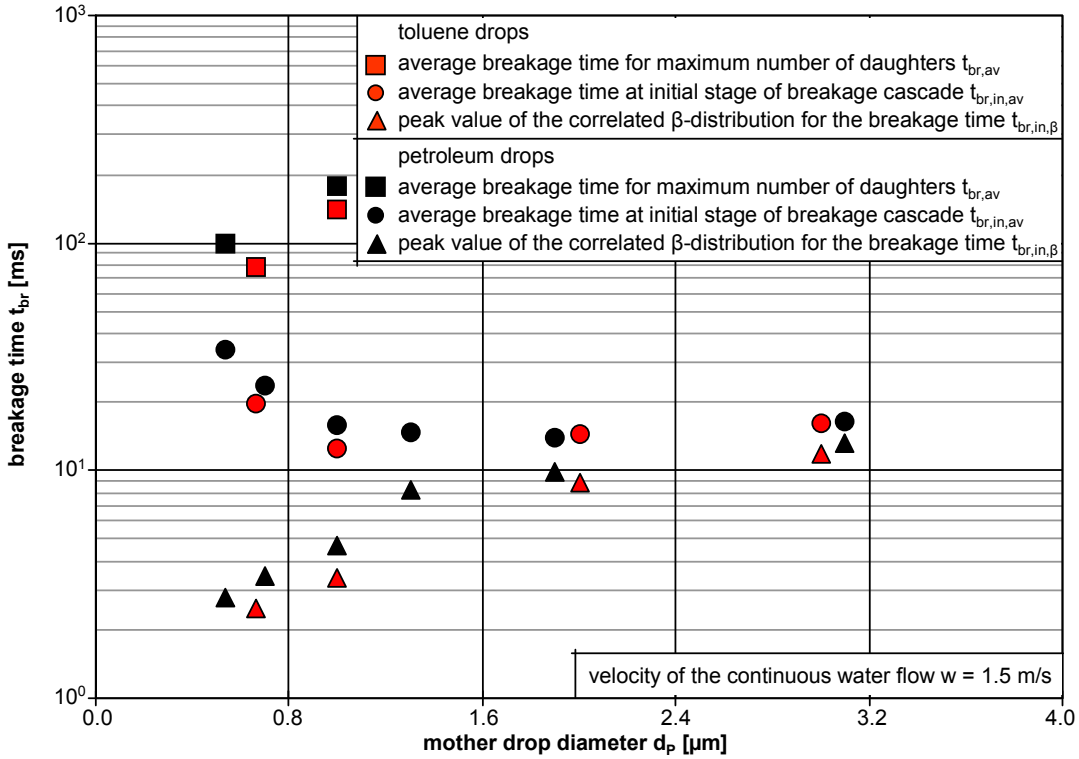

Figure 23 – Comparison of three different breakage times, the arithmetic average values for the time to achieve the maximum number of daughter drops, the arithmetic average value for the initial time of the first breakage event and the peak values of a β-distribution for the initial breakage times. Two different species are investigated at a constant flow rate of the continuous phase.

The experimental values are excellent reflected by the new model. Note that the standard models for the breakage time used in PBE simulations would also be able to predict one or the other system. As these models from literature are independent from any physical properties of the used chemicals, the variation between different chemicals can not be predicted. The new model overcomes this failure.

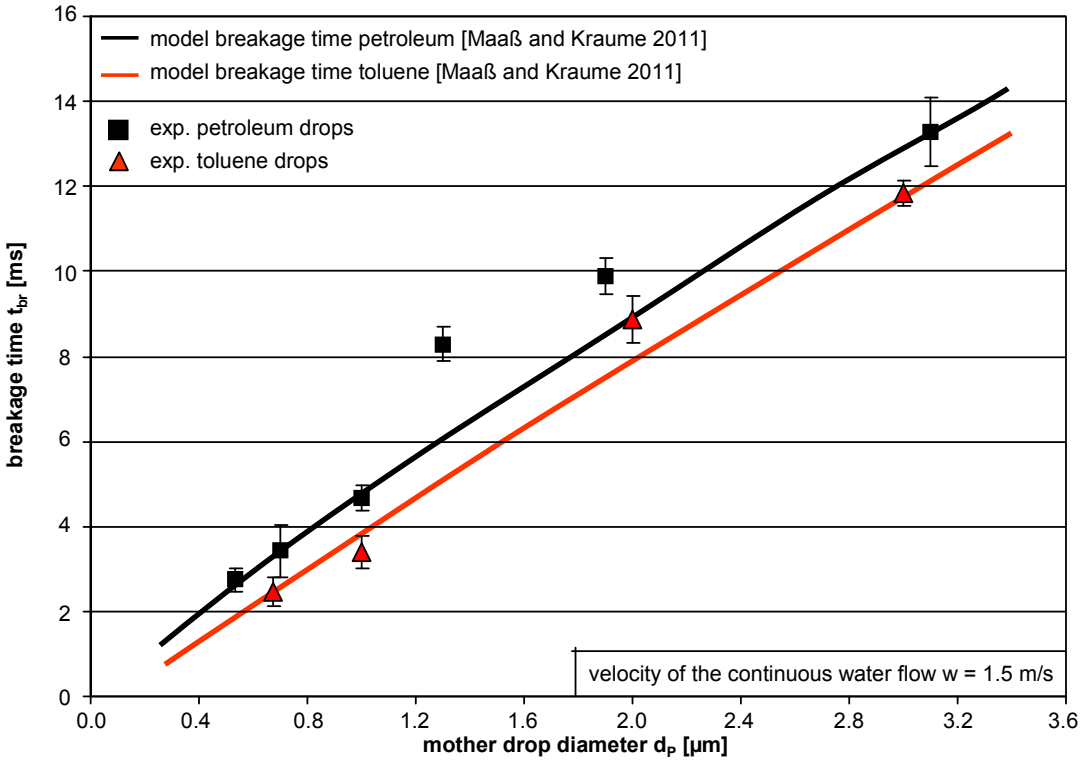

Figure 24 – Comparison between model data (lines) and experimental achieved values (symbols) for the breakage time at a constant flow rate.

The successful implementation of this model and promising simulation results are presented in publication X - Maaß et al. (2011e) and in chapter 6 (see page 57ff).

2. Daughter drop size distribution β

A mathematical formulation for the DDSD was derived in publication II - Zaccone et al. (2007). Daughter drop size distributions which often appeared in published works were analyzed in that publication concerning their ability to fulfill the mass balance. Often the sum of the predicted daughter drops volumes was not equal to the volume of the mother drop (see the work of Modes (2000) as one example).

Based on the general model by Hill and Ng (1996) and its further developments by Diemer and Olson (2002a) - (2000c) a very flexible formulation was derived in order to fit first experimental values achieved in the single drop breakage cell. The agreement with the experimental data was found to be very good, especially in comparison with other models most cited in the literature.

The model includes a dependency on physical parameters, such as the underlying turbulence via the Weber number, the mother drop diameter and the surface tension. Simulations have been carried out to verify the efficiency of the new model within the PBE framework in predicting transient drop size evolution in an agitated batch vessel. The agreement found with experimental transient drop size distributions for a toluene/water system was excellent (see Figure 25).

The developed model is still empirical, as the dependency on physical variables needs parameter fitting and further experimentation. Nevertheless, it represents achievements to a better knowledge of the physical situation and an advance in improving simulation efficiency of agitated liquid/liquid dispersions.

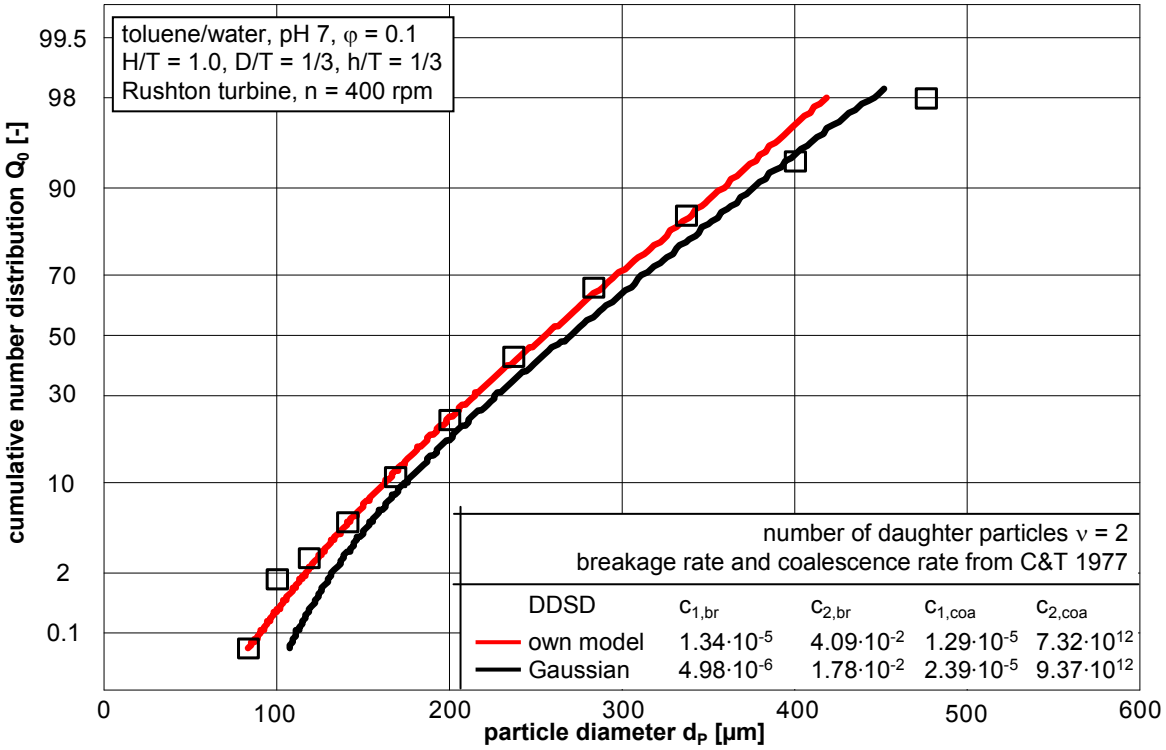

Figure 25 – Comparison between simulations and experimental data for a steady state drop size distribution in a stirred tank (Figure from publication I - Maaß et al. (2007) - reprinted with permission from Elsevier Science).

6. Results in the stirred vessel

The aim of this study was to investigate the influence of geometric factors, operating parameters and physical characteristic on the drop size distribution in an agitated liquid/liquid system with a focus on drop breakage. With the intention to evaluate the preciseness of the mathematical description of such l/l systems using population balances. The single drop experiments, discussed in the previous chapter, revealed already valuable insights in the drop breakage phenomena. Precise data for the number of daughter drops, the daughter drop size distribution and the breakage rate have been generated. Literature models have been evaluated based on these single drop results. Furthermore, own models for the DDSD and the breakage time have been developed to increase the prediction capacities of PBE models.

However, the industrial applications behind this thesis are agitated liquid/liquid dispersions. Therefore, the transient behavior of Sauter mean diameters and drop size distributions has been evaluated in different vessel. A complete list of the investigated parameters is given in the following section I, which is followed by the model evaluation and application section. There the prediction capacities of different PBE models applied to agitated systems are tested. Section III in this chapter presents a further model development based on experimental results in the stirred vessel.

I. Working program

The four organic liquids used as dispersed phase for this investigation were toluene, n-butyl chloride, anisole and cyclohexane - all with purities higher than 99.9 %. The continuous phase was always deionized water if no phase inversion occurred. The physical properties of each system are given in Table 8. A literature review on these values and more data including the influence of the used surfactant on the interfacial tension are given in publication X - Maaß et al. (2011e) and in the following subsection (see page 53ff).

In order to investigate the influence of different geometry factors and operation parameters on the drop size distribution in liquid/liquid systems, various experiments were carried out. An overview of the main influence parameter is given in Table 9. The size of the vessel, the aspect ratio, type and number of stirrer, the stirrer speed and the dispersed phase fraction variations are shown. Other parameters, like baffle immersion depth, baffle type, stirrer bottom clearance and stirrer height, which have also been investigated should be looked up in the publications IV - Maaß et al. (2010) and VI - Maaß et al. (2011b). The two different stirrer types, which have been used for the liquid/liquid experiments are a retreat curve impeller and a blade impeller with parallel (BI) and crossed blades (CBI).

Table 8 – Properties of used chemicals.

	γ [mN/m]	ρ [kg/m³] at 20°C	η_d [mPa·s]
n-butyl chloride	37	886	0.43
toluene	36	870	0.55
anisole	25	996	1.02
cyclohexane	51	774	1.15

II. Model evaluation and application

Based on the description of the flow field using CFD simulations, a PBE model was applied, which predicted the influence of broadly varying geometric factors, operating parameters and physical characteristics with satisfying results. To assure a breakage dominated system, the influence of polyvinyl alcohol as emulsifier was studied. These unpublished results are given in the next subsection. Furthermore, the results presenting the broad variety of parameters are summarized in the following subsections.

Table 9 – Overview of the measurement program - analyzing the influence of geometry factors and operation parameters on the n-butyl chloride/water system.

T [mm]	H/T [-]	stirrer type	number of stirrers	n [rpm]	φ [-]	source
155	1.0, 1.4, 1.5, 2.0, 2.3	RCI and BI	one	250, 400, 550, 700	0.25 and 0.45	Maaß et al. 2010
155	1.4, 2.8, 4.0, 5.0	BI and CBI	one and four	250, 410, 600	0.25	Maaß et al. 2011b
460	1.4 and 2.8	BI and CBI	one and four	200	0.25	Maaß et al. 2011b
155	1.4	BI	one	410	0.02 - 0.6	Maaß et al. 2011e

1. Influence of polyvinyl alcohol

The influence of surface agents in general and of polyvinyl alcohol (PVA) specifically on the l/l dispersion properties is extensively discussed in literature[i]. PVA is used as a stabilizer in different industrial fields, especially in suspension polymerization. It has been established that the stabilizing properties are dependent on the concentration, degree of hydrolysis and the molecular weight [Yang et al. 2000]. The degree of hydrolysis (72%) and the molecular weight (3586 g/mol) were kept constant for all experiments.

The exact knowledge of the interfacial tension in the used liquid/liquid systems is of great importance for the simulations of the drop size distributions. Furthermore, the measurements of the interfacial tension in dependency of the PVA concentration provide essential information of the coverage of interfacial active molecules (PVA molecules) at the l/l interface. In this work a breakage dominated system was observed, hence a complete coverage is needed to hinder the coalescence completely.

The interfacial tension was measured for different PVA concentrations (0-3 mg PVA/ g dispersed phase[ii]). The time the PVA molecules need to adsorb at the interface has to be considered. Therefore, transient pendant drop measurements have been carried out. The interfacial tension of a droplet of a certain volume was observed for a definite time. For high surfactant concentrations the time that the system need for reaching the steady state is reduced [Chatzi and Kiparissides 1995]. The results for the interfacial tension measurements are reported in publication X - Maaß et al. (2011e). While all PVA concentrations are less than 10 mg/g, the physical properties of the continuous phase do not significantly vary from those of pure water [Chatzi et al. 1991]. The physical properties of the four organics used as dispersed phase in this study are all given in publication X - Maaß et al. (2011e). Additionally, own measurements of the interfacial tensions for the pure components with deionized water are compared with literature values there.

The influence of the PVA concentrations on the transient Sauter mean diameter of n-butyl chloride/water is given in Figure 26. Independent from the concentration, all Sauter mean diameters are decreasing over time as expected. The influence of the PVA is strong. Already small amounts of the surfactant lead to a significant decrease in the drop size. The influence of the further increased concentration is much weaker. However, an increase in PVA concentration is leading to a consequent decrease in d_{32}.

The intense influence of already small amounts of a surfactant was explained by Koshi et al. (1988) with interfacial instabilities. They state that the breakage of drops in stirred dispersions is influenced by the presence of surfactants not only through the reduction of the interfacial tension, but also by the generation of an interfacial tension gradient[iii] across the drop. This results in an extra stress which adds to the turbulence stress and hence results in the easier breakup. The effects are small when the difference in dynamic and equilibrium

[i] See El-Hamouz (2009) for an updated literature review on published work related to liquid/liquid dispersions with respect to surfactant use. The work of Chatzi et al. (1991) as the work of Chatzi and Kiparissides (1994) are recommended for fundamental studies dealing with the influence of PVA on interfacial tension as on the drop sizes in l/l systems.

[ii] Note that the concentration of PVA is related to the amount of mass of the organic phase, opposed to standards in literature which relate it to the amount of mass of the aqueous phase. This procedural deviation from standard methods was received from our industrial cooperation partner. As it was their standard communication due to a constant phase fraction in all their processes. However, since density and dispersed phase fraction are always known in this study, these values can easily be transformed into the standard description for the interested reader.

[iii] The effect of interfacial tension gradients was discovered by Carlo Giuseppe Matteo Marangoni in the 19th century. For a detailed introduction into this field and extensive studies about this phenomenon the work of Wegner (2009) is recommended.

interfacial tension are small (Koshy et al. 1988). This effect was only detectable for low viscosity fluids as the ones used in this study. To better judge the order of magnitude of the influence of this phenomenon, the knowledge about the critical micelle concentration (CMC) is crucial.

The differences between the values for the dynamic and equilibrium interfacial tension are low for surfactant concentrations above the CMC. The values for the CMC concentrations of all investigated systems can be found in publication X - Maaß et al. (2011e). For the presented n-butyl chloride/water system it is around 0.9 mg/g. To avoid the influence of additional interfacial instabilities, mostly PVA concentrations above the CMC have been used in the drop swarm experiments.

The influence of the PVA concentration on the coalescence behavior can be seen in Figure 27. Here, the liquid/liquid system was first dispersed at 410 rpm (results are the same as in Figure 26). After 1 h of mixing the stirrer speed was decreased to 250 rpm (dashed line in Figure 27) and the drop size was still measured for 4 h.

The PVA concentration shows a significant impact on the coalescence behavior. A critical concentration exists, where the drops are completely stabilized as the measured d_{32} stays almost constant after the stirrer speed decrease for two of the three investigated cases. For the lowest surfactant concentration d_{32} is strongly increasing after the stirrer speed decrease. The complete hindrance of coalescence was used in all drop swarm studies (see the results in publication IV - Maaß et al. (2010), VI - Maaß et al. (2011b) and X - Maaß et al. (2011e).

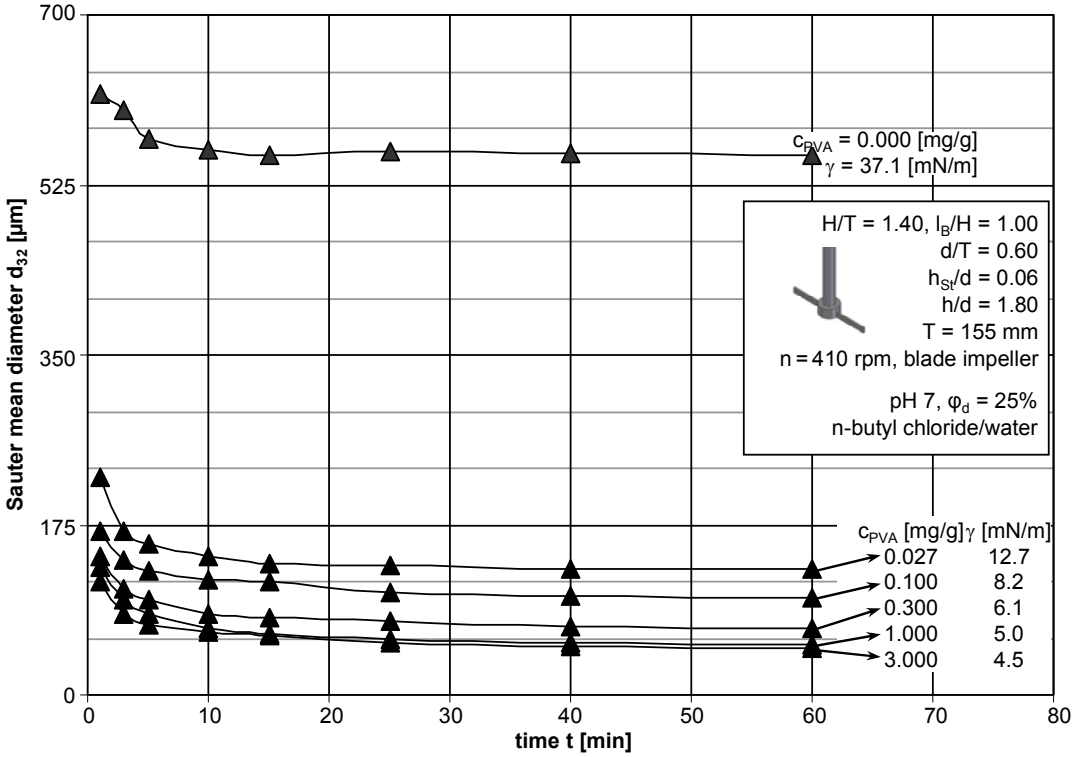

Figure 26 – Transient Sauter mean diameters d_{32} of n-butyl chloride/water systems for different PVA concentrations.

This critical concentration could be correlated with the CMC (see publication X - Maaß et al. (2011e) for details). If the PVA concentration is above the CMC, then the influence of PVA concentration on the timely drop size evolution can be predicted using PBE models. Such results are presented in Figure 28. The simulations for the two concentrations $c_{PVA} > 0.9$ mg/g are predicted in good agreement with the experiment. The possible occurrence of coalescence for $c_{PVA} = 0.3$ mg/g leads to an underestimation in the prediction of the drop sizes over time by the model. The breakage parameters have been set constant after fitting them against a long term breakage experiment. The experiment is presented in publication X - Maaß et al. (2011f) with $c_{PVA} = 3$ mg/g. For these high PVA concentrations the coalescence is completely inhibited and therefore the coalescence parameters are set to zero.

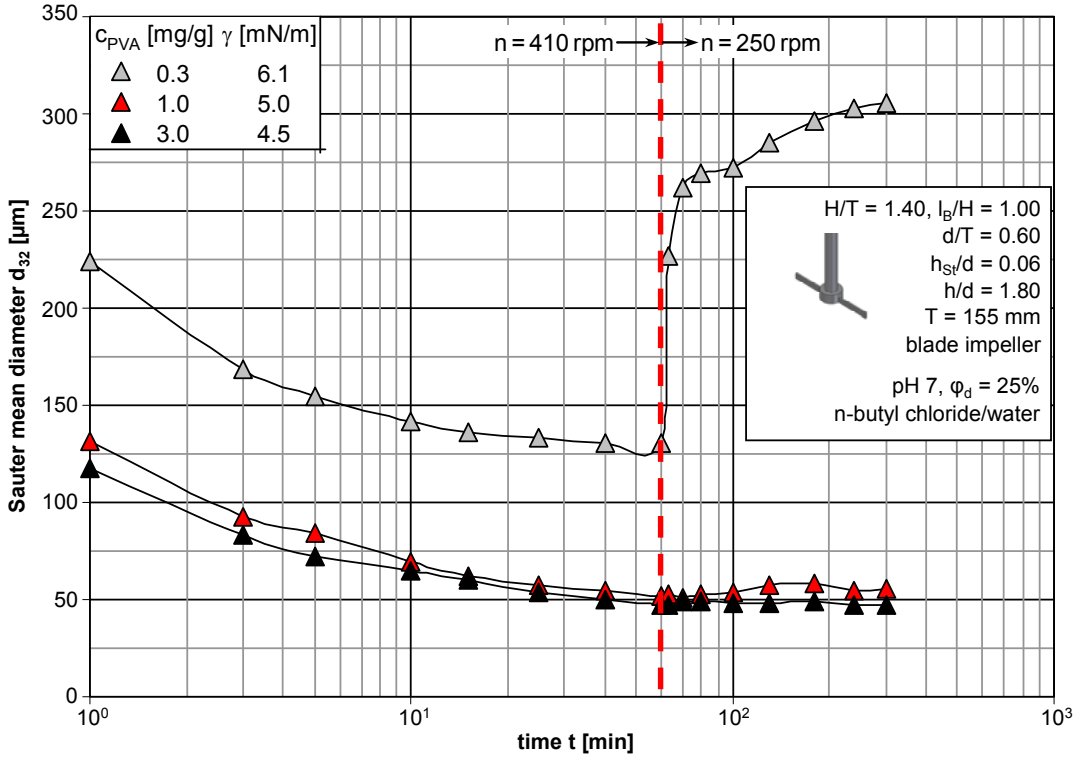

Figure 27 – Transient Sauter mean diameters of n-butyl chloride/water system for different PVA concentrations to evaluate the coalescence behavior.

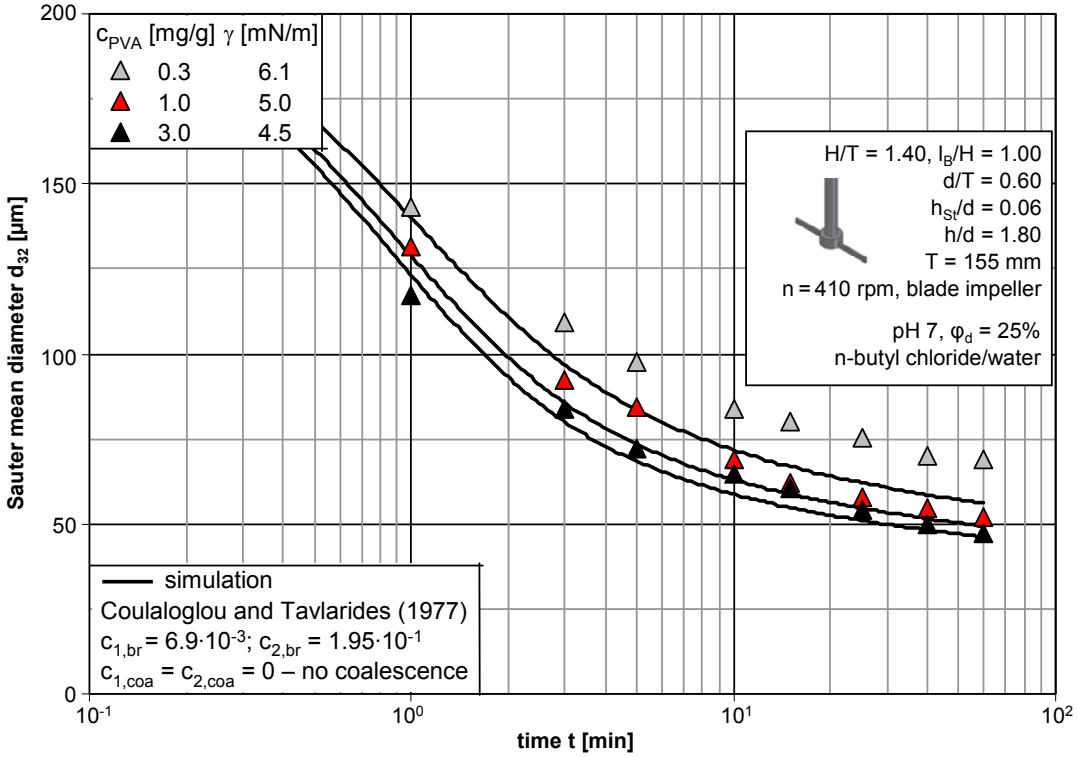

Figure 28 – Comparison between experiments (symbols) and simulations (lines) of the transient d_{32} for various PVA concentrations.

2. Prediction of the influence of geometric factors

The results in publication IV - Maaß et al. (2010) and VI - Maaß et al. (2011b) show clearly that the influence of geometric factors as liquid level, stirrer height, stirrer type, stirrer bottom clearance, baffles type and vessel size can be predicted for single stage impellers using constant numerical parameters in the PBE model. The achieved deviations between the measured and calculated transient Sauter mean diameters have been smaller than 10%. An experimental scale-up could be reproduced with the used PBE model and shows the promising capacities of such approaches.

One constrain for the successful use of these PBE models was the use of the already discussed 2-zone model. The assumption of the well mixed condition using only one average value for the energy dissipation failed to predict the discussed variation of geometric factors and operation parameters. The prediction capacities of the 1-zone and the 2-zone model have been additionally compared to prediction results using Weber number correlation ($d_{32} \sim \varepsilon^{-0.4}$). These results from publication IV - Maaß et al. (2010) are presented in Figure 29. The outstanding results for the scale-up of single stage impellers from publication VI - Maaß et al. (2011b) are shown in Figure 30.

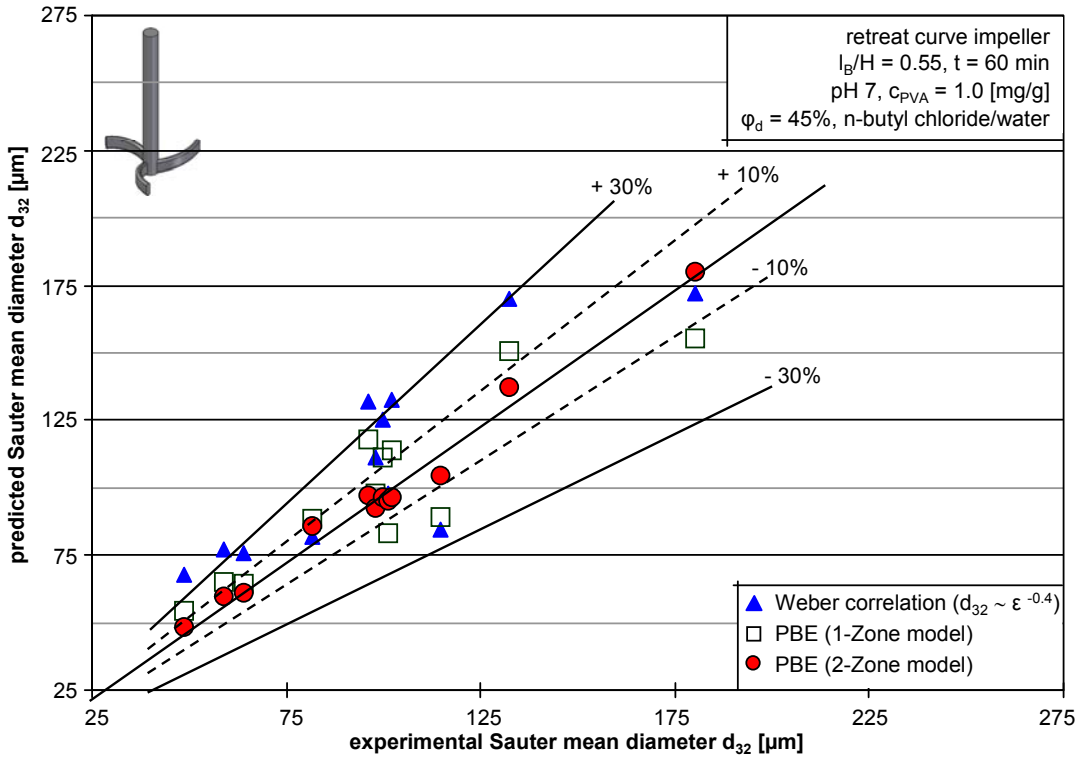

Figure 29 – Deviation of experimentally achieved d_{32} and three different drop size prediction methods after 60 min mixing at different stirrer speeds, different H/T (1.0 – 2.3) and with different retreat curve impellers (h_{St} = 0.12 and 0.24). Reprinted with permission from Elsevier Science.

The prediction results for multiple impeller systems have been excellent for the transient Sauter mean diameter, the number of stirrers, the stirrer - stirrer distances and the liquid level. Deviations smaller and around 10% have been achieved in those cases. The scale-up of a multiple impeller system by increasing the vessel diameter for geometric similarity do not lead to a clear conclusion. Although the simulations recommend the use of constant power input, the experiments could not support this. The experiments did not follow any traditional scale-up rule.

The prediction of the influence of the baffle length was unacceptable. The reason for this failure is not clear yet (see also the chapter 4 for a discussion on the influence of the immersion depth of the baffles on the flow field).

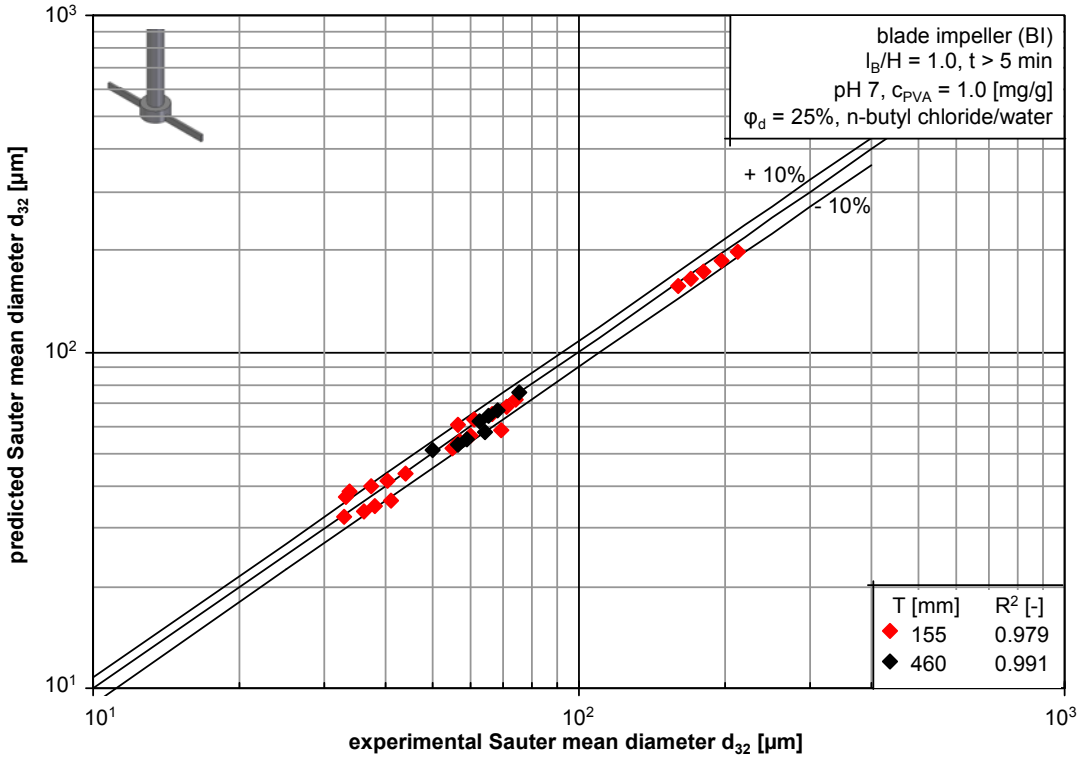

Figure 30 – Deviation between experimental and predicted d_{32} with the two-zone PBE simulations at different stirrer speeds (200 - 600rpm), H/T ratios (1.4 & 2.8) and different BI's (h_{St} = 0.06 and 0.24). Reprinted with permission from Elsevier Science.

3. Prediction of the influence of operating parameters

One major operating parameter in agitated industrial applications is the stirrer speed n. The influence of n was studied in publication IV - Maaß et al. (2010) and VI - Maaß et al. (2011b), for two different kinds of impellers with varying stirrer height (retreat curve impeller and flat blade impeller). The achieved prediction results were excellent. The deviations between the measured and calculated transient Sauter mean diameters were always lower than 5%. Problems only occurred when the system was not completely dispersed. This happened in both studies for low stirrer speeds. This ineffective operation procedure of the system lead to stronger deviations, especially in the beginning of the process, as the complete dispersion was mostly reached within 15 min even for the lower stirrer speeds which have been investigated.

The multi stage impellers have been tested against comparable single stage impellers in terms of power consumption, mixing time and minimum impeller speed. Especially for aspect ratios H/T larger than three, multi stage impellers successfully compete with the single stage ones.

The effect of the dispersed phase fraction on the evolving drop size distribution in different low viscous liquid/liquid systems was investigated. The analysis is presented in publication X - Maaß et al. (2011e). The measured drop sizes were increasing with increasing dispersed phase fraction. As coalescence was completely hindered and also the measured emulsion viscosity showed no influence on the dispersed phase hold-up, the size increase was a result of turbulence hindering. Therefore, the influence of the φ_d was well reproduced with PBE simulations. The used breakage models require a turbulence damping factor $(1+\varphi_d)$, which is used in most of the common models. As this is not the case for the model of Alopaeus et al. (2002), this model was extended (see the III. section: Model development in this chapter).

The accuracy of the PBE simulations was excellent (coefficient of determination $R^2 > 0.97$). The used Weber correlations ($d_{32}/D = C_1(1+C_2 \cdot \varphi)We^{-0.6}$, see publication X - Maaß et al. (2011e) for the parameter details) were also able to reproduce the linear interdependency between the drop size and the dispersed phase fraction. Challenges occurred for an increasing dispersed phase fraction above a critical value which led to phase inversion (see the IV. section: Occurrence and hindrance of phase inversion in this chapter) and could not be predicted with any of the tested model approaches. Also the change in the used organics caused some problems which will be discussed in the next section.

4. Prediction of the influence of physical characteristics

Four different organic solvents were used as dispersed phase: anisole, cyclohexane, n-butyl chloride and toluene. All associated physical properties are listed in publication X - Maaß et al. (2011e).

The pioneer model by Coulaloglou and Tavlarides (1977) was used to predict the time dependency drop size evolution as in all other already presented simulations. As this model does not take viscous effects into account, the model of Alopaeus et al. (2002) and an own developed model (already discussed in section III in chapter 5) were used.

The comparison between the simulation results by the model of Coulaloglou and Tavlarides (1977) and the own developed model show clearly, that the drop size evolutions of all four liquid/liquid systems are better described by the new model (see Figure 31, left - the results with Colulaloglou and Tavlarides (1977) and right - the results with the new model). Both models show only moderate, almost poor results for the cyclohexane/water system while the other three systems are predicted excellently.

The prediction results with the model based on Alopaeus et al. (2002) are worse for three of the four systems compared to the two other mentioned models. However, the absolute values are still acceptable. The results for the cyclohexane/water system are much better compared to the values achieved with Coulaloglou and Tavlarides (1977) and the own model. This shows some promising capacities in this model approach.

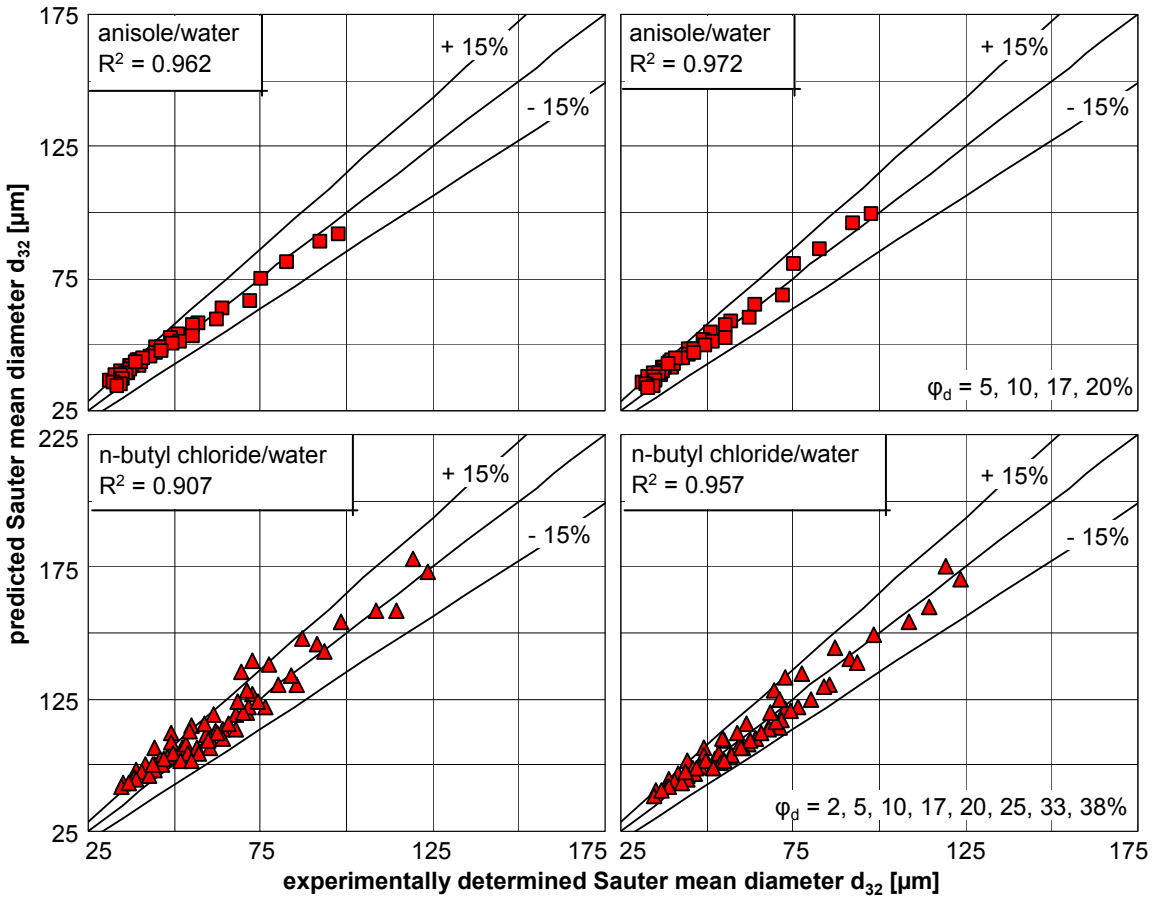

Figure 31 – parity plot evaluating the simulation results using the breakage rate of Coulaloglou and Tavlarides (1977) - left and the new model from publication X - Maaß et al. (2011e) - right.

III. Model development

The results, already discussed in the previous section, dealing with the influence of the dispersed phase fraction on drop breakage have been used to propose a new model. The simulations were reflecting the influence of φ_d on d_{32} excellently, if φ_d is not only considered via the mass balance, but with a direct affect on the breakage rate. If not, all simulations fall into the same curve as it was shown for the original model by Alopaeus et al. (2002) (see Figure 32 - left).

An extension of the standard model by Alopaeus et al. (2002) was derived. The inclusion of the assumption that the turbulence is damped by an increase in φ_d achieved excellent prediction results (see Figure 32 - right). The value achieved for the coefficient of determination R^2 was larger than 0.97. The influence of the dispersed phase fraction was expressed by a dampening of $\varepsilon^{1/3}$ by a factor of $(1+\varphi_d)^{-1}$. The slightly extended breakage rate model approach is given as follows:

$$g(d_p) = c_{1,b}\frac{\varepsilon^{1/3}}{(1+\varphi)}\cdot \mathrm{erfc}\left(\sqrt{\frac{c_{2,b}\gamma\,(1+\varphi)^2}{\rho_c d_P^{5/3}\varepsilon^{2/3}}+\frac{c_{3,b}\eta_d\,(1+\varphi)}{\sqrt{\rho_c\rho_d}\,d_P^{4/3}\varepsilon^{1/3}}}\right) \tag{15}$$

Further details on the model and the used PBE framework for this prediction study are given in publication X - Maaß et al. (2011e).

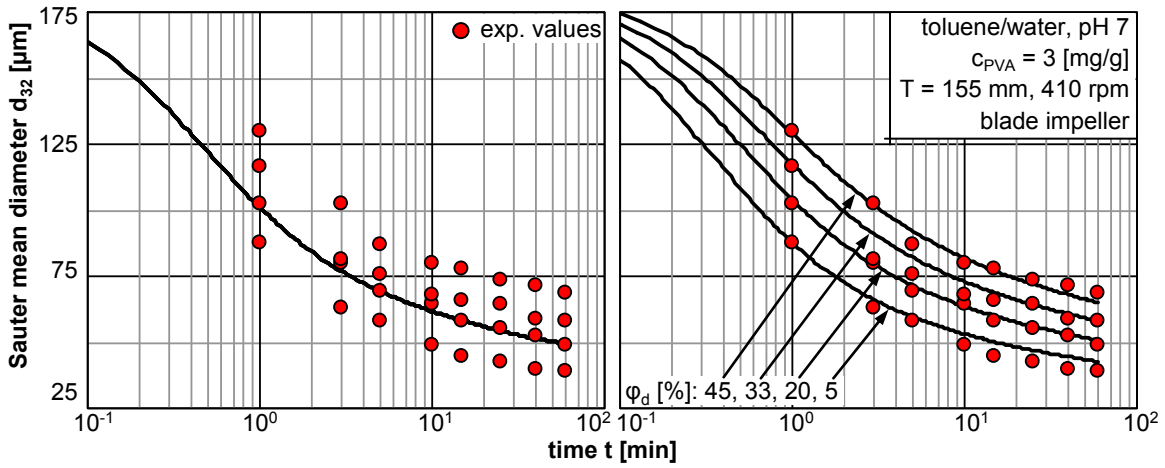

Figure 32 – Comparison of experiments (symbols) and simulations (lines) for the influence of dispersed phase fraction on transient Sauter mean diameter for the toluene/water system for the standard breakage model by Alopaeus et al. (2002) - left and the extended version of this model from equation (15) - right.

IV. Occurrence and hindrance of phase inversion

Phase inversion (PI) is the transitioning of oil dispersed in water (o/w) to water dispersed in oil (w/o), or vice versa. It can occur in more concentrated systems as a result of changes in stabilization, physical properties or phase proportions [Leng and Calabrese 2004].

The spontaneous inversion can be disastrous for most of the industrial processes presented earlier in this study. Many contradicting information exists on the ideas of phase inversion. Nienow (2004) summarizes his literature review on this field of research as follows: The fact that nothing better has been proposed for approximately 40 years shows how poorly the phenomenon is understood.

The study on the influence of the dispersed phase fraction (see publication X - Maaß et al. (2011e) for details) led to some boundaries in the dispersion process where PI occurred. The results of this process failure are presented in Figure 33. Example images of this process are given as a comparable transient series of single images in Figure 34. The dispersed phase fraction for the n-butyl chloride/water system was increased from 38 to 45% (see Figure 33 (a)). That led to a dramatic increase in the Sauter mean diameter. Additionally, the coalescence test (decreasing n to 250 rpm after 1h of agitating with 410 rpm) showed a strong increase in d_{32} (see Figure 33 (a)). As this was an unexpected behavior the same experiment was repeated and additionally two further experiments with $\varphi_d = 0.42$ and 0.5 have been carried out.

The results were concussive. The experiment with 45 % dispersed phase fraction, the retest, showed for the first 70 min of mixing exactly the same results as the first experiment with $\varphi_d = 45$ % shown in Figure 33 (a). Also the two other experiments showed the same behavior with unexpected large drops and strong coalescence behavior after decreasing the stirrer speed (see Figure 33 (b)). Furthermore, the retest run showed an unstable behavior after the stirrer speed decrease. The drop size was fluctuating (see also the example photos in Figure 34).

The separation behavior after the agitator was turned off, revealed the true nature of these systems. The dispersion had come to a point of phase inversion. The dispersed phase was now the heavier water phase which sank down after the shut down of the power input.

There are two types of phase inversions; transitional phase inversion and catastrophic phase inversion. For transitional phase inversion to happen the affinity of the surfactant(s) must be changed by either changing the temperature or changing the composition of the surfactant mixture at a constant temperature. A catastrophic phase inversion is triggered by increasing the rate of drop coalescence. This is usually brought about by increasing the effective volume fraction of dispersed phase either by continuous addition of the dispersed phase, or even by continuous stirring of the emulsion [Jahanzad et al. 2009].

As it is mentioned in literature, that the method of adding the disperse phase plays an essential role, a new filling procedure was used to produce the dispersion for a system with $\varphi_d = 0.6$. The stirrer bottom clearance was minimized and the agitation started in water which contained already the complete amount of the surfactant. After the agitation had started, the dispersed phase was added continuously. The stirrer position was changed back to the original position after the filling was complete. The values for the Sauter mean diameter achieved for the 60% dispersion are given in Figure 33 (c).

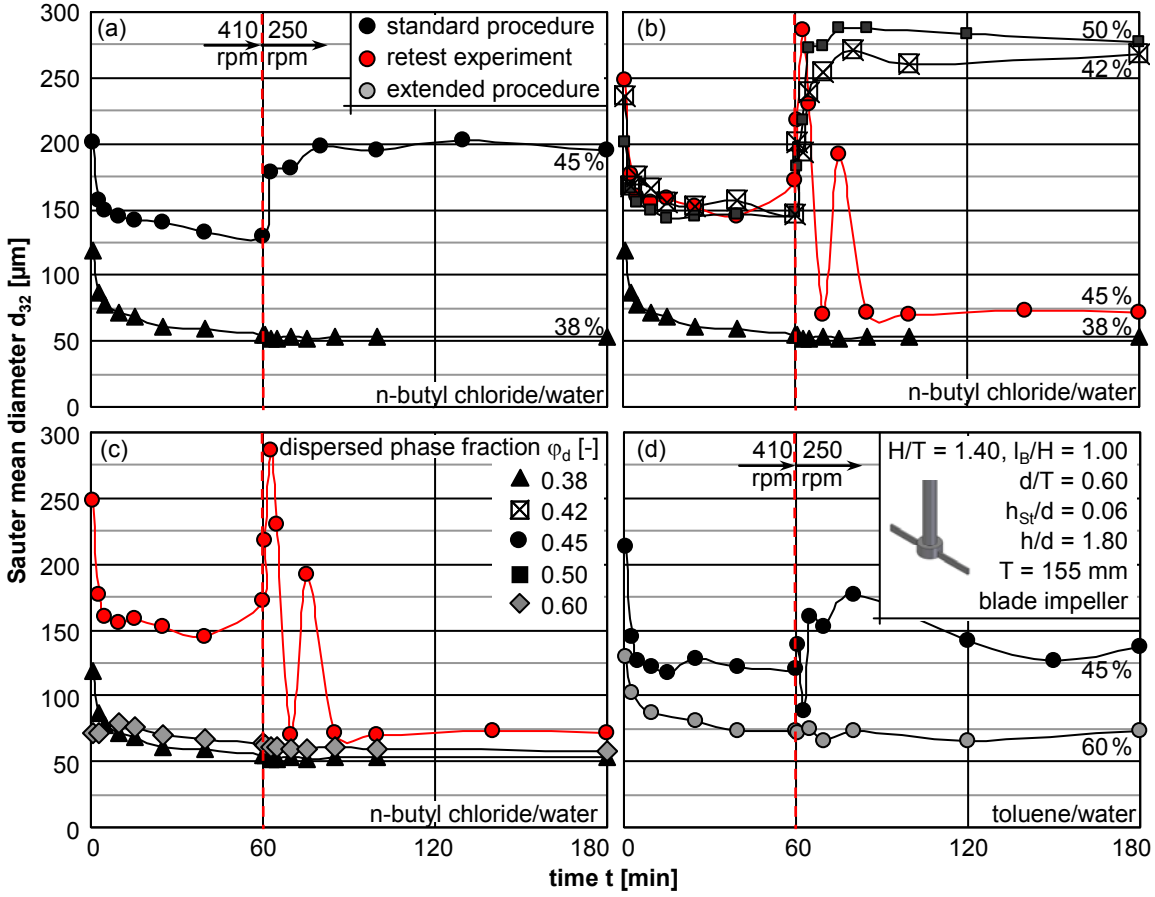

Figure 33 – Dependency of system phase inversion on the dispersed phase fraction and operation procedure (a) - (d) chronological order of experiments. (a) - occurrence of phase inversion above 38 % dispersed phase fraction, (b) - occurrence of phase inversion above 42 % dispersed phase fraction, (c) - hindrance of phase inversion by stirring during filling the reactor with 60 % dispersed phase fraction, (d) - repeated results of (c) with toluene instead of n-butyl chloride.

This procedure was successfully applied to another system. While catastrophic phase inversion also occurred to the toluene/water system for $\varphi_d = 0.45$, the experiment was repeated using the alternative filling method. The results are given in Figure 33 (d).

Catastrophic phase inversion occurred despite this filling method for a multiple impeller system with an aspect ratio of 5. This result is described in publication XI - Maaß et al. (2011f). Phase inversion with the building of a double emulsion (w/o/w) was observed at the top of the slim reactor while the expected o/w dispersion was measured at the bottom. A periodically decrease and strong increase and then decrease to the original stirrer speed broke up the double emulsion and the boundary of phase inversion. Homogeneous n-butyl chloride/water dispersion was reached with spatial independency throughout the complete reactor.

The used endoscope measurement technique (see publication V - Maaß et al. (2011a)) together with presented image analysis tool (see publication XI - Maaß et al. (2011e)) are able to monitor such process failure online. It provides therewith an interesting opportunity for observation based process control.

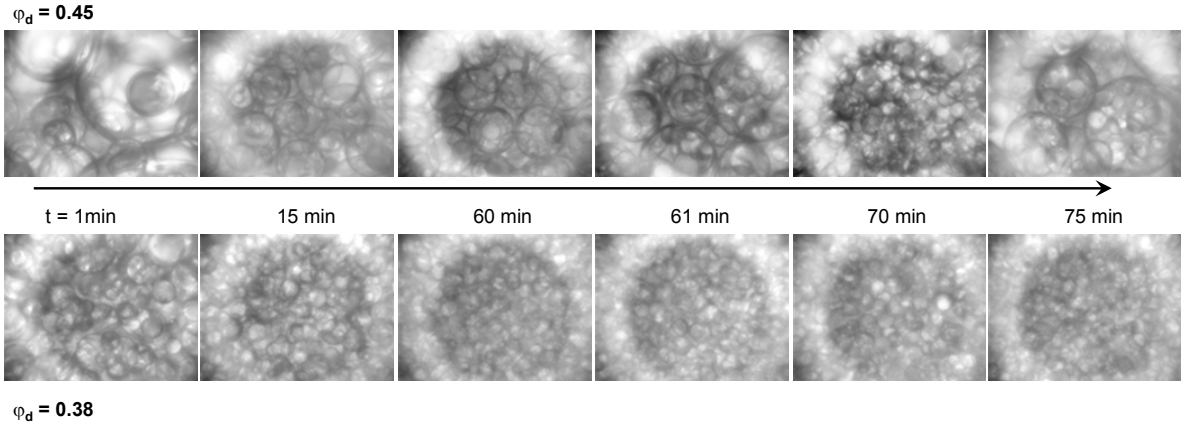

Figure 34 – Comparison of example images below and above the critical concentration of φ_d for the appearance of phase inversion. The stirrer speed was 410 rpm in the first 60 min for both investigated concentrations and was decreased after 60 min of mixing to 250 rpm. The water drops (φ_d = 0.45) are much larger than the n-butyl chloride drops (φ_d = 0.38).

V. Concluding remarks on the results in the stirred vessel

It was found in this project that the simulations using population balance equations were able to reproduce experimental drop size results for a broad variation of geometric factors, operating parameters and physical characteristics. The complete list and a short evaluation are given in Table 10. As it can be seen from the table, the PBE is already a powerful tool to provide trustful prediction results. Only the influence of the immersion depth of the baffles on the evolving drop sizes was reproduced with poor results. All variation of operation parameters and physical characteristics could be predicted with good too outstanding results. Although boundaries were reached in this study, they mostly occurred for systems were also coalescence was active. Therefore, it can be concluded that the simulation of breakage dominated systems is well represented by PBE models.

Further necessary development steps are a better implementation of physical characteristics (disperse phase viscosity seems most important - see publication X - Maaß et al. (2011e) for a more detailed discussion) and detailed studies on scale-up with multiple impeller system. Single stage impeller systems were scaled up without any objections.

Table 10 – Overview of the analyzed aspects in the drop size simulation studies and their accordance with results from own experimental investigations (+ good; +/- works for some cases; - poor) for breakage dominated systems.

	evaluation	publication
Geometric factors:		
reactor size T	+/-	VI - Maaß et al. (2011b)
reactor aspect ratio H/T	+	IV - Maaß et al. (2010) and VI - Maaß et al. (2011b)
stirrer type	+	IV - Maaß et al. (2010) and VI - Maaß et al. (2011b)
stirrer height h_{St}	+	IV - Maaß et al. (2010) and VI - Maaß et al. (2011b)
number of stirrers n	+	VI - Maaß et al. (2011b)
baffle type	+	VI - Maaß et al. (2010)
immersion depth of baffles l_B	-	VI - Maaß et al. (2011b)
Operating parameters:		
stirrer speed n	+	IV - Maaß et al. (2010) and VI - Maaß et al. (2011b)
dispersed phase fraction φ_d	+	X - Maaß et al. (2011e)
stabilizer concentration c	+	this study
Physical characteristics:		
interfacial tension between the immiscible liquids γ	+/-	this study
density of the dispersed phase ρ_d	+	X - Maaß et al. (2011e)
viscosity of the dispersed phase η_d	+/-	X - Maaß et al. (2011e)

7. Further steps in breakage modeling

Although all most tested models could predict the drop size distribution evolution reasonably well, the parameters needed to be adjusted at least once to fit the experiments well (see especially publication VI - Maaß et al. (2011b) for the parameter estimation procedures). More parameter adjustments may be necessary for a wider range of geometric factors, operating parameters or physical characteristics. Therefore, the physical meaning of the single model parts is discussed in this chapter to formulate more realistic and more reliable models for the breakage phenomena in liquid/liquid systems.

I. Initial breakage time versus sequence breakage time

It was shown in numerous studies [Janssen et al. 1994; Janssen and Meijer 1993; Megias-Alguacil and Windhab 2006; Stone 1994; Taylor 1934] experimentally, analytically and numerically that multiple drop breakage is common under laminar and shear flow conditions. Opposed, the likelihood of two or more breakage events taking place simultaneously, i.e., generating more than two daughter drops, precisely at the same time in turbulent flow is very small. This assumption was already discussed in publication IX - Maaß et al. (2011d). However, this is a general observation which led to the conclusion that binary breakage is most probable and therefore, is widely used in literature as in all publications associated with this thesis.

As it was shown in the previous chapter, this is only true if the initial breakage is considered as the described breakage event. If the description of the event stops there, the existing deformations and oscillations caused by the initial or previous breakage events are assumed to be fully dissipated before a new breakage takes place. The same is already true for the collision with a turbulent eddy which may have not lead to breakage but to a certain deformation or oscillation.

This assumption is questioned in Figure 35. A 3 mm drop, which is moving from left to right, broke at the tip of the stirrer blade into two fragments (see also the complete breakage sequence in Figure 18). The presentation in Figure 35 contains the original breakage sequence after image processing and a model representation of this breakage event which assumes the restoration of spherical drops after each breakage event. This restoration is equal to the assumption that all deformations or oscillations are dissipated after the first breakage and that they are not relevant for further events.

The model representation was illustrated under the condition to fulfill the mass balance for the initial mother drop. Figure 35 shows clearly that the discussed assumption is much too rough. Of course the surface deformations and oscillations do not completely disappear. Therefore, it is much easier to break up this already elongated lump into further individuals.

Note that not every elongated drop broke. In several instances drops that had stretched to cylinders of length several times their initial diameter were observed to retract. That showed, that it was still a question of probability if a drop broke.

However, from a physical point of view, these observations should be reflected by the drop breakage models. It means that the surface oscillation from previous collision should be at least partly remembered by the drop for example in form of a accumulated energy. It is commonly believed that this energy may have a contribution to the total energy required for the next breakage. Nevertheless, the energy contained in an oscillating droplet is difficult to be determined since the energy dissipation mechanism on the surface is still unclear [Han et al. 2011].

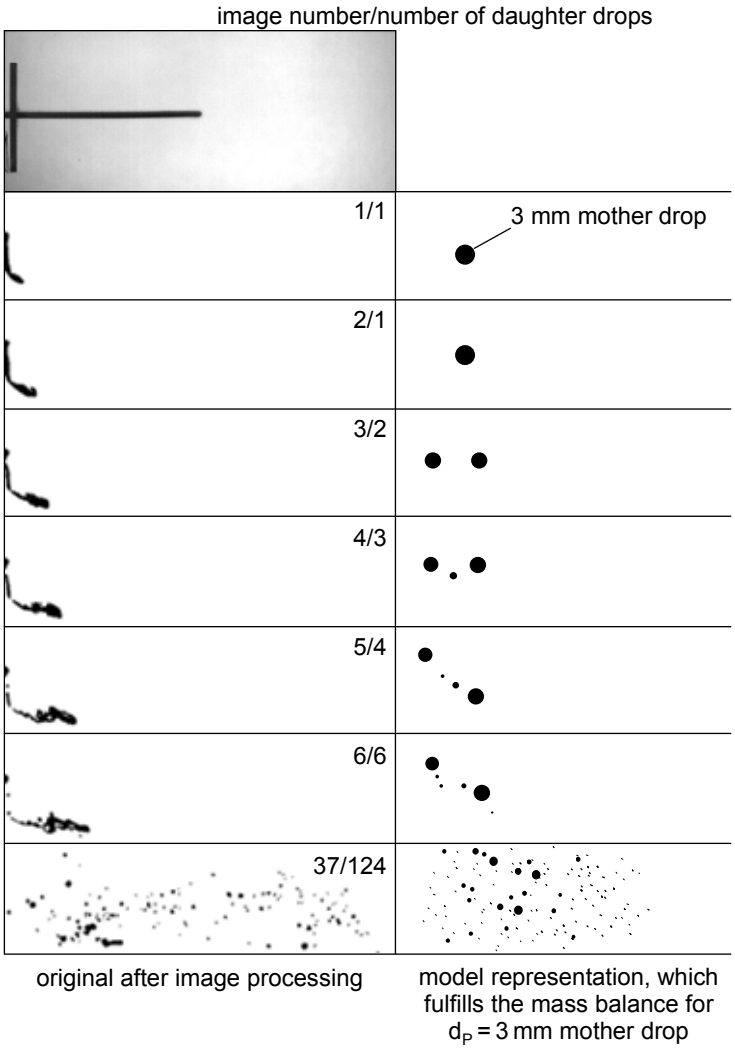

Figure 35 – Comparison between a real drop break-up and its corresponding sequence in terms of the assumption of spherical drops for a 3 mm toluene drop at a flow velocity of 1.5 m/s.

The description of such a breakage sequence does not necessarily need to track every single deformation and its consequence on the breakage. The single events could also be interpreted as the sum of the individual events. Therefore, only the initial drop is seen as a sphere and also the sum of the volume of the occurring daughter drops is seen as spherical. That this is a more precise assumption can be seen on the last image comparison in Figure 35. After several breakage events, the remaining fluid particles can be assumed as spherical drops with fair approximation. The same analysis as for the 3 mm toluene drop was carried out exemplary for one of the smallest investigated diameters, which are more relevant to agitated applications. The comparative results between the original images and the model representation are given for 0.65 mm toluene drop in Figure 36. Also the smaller drop was considerable elongated before it broke, which is in good agreements to the results of Konno et al. (1983). Again the assumption of only binary breakage would neglect the elongation which had a significant influence on the following breakage events.

With the interpretation of a breakage event as a sequence of breakages, the average number of daughter drops as its drop breakage time increases as shown in the previous chapter. The consequences on the PBE simulations will be discussed in the following paragraphs.

The choice of the number of daughter particles directly influences the other breakage model parts in the PBM framework [Ramkrishna 2000]. It is obvious, that the change of ν or the daughter drops size distribution $\beta(d_p, d_p')$ will directly effect the breakage rate $g(d_p)$ and therewith always the values of the numerical parameters. A computational sensitivity analysis for the number of daughter fragments is given in Figure 37. Experimental results for a coalescing (data from Gäbler et al. (2006)) and a non coalescing system (data from publication X - Maaß et al. (2011e)) are compared with simulation results using the standard model of Coulaloglou

and Tavlarides (1977) for various daughter drops. The increase in the number of daughters led to smaller drop sizes while everything else in the model remained constant.

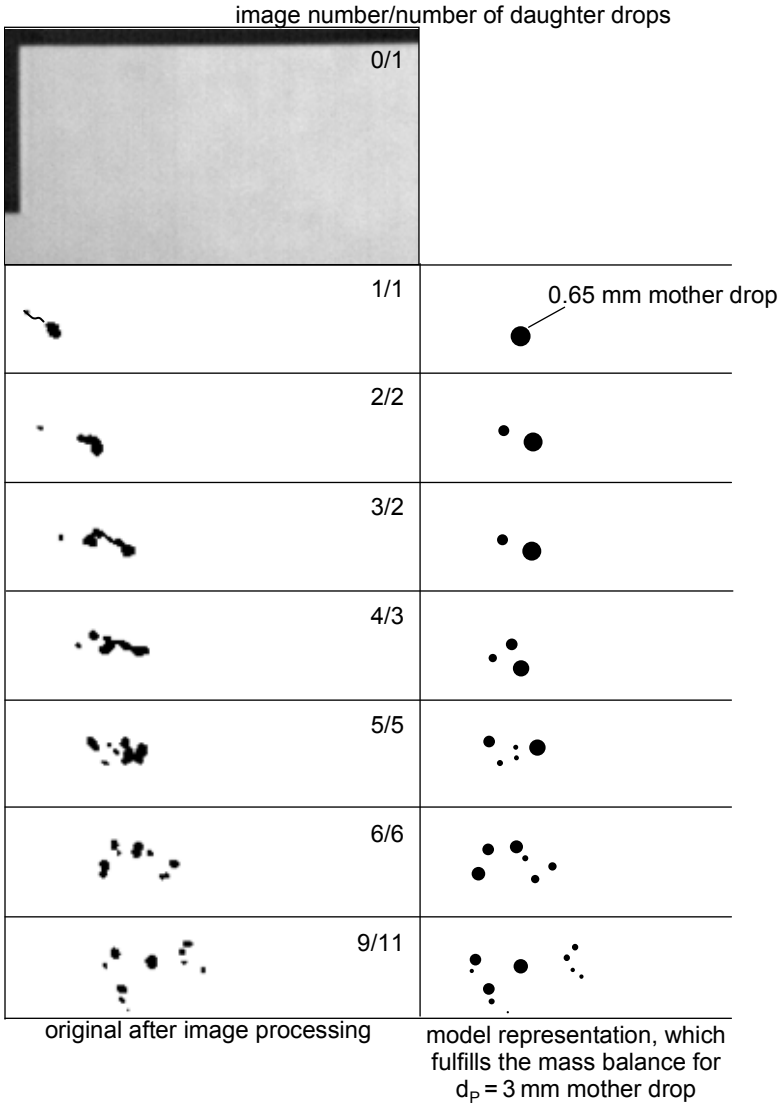

Figure 36 – Comparison between a real drop break-up and its corresponding sequence in terms of the assumption of spherical drops for a 0.65 mm toluene drop at a flow velocity of 1.5 m/s.

The coalescing system (represented by Figure 37 (a) and (b)) run into a steady state. The time to reach that condition decreased if ν was increased. The used values for ν represent the average values for the maximum number of daughter drops counted within the single drop experiments (see Figure 16 for a value listing).

An increase of ν to 51 led to numerical instabilities, which can be seen from the unphysical behavior of that drop size evolution over time. However, the drop sizes in the stirred tank are smaller than 1 mm - therefore, such high numbers of ν are unreasonable.

The dependency of ν on the mother drop diameter was shown in Figure 19 in chapter 5. The minimum number is 2 for the critical diameter, which is the smallest still breaking particle diameter under the given conditions. The experimental values of $\nu = f(d_p \leq 1\ mm)$ vary between 5 and 11 for the toluene drops and between 3 and 7 for the petroleum drops. These values are most relevant for the simulated application. An average value of 5 was used as constant for a further simulation of the coalescing system (Figure 37 (b)). With adaptation of three numerical parameters ($c_{1,br}$, $c_{2,br}$ and $c_{1,coa}$) the simulation fit the experiments. The ratio for $c_{1,br}/c_{1,coa}$ needs to be increased to decrease the dynamic of the breakage and the value for $c_{2,br}$ needs to be increased to increase the critical drop diameter.

This is in excellent agreements with the computational studies of Chatzi and Lee (1987), who were able to change the constant for the number of daughter drops up to 7 and could always adjust their simulations to corresponding experimental results with the change of the numerical constants.

The same procedure was carried out on a breakage dominated system (see Figure 37 (c) and (d)). The experimental results are from publication X - Maaß et al. (2011e). The same tendencies are observed as for the coalescing system. Different is the size range of the drops, which is clearly below the size range of the coalescing system. Therefore, the assumption was made, that also the number of daughter drops should be smaller than in the coalescing system. Smaller drops break into fewer particles than larger do for the same system properties (see Figure 19).

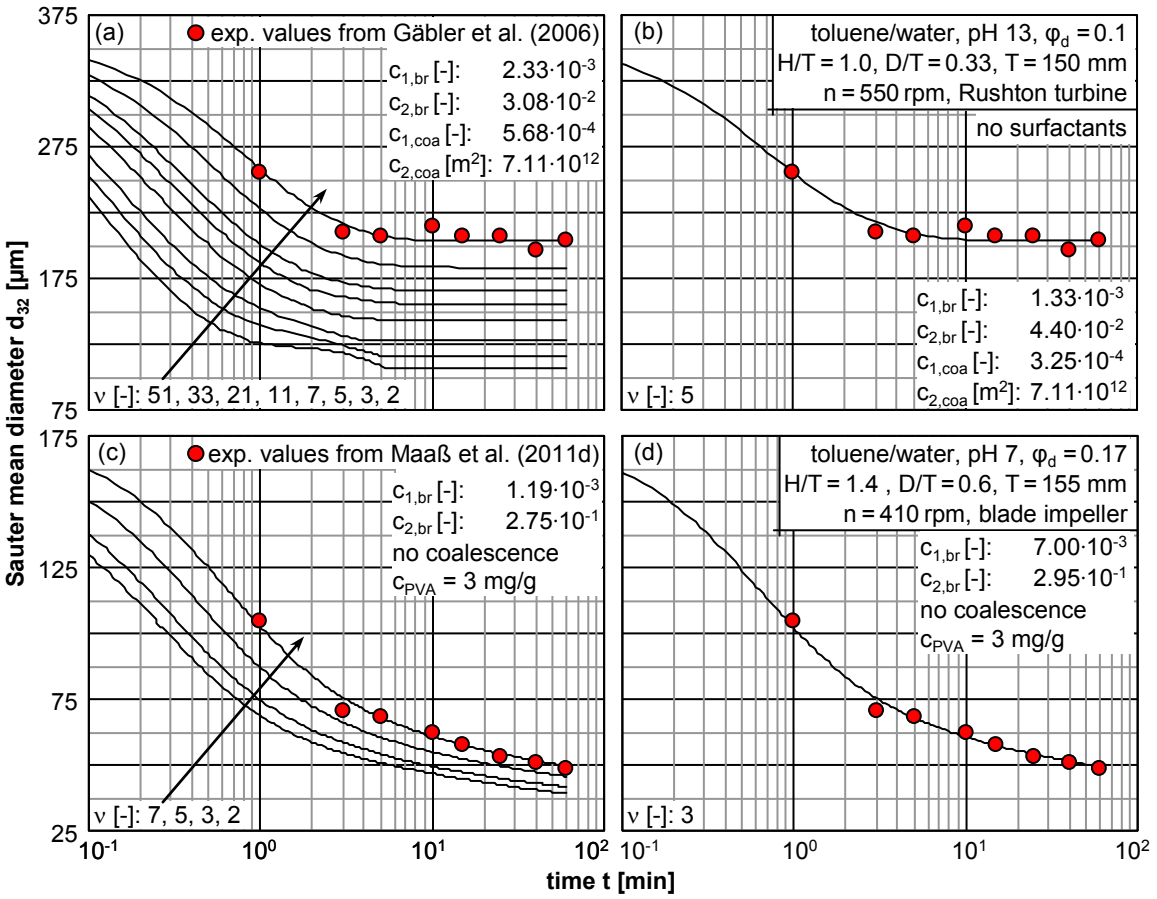

Figure 37 – Comparison of experimental results (symbols) with PBE simulations (lines) using the model of Coulaloglou and Tavlarides (1977) to analyze the influence of the average number of daughter drops for a coalescing ((a) and (b)) and a non coalescing ((c) and (d)) system. The parameter values in (a) are own optimized values from chapter two (see Table 1 and Figure 5). The parameters for the simulations in (c) are from publication IX - Maaß et al. (2011d). All simulations were using a Gaussian daughter drop size distribution. The parameters in (b) and (d) were fitted again after changing the number of daughter drops in the simulations.

The development of the fitted parameters for the simulation results from Figure 37 are now compared with the results of the single drop breakages as with the average values from the literature review presented in chapter 2. These comparative results are given in Table 11.

The increase of ν in the simulations led to smaller drops while all other parameter and the physical conditions remained constant. To fit the simulations using a higher ν with the experimental values, the parameter of $c_{2,br}$ was increased. That new value (see Table 11) led to slightly closer agreements between the results of the simulations and the single drop breakage experiments. Furthermore, the use of higher values of the number of daughter drops which is also associated with modeling of the whole breakage sequence rather than modeling only the initial event, led to closer agreements for the values of $c_{1,br}$ used in the simulations and the single drop experiments. A comparison with the literature values showed, that this value is now in reasonable agreements

with most of the parameters reported in literature (compare the values in Table 2 in the 2. Population balances). Therefore, multiple breakages modeled by the whole sequence are proposed for further simulations.

Table 11 – Influence of the number of daughter drops on the numerical parameters in the model of Coulaloglou and Tavlarides (1977) for different applications.

application	number of zones [-]	$c_{1,br}$ [-]	$c_{2,br}$ [-]	ν [-]
Gäbler et al. (2006)	1	$2.33 \cdot 10^{-3}$	$3.08 \cdot 10^{-2}$	2
this study	1	$1.33 \cdot 10^{-3}$	$4.40 \cdot 10^{-2}$	5
X - Maaß et al. (2011e)	2	$1.19 \cdot 10^{-2}$	$1.95 \cdot 10^{-1}$	2
this study	2	$7.00 \cdot 10^{-3}$	$2.95 \cdot 10^{-1}$	3
single drop experiment - initial breakage	2	$9.10 \cdot 10^{-1}$	$3.90 \cdot 10^{-1}$	-
single drop experiment - sequence breakage	2	$4.50 \cdot 10^{-2}$	$3.90 \cdot 10^{-1}$	-
average value from literature review	various	$1.29 \cdot 10^{-1}$	$5.47 \cdot 10^{-1}$	

II. Modeling of the number of daughter drops

The necessity for including multiple breakages into PBE simulations was already proposed by Raikar et al. (2010). They quoted Tcholakova et al. (2007), who observed the occurrence of multiple breakage by analyzing the evolution of DSD in a "narrow-gap" homogenizer with an axially symmetric, cylindrical mixing head [Vankova et al. 2007]. They furthermore observed that the number of daughter drops strongly increases with the viscosity of the dispersed phase due to the increase of capillary instabilities of long dispersed threads (see Figure 38). They were probably formed and broken mainly by capillary driven subdivision or shear strain by macroscopic turbulence rather than by the collision with microscopic turbulent eddies.

The development of a sound model, which also reflects the results from the single drop experiments in Figure 16 to Figure 19 is even more complicated as the two low viscous fluids show the opposed tendency. The toluene drops which are heavier, low viscous with lower interfacial energy than the investigated petroleum drops break into more daughter drops. Both systems show an increase in ν with an increase in d_p.

Future simulations should therefore not only use a higher value for ν which is still a single value but model functions instead. These models should reflect the influence of the size of the mother drop diameter, the viscosity ratio, the density ratio and the interfacial tension between the two liquid phases. Furthermore, different breakage mechanisms should be considered for more precise and reliable modeling.

The same is true for the other breakage models in the PBE framework, the breakage rate and the daughter drop size distribution.

III. Breakage time versus residence time

Coulaloglou and Tavlarides (1977) calculated the time available for breakage to be $t_{br} \sim d_P^{2/3} \varepsilon^{-1/3}$ (see equation (4)). This expression leads to an absolute maximum in the breakage rate $g(d_p)$ which was criticized by Chen et al. (1998) as physically not realistic. They assumed that the characteristic breakage time is constant. Alopaeus et al. (2002) did not follow this drastic simplification. They proposed based on the turbulence theory a dependency of $t_{br} \sim \varepsilon^{-1/3}$. Both assumptions combined with a monotone increasing breakage probability (see the original sources for details) lead to a monotone growing breakage frequency over the particle diameter. That assumes that as larger the particles get as easier they are going to break. That is in contrast to the relation developed by Coulaloglou and Tavlarides (1977).

These contradicting ideas have been intensively discussed in publication VII - Maaß and Kraume (2011). The results of the single drop experiments there, analyzing the initial phase of the breakage events and also the results from the Chapter 5, analyzing the complete breakage sequence, show clearly an increase of the breakage time with increasing mother drop diameter.

The breakage rate per definition combines an inverse time and a probability. Therefore, a different question should be asked: Is it suitable to combine the specific breakage time of the individual drops with a probability of the breakage to take place? Many authors describe this characteristic time as a residence time in the breakage region, which is not necessarily a function of the drop diameter but a bulk flow fluid dynamic parameter, not directly related to the breakage rate model. The average lifetime of the different drop sizes is then de-

scribed by the actual breakage rate, which predicts the frequency of breakage events during these residence times.

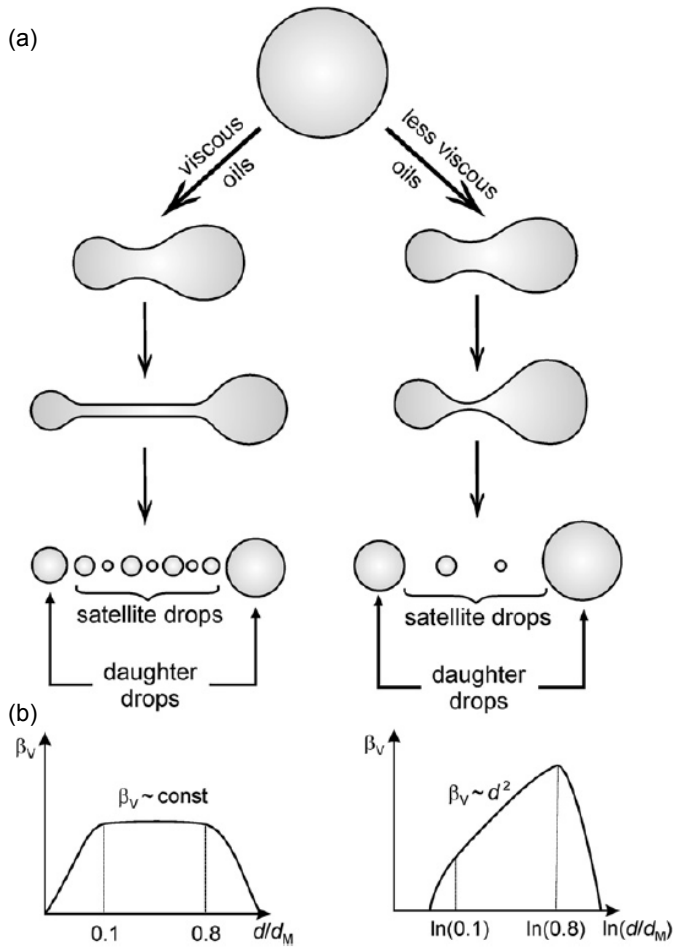

Figure 38 – Schematic presentation of the process of drop breakage of mother drops d_M of less-viscous and more viscous oil with the mother drop diameter in the range of the maximum stable diameter - (a) and graphical presentation of the resulting volume daughter drop size distribution β_V [Tcholakova et al. 2007]. Reprinted with permission from Elsevier Science.

It is well known that the turbulence intensity and energy dissipation rapidly decrease with the distance from the impeller. In order that the drop can break up, it has to enter a region in the vessel where the energy dissipation is higher than a critical value necessary for its breakage[i]. The smaller the drop, the smaller the volume in which the drop can break and so the residence time of the drop for macroscopic timely constant fluid dynamic conditions.

If a drop with a constant diameter is introduced in the same vessel with different stirrer speeds than the drop would break most probable first in the vessel with the highest stirrer speed. The larger the speed is, the larger is the volume of regions where the drop can break, the larger is the characteristic residence time. That line of argumentation would support model ideas like the one proposed by Alopaeus et al. (2002) but it contradicts the drastic simplification of Chen et al. (1998) assuming a constant breakage time independend from the operating parameters.

[i] This line of argumentation was used already by Hancil and Rod (1988) to explain the increase of the average number of daughter drops for increasing mother drop diameter.

IV. Influence of the breakage rate shape on simulated drop size distributions

Raikar et al. (2009) have used the model of Coulaloglou and Tavlarides (1977) and further developments of this breakage model which all show a monotone increase until a certain diameter and than a monotone decrease until the breakage frequency turns to zero. Raikar et al. (2009) showed that the decreasing part of the breakage frequency above the critical diameter appeared to have a relatively small effect on the simulation results. That was true for all three models in their investigations. The major bandwidths of the affected drop sizes were always smaller than this critical diameter. These results were achieved for several parameter estimation runs.

The same is true for the simulations associated with this thesis. The largest drops occurring in the simulations in publication IV - Maaß et al. (2010), VI - Maaß et al. (2011b), IX - Maaß et al. (2011d) and X - Maaß et al. (2011e) are always smaller or in the same range as the critical diameter which determines the maximum of the breakage rate. See especially publication X - Maaß et al. (2011e) for this analysis, as the breakage rates are given graphically as the experimental and simulated drop sizes.

These results support the assumption that the breakage rate should be described rather by a monotone increasing function than by one with a maximum. This directly forces the use of a characteristic residence time rather than a breakage time in the breakage modeling framework.

The model of Coulaloglou and Tavlarides was transformed eliminating the dependence of d_p in the pre exponential term based on the ideas of using a residence time rather than a drop associated breakage time. Only considering the influence of the energy dissipation rate and simplifying all further dependencies of the residence time into the empirical constant $c_{1,br}$ the model is written as follows:

$$g(d_p) = c_{1,br} \frac{\varepsilon^{1/3}}{(1+\varphi_d)} \exp\left(- c_{2,br} \frac{\gamma(1+\varphi_d)^2}{\rho \varepsilon^{2/3} d_P^{5/3}} \right) \tag{16}$$

V. Influence of the breakage models on the self similarity of the simulated distributions

The following discussion deals with simulation results using the traditional model of Coulaloglou and Tavlarides (1977) and its modified version from equation (16). It will specify the influence of the shape of the breakage rate on the solution of the PBE. Specifically the self similarity is analyzed. These properties are of considerable importance for the identification of key model behavior associated with system behavior [Ramkrishna 2000].

The experimental evidence for self similar behavior of agitated l/l system has a long history. Molag et al. (1980) carried out experiments in a baffled and unbaffled tank with four types of agitators (see original source for details). The cumulative volume drop size distributions were observed to be normal distributions. These DSD plotted over the normalized drop diameter d_p/d_{32} were self similar. The standard deviation of the normalized distribution function did not depend very much upon either the stirrer type or its speed; its mean value was about 0.30. This is in absolute agreement with the results of Gäbler (2007) and Kraume (2004) achieved almost 30 years later, who found the same value of the standard deviation for coalescing toluene/water and anisole/water systems.

Calabrese et al. (1992) found similar results. All investigated cumulative number size distributions of their investigated evolving liquid/liquid systems were similar when normalized with instantaneous d_{32}. This result was independent of time, physical characteristics of the dispersion and conditions of agitation.

The same was found by Kraume et al. (2004) analyzing transient strongly coalescing toluene/water systems for various dispersed phase fractions.

Else wise as Kraume et al. (2004) the toluene/water system, discussed in publication IX - Maaß et al. (2011d), was stabilized. Nevertheless, the breakage dominated l/l dispersion showed also self similar behavior. The results are given in Figure 39. The cumulative number distribution is converted into the probability density net. This diagram shows that all the distributions are strongly self-similar and total agreement between the results has to be stated. All little deviations are most probable related to measurement errors.

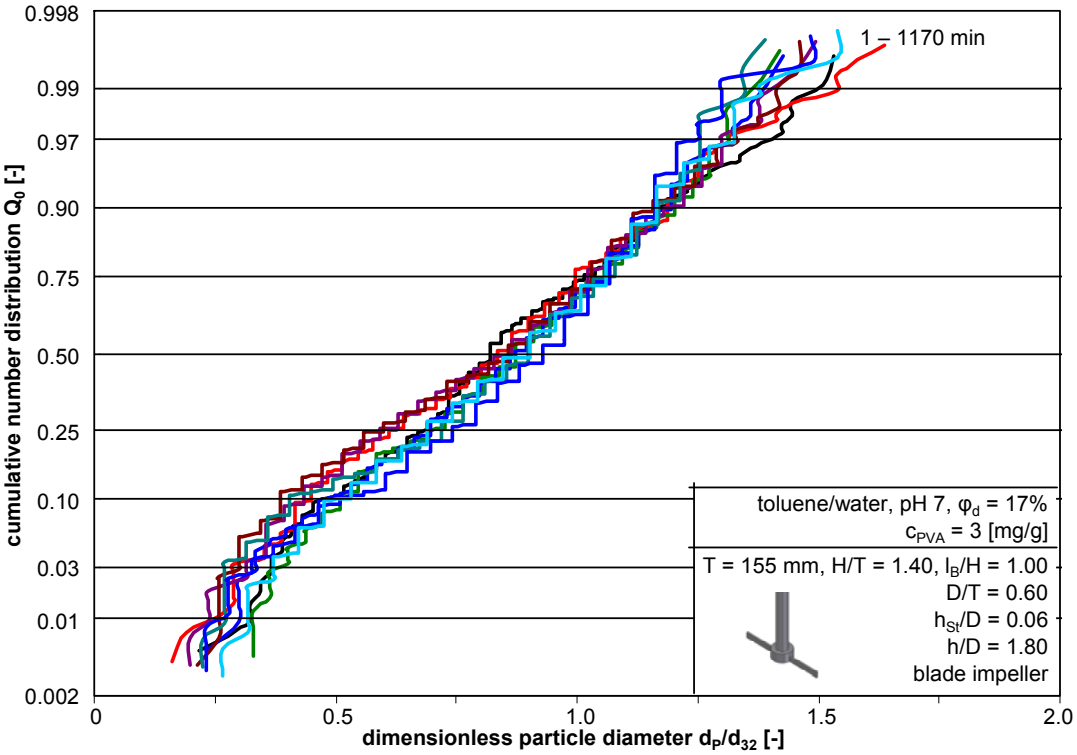

Figure 39 – Dimensionless analysis of experimentally determined transient DSD (data from publication IX - Maaß et al. (2011d)). The DSD at each point in time is divided by the corresponding Sauter mean diameter,

Opposed to the experiments, the simulations presented in Figure 40 using different DDSDs led to no self similarity (for a detailed description of all used DDSD see publication IX - Maaß et al. (2011d)). The simulation results show the transient DSD divided by the corresponding Sauter mean diameter over time. Four different daughter drop size distributions have been used. All simulation results showed a clear tendency to more narrow distributions over time. The enveloping curves (3 min and 1170 min) are especially pointed out in the diagram. The other curves develop monotone within these two.

This behavior was especially obvious for the drops larger than $1.2 \cdot d_{32}$ at the top of the distribution. The same tendency was noticed at the bottom of the distribution for drops smaller than $0.75 \cdot d_{32}$, but not as strong as at the top. Although all investigated daughter drop size distributions showed this behavior. It was especially strong for the Gaussian distribution.

The M-shaped Gaussian distribution and the β-distribution after Lee et al. (1987a) & (1987b) showed better results. The simulation results based on those DDSD were almost self-similar and reflect therewith the experimental findings better than the results achieved with the Gaussian distribution. Additionally, the agreements of the experimental distributions with the simulations were best for the M-shaped Gaussian distribution and the β-distribution (see publication IX - Maaß et al. (2011d) for details).

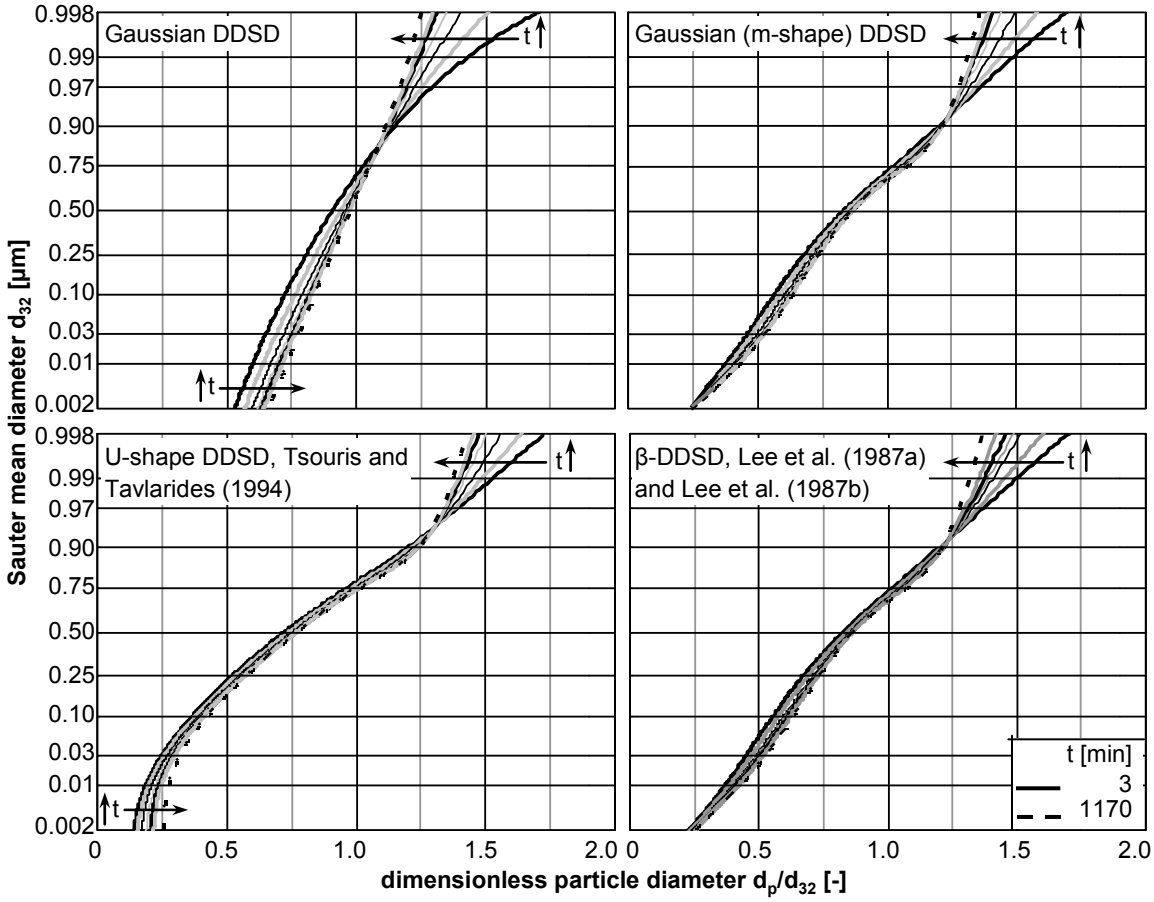

Figure 40 – Dimensionless analysis of computationally determined transient DSD using four different DDSD

The Gaussian distribution led to the strongest deviations. An improvement in self similarity using different breakage rates seems most visiable using this DDSD.

All simulations in publication IX - Maaß et al. (2011d) were using the model of Coulaloglou and Tavlarides (1977) for the breakage rate. The coefficient of determination R^2 to predict the transient d_{32} for 1170 min of mixing a toluene/water system with $\varphi_d = 0.17$ was reported with 0.988 using a Gaussian DDSD.

The same simulations were carried out for the modified model described in equation (16). The achieved R^2 was even better with 0.999. The transient cumulative number distributions are shown in Figure 41 over the dimensionless particle diameter d_p/d_{32}. The simulations for 3 and 1170 min are compared with the simulation results of the standard model by Coulaloglou and Tavlarides (1977) - see the red lines. Although, both model approaches do not lead into self similar solutions, the differences are clear. The standard model of Coulaloglou and Tavlarides (1977) produces distributions which are much narrower than the ones produced by the modified model. Furthermore, the top of the distribution achieved with the standard model showed worse result than the modified one. The results of the shape at bottom of the distribution are equal for both approaches.

This gives only a weak hint that a self similar solution is more probable to achieve with a monotone increasing breakage rate, than one with a maximum. However, the influence of the daughter drop size distribution on the self similarity is dominant.

Therefore, it can be concluded that the modeling of drop breakage in the population balance framework needs careful adjustment of all sub-models because they strongly interfere with each other mathematically but also conceptual:

If binary breakage is assumed as a fixed single value, the initial breakage is described. That has consequences on the used characteristic time which is automatically the initial breakage time. The used daughter drop size distribution should definitely bimodal and not a normal distribution. Furthermore, drop deformation needs to be considered as additional information about the individual drops. It should be tracked as one addi-

tional attribute besides volume. As this procedure is computational expensive and arguable due to the unknown deformations happening on the single drop level, it is not recommended by this work.

The description of the complete breakage sequence as one event increases the characteristic time. This opens the opportunity for coarser timely discretization, which would be computational friendly. Furthermore, the characteristic time can be associated with the fluid dynamics only rather than with fluid dynamics and the single drop. That was supported by the range of the used breakage rates in this study and in literature examples. It would also allow the use of a function describing the number of daughter drops rather than a fixed single value.

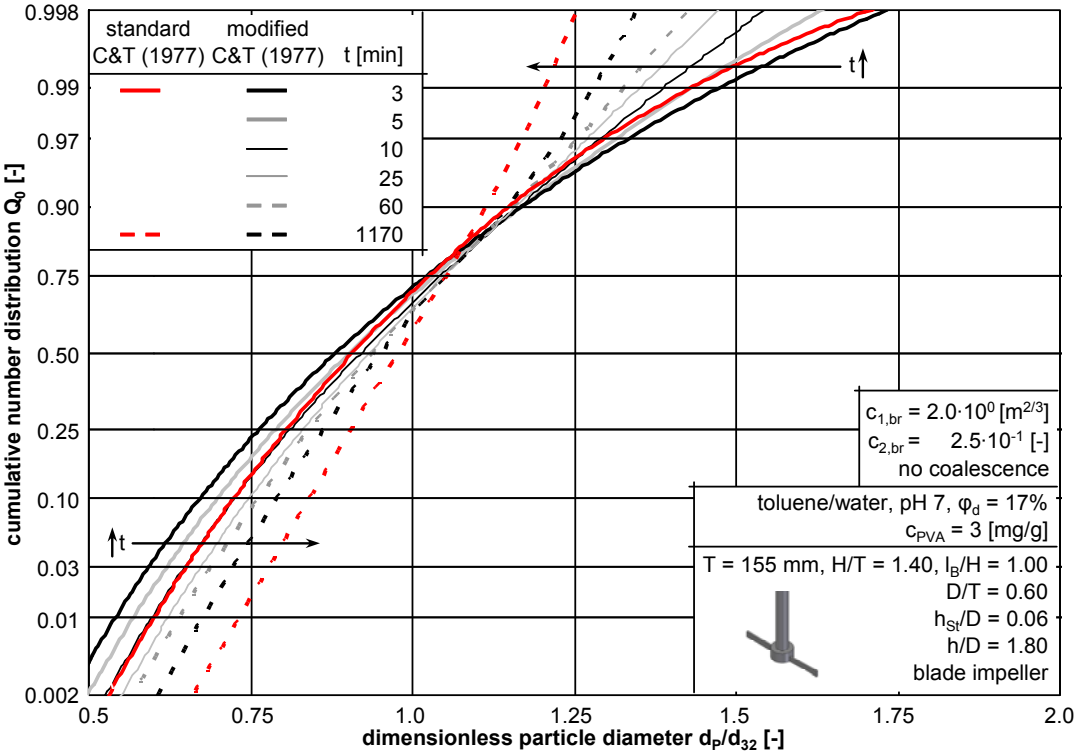

Figure 41 – Computational analysis for self similarity of transient drop size distributions using the standard breakage rate from Coulaloglou and Tavlarides (1977) and the modified model displayed in equation (16).

These recommendations are not necessary for precise simulation results. It was shown in this study and in the associated publications (IV - Maaß et al. (2010); VI - Maaß et al. (2011b); IX - Maaß et al. (2011d) and X - Maaß et al. (2011e) that precise reproduction of experimental Sauter mean diameters for a broad variation in geometry factors, operating parameters and physical characteristics is already possible with common models in the investigated breakage dominated systems.

Nevertheless, the more physical the description will become, the more trustful the simulation results will be. The change in the number of daughter drops and the use of bimodal daughter drop size distributions for example broadened the simulated drop size distribution and led to much better accordance with the experimental results.

These examples showed the opportunity for model improvement based on single drop experiments, which will help to predict characteristics of drop swarms in complex industrial applications much better. Further necessary steps in research field will be proposed in the last chapter.

8. Summary

Consequently growing requirements for operation efficiency and environmental compatibility on industrial processes and technologies will increase the value of process understanding and the frequency of process optimization. In the context of increasing competition in a globalizing world and sinking availabilities for commodities this will have to be carried out with as small labor and material costs as possible. Process simulation plays the major role fulfilling those needs in this continuing dynamic. Physically based, accurate models, which were experimentally sufficiently validated, are the base for sustainable simulation results.

I. Concluding remarks

The major focus of this work was on analyzing turbulent liquid/liquid dispersions in agitated vessels. These kinds of apparatus still belong to the most frequently used apparatuses in the process industry. A short overview of some industrial applications is given in chapter one.

The experimental evaluation is based on photo-optical measurement techniques with image processing. The manually very time consuming procedures were fully automated.

It became generally accepted in the last two decades to describe the evolution as well as the spatial distribution of liquid/liquid dispersion by population balances. Therefore, this tool became the simulation standard of this work.

The broad variety of existing models as well as the challenges with the missing of an absolute solution of these integro- partial differential equations is discussed broadly in the literature. In the context of this work this discussion was led mainly by the example of the model by Coulaloglou and Tavlarides (1977).

Nevertheless, the final statement from literature is approved: The opposed phenomena of drop breakage and drop coalescence impede a clear model analysis. Therefore, a separation of both phenomena was carried out in the experiments as in the simulation work to focus on drop breakage.

On the one hand investigations of drop swarms were accomplished under high polyvinyl alcohol concentrations. Since the used quantity of this water-soluble polymer was clearly above the critical micelle concentration, coalescence was completely hindered. A broad variation of geometry factors, operating parameters and physical characteristics was studied here under breakage dominant conditions.

On the other hand drop breakage was analyzed with single drops experiments. These helped to quantify the influence of flow rate of the continuous phase as well as viscosity of the dispersed phase and interfacial tension between the two phases on the turbulent drop break-up.

The experimental results of both analysis procedures (the drop swarm analysis as well as the single drop analysis) were used for the validation of existing population balance models with the focus on the breakage models used in the population balances. These are the breakage rate, the number of daughter drops as well as the daughter drop size distribution.

First and foremost the single drop investigations revealed specific information for the evaluation of the sub-models. So on the one hand, the usual and easy assumption of Gaussian distributed daughter drop size distribution was disproved. An uneven break-up into a small and a large daughter drop is clearly more probable for binary breakage.

But also the binary breakage, which is the most frequent used assumption for the number of daughter drops in the literature, is only a rough assessment of the physically truth. With increasing mother drop diameter also the number of occurring daughter drops rises rapidly. Thus for a 3 mm toluene drop up to 212 daughter drops as consequence of an entire break sequence were counted. These multiple breakages could be broken down into a cascade of binary breakages by highspeed imaging. However, the isolation of these individual breakages is a strong simplification of the breakage process. It is much more meaningful to evaluate not only the initiation of a drop breakage but the whole sequence.

The observed breakage probability of the single drop analysis remains uninfluenced by this discussion, since the statement whether a drop breaks is detached from the question of how many fragments are generated by the breakage event. The breakage probability represents one out of two parts in the breakage rate. Multiplied by the inverse breakage time it results into the breakage rate.

Different models from literature were correlated well with the experimental data of the breakage probability from the single drop analyses. Even a change of the dispersed phase from petroleum to toluene was pre-

dictable without additional parameter adjustment. The obtained model parameter values after fitting against the experimental data from the single drop investigations could even be used for simulations of an agitated toluene/water system with acceptable success.

This was not the case for the breakage time. It is defined in this work as the duration between the entrance of the drop into the impeller region and the first breakage of the particle. The measured values for the breakage time were found to be one or two magnitudes smaller than the used values of the characteristic time for PBE simulations. Opposed they agree very well with experimentally determined breakage times of other working groups.

This discrepancy led to the conclusion to differentiate on the one hand between drop residence time in breakage relevant parts of the agitated vessel and on the other hand the drop breakage time, which is measured experimentally.

Considerations of other breakage mechanisms than only the turbulent fluctuations were possible by including the droplet capillary number. A new developed breakage model considers additionally to the turbulent break mechanisms the drop elongation, resulting from the acceleration of the continuous phase in the vicinity of the impeller. This development based on single drop results led to a more precise description of drop breakage in the population balance equation which was shown with simulation results for varying dispersed phase.

The drop swarm analysis in the agitated vessel showed clearly that a reproduction of the experimental data by means of the population balance can be achieved already with common models from literature. One constraint for such a successful implementation is the use of a 2-zone model to consider spatial inhomogeneities of the energy dissipation and velocities. It was shown in this work, that with one pair of adjusted parameters, using the model of Coulaloglou and Tavlarides (1977), a variation of geometry factors and operating parameters (e.g. stirrer speed, reactor size or type of agitator) is possible without further parameter adaptation. Even severe changes, like the one from a single to a quadruple impeller system with parallel four times increasing liquid level with constant reactor diameter, could be predicted with deviations smaller 10%.

The major advantage of the new developed model is first and foremost, the increased prediction capacities for the variation of the dispersed phase. After the adaptation of the model to a toluene/water system also the anisole/water as well as the n-butyl chloride/water systems has been predicted with deviations less than 5% of the transient Sauter mean diameter to experimental values.

A further substantial operation parameter of agitated liquid/liquid dispersions is the dispersed phase fraction. Predictions of the influence of this parameter for the investigated breakage dominated systems were possible, if the turbulence dampening was considered by the variation of the quantity of the dispersed phase. Usual assumptions from the literature have been used as description for this phenomenon.

This work proofed the opportunity for model improvement based on single drop and drop swarm experiments, which will help to predict liquid/liquid dispersions in complex industrial applications much better.

II. Outlook

Following four main directions can be identified to improve the prediction qualities of breakage models and to increase the use of PBE models for process analysis, optimization, intensification and control:

1. Precise optimization of the stirrer configuration in slim reactors for industrial practice.
2. Implementation of further parameters (surfactant concentration, mass transfer, reaction kinetics) in PBE models, especially in the coalescence terms.
3. Development of a sound understanding of drop breakage, which includes a concept of interconnection of the various sub-models (number and size of daughter drops, breakage time and breakage probability).
4. Increase the accuracy and speed of the drop size prediction for model based process control.

While point 4 is very general and also true for the experimental analysis technique of drop size distributions, points 1 to 3 are very specific and aiming for different goals. Pure process optimization may be the goal for the first point, while it is model improvement for the second. The development of a phenomenological theory concerning drop breakage is the major goal of the third point. The first three points will be discussed in detail within the following subsections.

1. Optimization of the stirrer configuration

The experimental results have shown, that it was possible to increase the production capacities of liquid/liquid systems by increasing the aspect ratio H/T. Parallel, with the use of a quadruple crossed blade impeller, the energy demands have been dramatically decreased, compared to the energy demands of a number of single reactors with H/T = 1 with the same production capacity. However, the used CBI is a very simple impeller. Various combinations of down pumping turbines at the top of a slim reactor with high shear turbines at the bottom seem more promising. This could improve the performance of the analyzed reactor configurations in terms of mixing efficiency and minimum dispersion speed. Additionally the stirrer-stirrer distance and therewith the number of stirrers would be one very obvious optimization parameter.

2. Model improvement by including further influence parameters

The influence of surfactant concentration on the drop size may be the example for the named concept of model improvement.

The influence of surfactants in PBE models is mainly displayed by the changes of the interfacial tension. The results in this study showed clearly, for the example of polyvinyl alcohol, that the change in surfactant concentration could only be reflected with PBE simulations for surfactant concentrations above the CMC. For systems where coalescence still existed, the simulation failed to predict the drop size change based on the interfacial tension changes.

These results also showed that the influence is mainly on the coalescence terms and should therefore be applied to the according sub-models. They same is assumed to be true for mass transfer or chemical reactions.

3. Drop breakage model development

Experimental methods analyzing single drop breakages and breakage dominated drop swarms are still limited. Although a definition for the drop breakage time was set, the interpretation of the single drop data is complex.

The discussion for the definition of a single drop breakage event is still open. Based on the results achieved in this study, it seems obvious, that the breakage of a drop should be considered as a complete cascade of single breakage events. They single breakages are strongly connected to each other. Up to now, that is not considered in PBE models.

It is possible to implement it by increasing the possible number of daughter drops. However, this would still only be a statistical estimation but is a first step in the right direction. The choice of the used value for the number of daughter drops should be based on a sound model. A further step would be the implementation not only of a fixed value for ν, but rather a phenomenological model, which describes the number of expected daughter drops as a function of mother drop diameter, physical properties of the drops and process parameters over time. Up to now only empirical equations are available as the ones presented in this study.

This development would automatically influence the choice of the daughter drop size distribution. It could be shown that DDSD after the initial breakage event is bimodal. However, the description of the complete breakage sequence would also effect the description of the resulting daughter drop size distribution. An experimental evaluation of these data although recorded was not possible in this work, due to the limited resolution of the available camera technique.

This was not the case for the breakage time. It was measured for the initial breakage event and also for the time until a maximum number of daughter drops was detected. However, both definitions are open to question. An analysis of drop deformation using a high resolution highspeed camera seems more promising in defining the real breakage time.

Therefore more detailed and fundamental research is necessary to include all these findings as they interconnect with each other, to describe drop breakage more accurate.

Table of figures

Image on page iii from http://hozzamedia.co.uk/pictures: "Drop in the ocean"

List of references

Alban, F.B., Sajjadi, S. and Yianneskis, M., 2004. Dynamic tracking of fast liquid-liquid dispersion processes with a real-time in-situ optical technique. Chem. Eng. Res. Des., 82(A8): 1054-1060.

Alopaeus, V., Koskinen, J. and Keskinen, K.I., 1999. Simulation of the population balances for liquid-liquid systems in a nonideal stirred tank. Part 1 - Description and qualitative validation of the model. Chem. Eng. Sci., 54(24): 5887-5899.

Alopaeus, V., Koskinen, J., Keskinen, K.I. and Majander, J., 2002. Simulation of the population balances for liquid-liquid systems in a nonideal stirred tank. Part 2 - Parameter fitting and the use of the multiblock model for dense dispersions. Chem. Eng. Sci., 57(10): 1815-1825.

Alopaeus, V., Moilanen, P. and Laakkonen, M., 2009. Analysis of stirred tanks with two-zone models. AIChE J., 55(10): 2545-2552.

Angle, C.W. and Hamza, H.A., 2006. Predicting the sizes of toluene-diluted heavy oil emulsions in turbulent flow - Part 2: Hinze-Kolmogorov based model adapted for increased oil fractions and energy dissipation in a stirred tank. Chem. Eng. Sci., 61(22): 7325-7335.

Attarakih, M.M., Drumm, C. and Bart, H.-J., 2009. Solution of the population balance equation using the sectional quadrature method of moments (SQMOM). Chem. Eng. Sci., 64(4): 742-752.

Azizi, F. and Al Taweel, A.M., 2010. Algorithm for the accurate numerical solution of PBE for drop breakup and coalescence under high shear rates. Chem. Eng. Sci., 65(23): 6112-6127.

Azizi, F. and Al Taweel, A.M., 2011. Turbulently flowing liquid-liquid dispersions. Part I: Drop breakage and coalescence. Chem. Eng. J., 166(2): 715-725.

Bae, J.H. and Tavlarides, L.L., 1989. Laser capillary spectrophotometry for drop-size concentration measurements. AIChE J., 35(7): 1073-1084.

Bahmanyar, H. and Slater, M.J., 1991. Studies of drop break-up in liquid-liquid systems in a rotating disc contactor. Part I: Conditions of no mass transfer. Chem. Eng. Technol., 14(2): 79-89.

Bakker, A. and Oshinowo, L.M., 2004. Modelling of turbulence in stirred vessels using large eddy simulation. Chem. Eng. Res. Des., 82(A9): 1169-1178.

Baldi, S. and Yianneskis, M., 2004. On the quantification of energy dissipation in the impeller stream of a stirred vessel from fluctuating velocity gradient measurements. Chem. Eng. Sci., 59(13): 2659-2671.

Bapat, P.M., Tavlarides, L.L. and Smith, G.W., 1983. Monte-Carlo simulation of mass-transfer in liquid-liquid dispersions. Chem. Eng. Sci., 38(12): 2003-2013.

Bapat, P.M. and Tavlarides, L.L., 1985. Mass-transfer in a liquid-liquid CFSTR. AIChE J., 31(4): 659-666.

Bart, H.J., Garthe, D., Grömping, T., Pfennig, A., Schmidt, S. and Stichlmair, J., 2006. Vom Einzeltropfen zur Extraktionskolonne. Chem. Ing. Tech., 78(5): 543-547 (in German).

Barth, H.G. and Flippen, R.B., 1995. Particle-Size Analysis. Anal. Chem., 67(12): R257-R272.

Batchelor, G.K., 1952. Diffusion in a field of homogeneous turbulence: II. The relative motion of particles. Math. Proc. Cambridge Philos. Soc., 48: 345-362.

Bey, M. and Dienes, C., 2010, Ausgewählte Probleme der industriellen Rührtechnik, oral presentation at: ProcessNet Jahrestreffen der Fachausschüsse Agglomeration, Zerkleinern/Klassieren und Mischvorgänge, Fulda, 21.-23.02., (in German).

Boxall, J.A., Koh, C.A., Sloan, E.D., Sum, A.K. and Wu, D.T., 2010. Measurement and calibration of droplet size distributions in water-in-oil emulsions by particle video microscope and a focused beam reflectance method. Ind. Eng. Chem. Res., 49(3): 1412-1418.

Brás, L.M.R., Gomes, E.F., Ribeiro, M.M.M. and Guimarães, M.M.L., 2009. Drop distribution determination in a liquid-liquid dispersion by image processing. Int. J. Chem. Eng.(Article ID 746439): pp. 6.

Brown, D.A.R., Jones, P.N. and Middelton, J.C., 2004. Experimental methods - part A: Measuring tools and techniques for mixing and flow visualization studies. In: E.L. Paul, V.A. Atiemo-Obeng and S.M. Kresta (Editors), Handbook of Industrial Mixing: Science and Practice. John Wiley & Sons, Inc., Hoboken, New Jersey, pp. 145-202.

Bürkholz, A. and Polke, R., 1984. Laser diffraction spectrometers / experience in particle size analysis. Part. Charact., 1: 153-160.

Cabassud, M., Gourdon, C. and Casamatta, G., 1990. Single drop break-up in a Kuhni column. Chem. Eng. J., 44(1): 27-41.

Calabrese, R.V., Wang, M.H., Zhang, N. and Gentry, J.W., 1992. Simulation and analysis of particle breakage phenomena. Chem. Eng. Res. Des., 70(2): 189-191.

Calabrese, R.V., Cheng, S.H., Lin, J.C. and Gentry, J.W., 1995. Effect of kernel on aggregation or coalescence of large clusters. Part. Sci. Technol., 13(1): 37-53.
Cents, A.H.G., Brilman, D.W.F., Versteeg, G.F., Wijnstra, P.J. and Regtien, P.P.L., 2004. Measuring bubble, drop and particle sizes in multiphase systems with ultrasound. AIChE J., 50(11): 2750-2762.
Chatzi, E.G. and Lee, J.M., 1987. Analysis of interactions for liquid liquid dispersions in agitated vessels. Ind. Eng. Chem. Res., 26(11): 2263-2267.
Chatzi, E.G., Boutris, C.J. and Kiparissides, C., 1991. Online monitoring of drop size distributions in agitated vessels: 2. Effect of stabilizer concentration. Ind. Eng. Chem. Res., 30(6): 1307-1313.
Chatzi, E.G. and Kiparissides, C., 1994. Drop size distributions in high holdup fraction dispersion systems: Effect of the degree of hydrolysis of PVA stabilizer. Chem. Eng. Sci., 49(24B): 5039-5052.
Chatzi, E.G. and Kiparissides, C., 1995. Steady-state drop-size distributions in high holup fraction dispersion systems. AIChE J., 41(7): 1640-1652.
Chen, Z., Prüss, J. and Warnecke, H.J., 1998. A population balance model for disperse systems: Drop size distribution in emulsion. Chem. Eng. Sci., 53(5): 1059-1066.
Coulaloglou, C.A. and Tavlarides, L.L., 1977. Description of Interaction Processes in Agitated Liquid-Liquid Dispersions. Chem. Eng. Sci., 32(11): 1289-1297.
Cull, S.G., Woodley, J.M. and Lye, G.J., 2001. Process selection and characterisation for the biocatalytic hydration of poorly water soluble aromatic dinitriles. Biocatal. Biotransform., 19(2): 131-154.
Cull, S.G., Lovick, J.W., Lye, G.J. and Angeli, P., 2002. Scale-down studies on the hydrodynamics of two-liquid phase biocatalytic reactors. Bioprocess. Biosyst. Eng., 25(3): 143-153.
Delafosse, A., Morchain, J., Guiraud, P. and Liné, A., 2009. Trailing vortices generated by a Rushton turbine: Assessment of URANS and large Eddy simulations. Chem. Eng. Res. Des., 87: 401-411.
Desnoyer, C., Masbernat, O. and Gourdon, C., 2003. Experimental study of drop size distributions at high phase ratio in liquid-liquid dispersions. Chem. Eng. Sci., 58(7): 1353-1363.
Deziél, E., Comeau, Y. and Villemur, R., 1999. Two-liquid-phase bioreactors for enhanced degradation of hydrophobic/toxic compounds. Biodegradation, 10(3): 219-233.
Diemer, R.B. and Olson, J.H., 2002a. A moment methodology for coagulation and breakage problems: Part 1 - analytical solution of the steady-state population balance. Chem. Eng. Sci., 57(12): 2193-2209.
Diemer, R.B. and Olson, J.H., 2002b. A moment methodology for coagulation and breakage problems: Part 2 - Moment models and distribution reconstruction. Chem. Eng. Sci., 57(12): 2211-2228.
Diemer, R.B. and Olson, J.H., 2002c. A moment methodology for coagulation and breakage problems: Part 3 - generalized daughter distribution functions. Chem. Eng. Sci., 57(19): 4187-4198.
Drumm, C., Tiwari, S., Kuhnert, J. and Bart, H.-J., 2008. Finite pointset method for simulation of the liquid-liquid flow field in an extractor. Comp. Chem. Eng., 32(12): 2946-2957.
Drumm, C., Attarakih, M., Hlawitschka, M.W. and Bart, H.J., 2010. One-Group Reduced Population Balance Model for CFD Simulation of a Pilot-Plant Extraction Column. Ind. Eng. Chem. Res., 49(7): 3442-3451.
Drumm, C., Hlawitschka, M.W. and Bart, H.J., 2011. CFD Simulations and Particle Image Velocimetry Measurements in an Industrial Scale Rotating Disc Contactor. AIChE J., 57(1): 10-26.
Dukhin, A.S. and Goetz, P.J., 2001. Acoustic and electroacoustic spectroscopy characterizing concentrated dispersions emulsions. Adv. Colloid Interface Sci., 92(1-3): 73-132.
El-Hamouz, A., Cooke, M., Kowalski, A. and Sharratt, P., 2009. Dispersion of silicone oil in water surfactant solution: Effect of impeller speed, oil viscosity and addition point on drop size distribution. Chem. Eng. Process., 48(2): 633-642.
Escudie, R., Bouyer, D. and Line, A., 2004. Characterization of trailing vortices generated by a Rushton turbine. AIChE J., 50(1): 75-86.
Frauendorfer, E., Wolf, A. and Hergeth, W.D., 2010. Polymerization online monitoring. Chem. Eng. Technol., 33(11): 1767-1778.
Gäbler, A., Wegener, M., Paschedag, A.R. and Kraume, M., 2006. The effect of pH on experimental and simulation results of transient drop size distributions in stirred liquid-liquid dispersions. Chem. Eng. Sci., 61(9): 3018-3024.
Gäbler, A., 2007. Experimentelle Untersuchungen, Modellierung und Simulation gerührter Flüssig/flüssig-Systeme mit veränderlichen Stoff- und Betriebsparametern. dissertation, Technische Universität Berlin, pp. 141, (in German).
Gaitzsch, F., Kamp, J., Kraume, M. and Gäbler, A., 2011. Vergleich des Koaleszenzverhaltens ruhender und umströmter Wasser-in-Öl-in-Wasser-Einzeltropfen. Chem. Ing. Tech., 83(4): 511-517 (in German).
Galindo, E., Pacek, A.W. and Nienow, A.W., 2000. Study of drop and bubble sizes in a simulated mycelial fermentation broth of up to four phases. Biotechnol. Bioeng., 69(2): 213-221.
Gopalan, R. and Jacobs, D., 2010. Comparing and combining lighting insensitive approaches for face recognition. Comput. Vis. Image Underst., 114(1): 135-145.

Gourdon, C., Casamatta, G. and Angelino, H., 1991. Single drop experiments with liquid test systems - a way of comparing 2 types of mechanically agitated extraction columns. Chem. Eng. J., 46(3): 137-148.

Gramdorf, S., Hermann, S., Hentschel, A., Schrader, K., Müller, R.H., Kumpugdee-Vollrath, M. and Kraume, M., 2008. Crystallized miniemulsions: Influence of operating parameters during high-pressure homogenization on size and shape of particles. Colloid Surf. A-Physicochem. Eng. Asp., 331(1-2): 108-113.

Greaves, D., Boxall, J., Mulligan, J., Montesi, A., Creek, J., Sloan, E.D. and Koh, C.A., 2008. Measuring the particle size of a known distribution using the focused beam reflectance measurement technique. Chem. Eng. Sci., 63(22): 5410-5419.

Grünig, J., Skale, T. and Kraume, M., 2011. Liquid flow on a vertical wire in a countercurrent gas flow. Chem. Eng. J., 164(1): 121-131.

Haggag, A.A., 1981. A Variant of the Generalized Reduced Gradient Algorithm for Non-Linear Programming and Its Applications. Eur. J. Oper. Res., 7(2): 161-168.

Hakansson, A., Trägardh, C. and Bergenstahl, B., 2009. Dynamic simulation of emulsion formation in a high pressure homogenizer. Chem. Eng. Sci., 64(12): 2915-2925.

Han, L.C., Luo, H.A. and Liu, Y.J., 2011. A theoretical model for droplet breakup in turbulent dispersions. Chem. Eng. Sci., 66(4): 766-776.

Hancil, V. and Rod, V., 1988. Break-up of a Drop in a Stirred Tank. Chem. Eng. Process., 23(3): 189-193.

Henschke, M., Schlieper, L.H. and Pfennig, A., 2002. Determination of a coalescence parameter from batch-settling experiments. Chem. Eng. J., 85(2-3): 369-378.

Hentschel, A., Gramdorf, S., Müller, R.H. and Kurz, T., 2008. Beta-Carotene-loaded nanostructured Lipid carriers. J. Food Sci., 73(2): N1-N6.

Hermann, S., Erdt, R., Maaß, S. and Kraume, M., 2011, Untersuchungen zur Steuerung von Tropfengrößenverteilungen, in proceedings of 13. Köthener Rührerkolloquium, Köthen, 17.06.2010, ISBN: 978-3-86011-026-3, pp. 17 (in German).

Hill, P.J. and Ng, K.M., 1996. Statistics of multiple particle breakage. AIChE J., 42(6): 1600-1611.

Himmelsbach, W., 2009. Herausforderungen und Lösungen in der industriellen Mischtechnik. CIT Plus, 11-12: 36-39 (in German).

Hinze, J.O., 1955. Fundamentals of the Hydrodynamic Mechanism of Splitting in Dispersion Processes. AIChE J., 1(3): 289-295.

Höfken, M., Schäfer, M. and Durst, F., 1996. Detailierte Untersuchung des Strömungsfeldes innerhalb eines Sechs-Blatt-Scheibenrührers. Chem. Ing. Tech., 68(7): 803-809 (in German).

Hsia, M.A. and Tavlarides, L.L., 1983. Simulation analysis of drop breakage, coalescence and micromixing in liquid-liquid stirred tanks. Chem. Eng. J., 26(3): 189-199.

Hu, B., Angeli, P., Matar, O.K., Lawrence, C.J. and Hewitt, G.F., 2006. Evaluation of drop size distribution from chord length measurements. AIChE J., 52(3): 931-939.

Hulburt, H.M. and Katz, S., 1964. Some problems in particle technology - a statistical mechanical formulation. Chem. Eng. Sci., 19(8): 555-574.

Jahanzad, F., Crombie, G., Innes, R. and Sajjadi, S., 2009. Catastrophic phase inversion via formation of multiple emulsions: A prerequisite for formation of fine emulsions. Chem. Eng. Res. Des., 87(4A): 492-498.

Jahoda, M., Mostek, M., Kukukova, A. and Machon, V., 2007. CFD modelling of liquid homogenization in stirred tanks with one and two impellers using large eddy simulation. Chem. Eng. Res. Des., 85(A5): 616-625.

Janssen, J.J.M., Boon, A. and Agterof, W.G.M., 1994. Influence of dynamic interfacial properties on droplet breakup in simple shear flow. AIChE J., 40(12): 1929-1939.

Janssen, J.M.H. and Meijer, H.E.H., 1993. Droplet Breakup Mechanisms - Stepwise equilibrium versus transient dispersion. J. Rheol., 37(4): 597-608.

Jaworski, Z., Bujalski, W., Otomo, N. and Nienow, A.W., 2000. CFD study of homogenization with dual Rushton turbines - Comparison with experimental results part I: Initial studies. Chem. Eng. Res. Des., 78(A3): 327-333.

Jon, D.I., Rosano, H.L. and Cummins, H.Z., 1986. Toluene Water/1-Propanol Interfacial-Tension Measurements by Means of Pendant Drop, Spinning Drop, and Laser Light-Scattering Methods. J. Colloid Interface Sci., 114(2): 330-341.

Joshi, J.B., Nere, N.K., Rane, C.V., Murthy, B.N., Mathpati, C.S., Patwardhan, A.W. and Ranade, V.V., 2011. CFD simulation of stirred tanks: Comparison of turbulence models. part I: radial flow impellers. Can. J. Chem. Eng., 89(1): 23-82.

Junker, B., Maciejak, W., Darnell, B., Lester, M. and Pollack, M., 2007. Feasibility of an in situ measurement device for bubble size and distribution. Bioprocess. Biosyst. Eng., 30(5): 313-326.

Khalil, A., Puel, F., Chevalier, Y., Galvan, J.M., Rivoire, A. and Klein, J.P., 2010. Study of droplet size distribution during an emulsification process using in situ video probe coupled with an automatic image analysis. Chem. Eng. J., 165(3): 946-957.
Kiparissides, C., Alexopoulos, A., Roussos, A., Dompazis, G. and Kotoulas, C., 2004. Population balance modeling of particulate polymerization processes. Ind. Eng. Chem. Res., 43(23): 7290-7302.
Koch, J., Hackbusch, W. and Sundmacher, K., 2006. Simulation of the population balance for droplet breakage in a liquid-liquid stirred tank reactor using H-matrix methods. In: W. Marquardt and C. Pantelides (Editors), Computer Aided Chemical Engineering. Elsevier, pp. 261-266.
Kolmogoroff, A.N., 1941. Local structure of turbulence in an incompressible viscous fluid at very high Reynolds numbers. Dokl. Akad. Nauk SSSR 30: 299-303.
Konno, M., Matsunaga, Y., Arai, K. and Saito, S., 1980. Simulation-Model for Breakup Process in an Agitated Tank. J. Chem. Eng. Jpn., 13(1): 67-73.
Konno, M., Aoki, M. and Saito, S., 1983. Scale Effect on Breakup Process in Liquid Liquid Agitated Tanks. J. Chem. Eng. Jpn., 16(4): 312-319.
Koshy, A., Das, T.R. and Kumar, R., 1988. Effect of Surfactants on Drop Breakage in Turbulent Liquid Dispersions. Chem. Eng. Sci., 43(3): 649-654.
Kostoglou, M., Dovas, S. and Karabelas, A.J., 1997. On the steady-state size distribution of dispersions in breakage processes. Chem. Eng. Sci., 52(8): 1285-1299.
Kostoglou, M. and Karabelas, A.J., 1997. An explicit relationship between steady-state size distribution and breakage kernel for limited breakage processes. J. Phys. A-Math. Gen., 30(20): L685-L691.
Kostoglou, M. and Karabelas, A.J., 2005. Toward a unified framework for the derivation of breakage functions based on the statistical theory of turbulence. Chem. Eng. Sci., 60(23): 6584-6595.
Kraume, M., Gäbler, A. and Schulze, K., 2004. Influence of physical properties on drop size distributions of stirred liquid-liquid dispersions. Chem. Eng. Technol., 27(3): 330-334.
Kukukova, A., Mostek, M., Jahoda, M. and Machon, V., 2005. CFD prediction of flow and homogenization in a stirred vessel: Part I vessel with one and two impellers. Chem. Eng. Technol., 28(10): 1125-1133.
Kumar, S., Kumar, R. and Gandhi, K.S., 1991. Alternative mechanisms of drop breakage in stirred vessels. Chem. Eng. Sci., 46(10): 2483-2489.
Kumar, S., Ganvir, V., Satyanand, C., Kumar, R. and Gandhi, K.S., 1998. Alternative mechanisms of drop breakup in stirred vessels. Chem. Eng. Sci., 53(18): 3269-3280.
Laakkonen, M., Moilanen, P., Alopaeus, V. and Aittamaa, J., 2007. Modelling local gas-liquid mass transfer in agitated vessels. Chem. Eng. Res. Des., 85(A5): 665-675.
Lasheras, J.C., Eastwood, C., Martínez-Bazán, C. and Montanés, J.L., 2002. A review of statistical models for the break-up of an immiscible fluid immersed into a fully developed turbulent flow. Int. J. Multiphase Flow, 28(2): 247-278.
Lee, C.H., Erickson, L.E. and Glasgow, L.A., 1987a. Dynamics of Bubble-Size Distribution in Turbulent Gas-Liquid Dispersions. Chem. Eng. Commun., 61(1-6): 181-195.
Lee, C.H., Erickson, L.E. and Glasgow, L.A., 1987b. Bubble Breakup and Coalescence in Turbulent Gas-Liquid Dispersions. Chem. Eng. Commun., 59(1-6): 65-84.
Lehr, F., Millies, M. and Mewes, D., 2002. Bubble-Size distributions and flow fields in bubble columns. AIChE J., 48(11): 2426-2443.
Leng, D.E. and Calabrese, R.V., 2004. Immiscible liquid-liquid systems. In: E.L. Paul, V.A. Atiemo-Obeng and S.M. Kresta (Editors), Handbook of Industrial Mixing: Science and Practice. John Wiley & Sons, Inc., Hoboken, New Jersey, pp. 639-753.
Lewis, J.P., 1995. Fast Normalized Cross-Correlation. Vision Interface: pp. 7.
Li, M.Z., White, G., Wilkinson, D. and Roberts, K.J., 2005. Scale up study of retreat curve impeller stirred tanks using LDA measurements and CFD simulation. Chem. Eng. J., 108(1-2): 81-90.
Li, M.Z. and Wilkinson, D., 2005. Determination of non-spherical particle size distribution from chord length measurements. Part 1: Theoretical analysis. Chem. Eng. Sci., 60(12): 3251-3265.
Liao, Y. and Lucas, D., 2009. A literature review of theoretical models for drop and bubble breakup in turbulent dispersions. Chem. Eng. Sci., 64(15): 3389-3406.
Liao, Y. and Lucas, D., 2010. A literature review on mechanisms and models for the coalescence process of fluid particles. Chem. Eng. Sci., 65(10): 2851-2864.
Lovick, J., Mouza, A.A., Paras, S.V., Lye, G.J. and Angeli, P., 2005. Drop size distribution in highly concentrated liquid-liquid dispersions using a light back scattering method. J. Chem. Technol. Biotechnol., 80(5): 545-552.
Maaß, S., Gäbler, A., Zaccone, A., Paschedag, A.R. and Kraume, M., 2007. Experimental investigations and modelling of breakage phenomena in stirred liquid/liquid systems. Chem. Eng. Res. Des., 85(A5): 703-709.

Maaß, S., Wollny, S., Sperling, R. and Kraume, M., 2009. Numerical and experimental analysis of particle strain and breakage in turbulent dispersions. Chem. Eng. Res. Des., 87(4): 565–572.
Maaß, S., Metz, F., Rehm, T. and Kraume, M., 2010. Prediction of drop sizes for liquid-liquid systems in stirred slim reactors - Part I: Single stage impellers. Chem. Eng. J., 162(2): 792-801.
Maaß, S., Wollny, S., Voigt, A. and Kraume, M., 2011a. Experimental comparison of measurement techniques for drop size distributions in liquid/liquid dispersions. Exp. Fluids, 50(2): 259-269.
Maaß, S., Rehm, T. and Kraume, M., 2011b. Prediction of drop sizes for liquid-liquid systems in stirred slim reactors - Part II: Multi stage impellers. Chem. Eng. J., 168(2): 827–838.
Maaß, S., Eppinger, T., Altwasser, S., Rehm, T. and Kraume, M., 2011c. Flow field analysis of stirred liquid-liquid systems in slim reactors. Chem. Eng. Technol., 34(8): 1215-1227.
Maaß, S., Buscher, S., Hermann, S. and Kraume, M., 2011d. Analysis of particle strain in stirred bioreactors by drop breakage investigations. Biotechnol. J., 6(8): 979-992.
Maaß, S. and Kraume, M., 2011. Determination of breakage rates using single drop experiments. Chem. Eng. Sci.(DOI: 10.1016/j.ces.2011.08.027): pp. 20.
Maaß, S., Paul, N. and Kraume, M., 2011e. Influence of the dispersed phase fraction on experimental and predicted drop size distributions in breakage dominated stirred liquid-liquid systems. Chem. Eng. Sci.(submitted): pp. 12.
Maaß, S., Rojahn, J., Hänsch, R. and Kraume, M., 2011f. Automated drop detection using image analysis for online particle size monitoring in multiphase systems. Comput. Chem. Eng.(submitted): pp. 10.
Marchisio, D.L., Pikturna, J.T., Fox, R.O., Vigil, R.D. and Barresi, A.A., 2003. Quadrature method of moments for population-balance equations. AIChE J., 49(5): 1266-1276.
Marinova, K.G., Alargova, R.G., Denkov, N.D., Velev, O.D., Petsev, D.N., Ivanov, I.B. and Borwankar, R.P., 1996. Charging of oil-water interfaces due to spontaneous adsorption of hydroxyl ions. Langmuir, 12(8): 2045-2051.
Martín, M., Montes, F.J. and Galán, M.A., 2009. Theoretical modelling of the effect of surface active species on the mass transfer rates in bubble column reactors. Chem. Eng. J., 155(1-2): 272-284.
Martínez-Bazán, C., Montanés, J.L. and Lasheras, J.C., 1999. On the breakup of an air bubble injected into a fully developed turbulent flow. Part 1. Breakup frequency. J. Fluid Mech., 401: 157-182.
McGraw, R., 1997. Description of aerosol dynamics by the quadrature method of moments. Aerosol Sci. Technol., 27(2): 255-265.
Megias-Alguacil, D. and Windhab, E.J., 2006. Experimental study of drop deformation and breakup in a model multitoothed rotor-stator. 128(6): 1289-1294.
Mickler, M., Didas, S., Jaradat, M., Attarakih, M. and Bart, H.-J., 2011. Droplet swarm analysis by image processing for simulation of extraction columns with population balances. Chem. Ing. Tech., 83(3): 227-236 (in German).
Mima, H. and Kitamori, N., 1966. Stability and flocculation of oil droplets in dilute emulsions. J. Pharm. Sci., 55(1): 44-48.
Modes, G., 2000. Grundsätzliche Studie zur Populationsdynamik einer Extraktionskolonne auf Basis von Einzeltropfenuntersuchungen. dissertation, Universität Kaiserslautern, pp. 163, (in German).
Molag, M., Joosten, G.E.H. and Drinkenburg, A.A.H., 1980. Droplet breakup and distribution in stirred immiscible two-liquid systems. Ind. Eng. Chem. Fundam., 19(3): 275-281.
Montante, G. and Magelli, F., 2004. Liquid homogenization characteristics in vessels stirred with multiple rushton turbines mounted at different spacings - CFD study and comparison with experimental data. Chem. Eng. Res. Des., 82(A9): 1179-1187.
Nanda, A.K. and Sharma, M.M., 1966. Effective Interfacial Area in Liquid-Liquid Extraction. Chem. Eng. Sci., 21(8): 707-713.
Nienow, A.W., 2004. Break-up, coalescence and catastrophic phase inversion in turbulent contactors. Adv. Colloid Interface Sci., 108: 95-103.
Niknafs, N., Spyropoulos, F. and Norton, I.T., 2011. Development of a new reflectance technique to investigate the mechanism of emulsification. J. Food Eng., 104(4): 603-611.
O'Rourke, A.M. and MacLoughlin, P.F., 2005. A comparison of measurement techniques used in the analysis of evolving liquid-liquid dispersions. Chem. Eng. Process., 44(8): 885-894.
O'Rourke, A.M. and MacLoughlin, P.F., 2010. A study of drop breakage in lean dispersions using the inverse-problem method. Chem. Eng. Sci., 65(11): 3681-3694.
Ochieng, A., Onyango, M. and Kiriamiti, K., 2009. Experimental measurement and computational fluid dynamics simulation of mixing in a stirred tank: a review. S. Afr. J. Sci., 105(11-12): 421-426.
Pacek, A.W., Moore, I.P.T., Nienow, A.W. and Calabrese, R.V., 1994. Video technique for measuring dynamics of liquid-liquid dispersion during phase inversion. AIChE J., 40(12): 1940-1949.
Pacek, A.W. and Nienow, A.W., 1995. Measurement of drop size distribution in concentrated liquid-liquid dispersions - video and capillary techniques. Chem. Eng. Res. Des., 73(A5): 512-518.

Pacek, A.W., Man, C.C. and Nienow, A.W., 1998. On the Sauter mean diameter and size distributions in turbulent liquid/liquid dispersions in a stirred vessel. Chem. Eng. Sci., 53(11): 2005-2011.
Petrak, D., 2002. Simultaneous measurement of particle size and particle velocity by the spatial filtering technique. Part. Part. Sys. Char., 19(6): 391-400.
Qin, S.J. and Badgwell, T.A., 2003. A survey of industrial model predictive control technology. Control Eng. Practice, 11(7): 733-764.
Quadros, P.A. and Baptista, C.M.S.G., 2003. Effective interfacial area in agitated liquid-liquid continuous reactors. Chem. Eng. Sci., 58(17): 3935-3945.
Raikar, N.B., Bhatia, S.R., Malone, M.F. and Henson, M.A., 2009. Experimental studies and population balance equation models for breakage prediction of emulsion drop size distributions. Chem. Eng. Sci., 64(10): 2433-2447.
Raikar, N.B., Bhatia, S.R., Malone, M.F., McClements, D.J., Almeida-Rivera, C., Bongers, P. and Henson, M.A., 2010. Prediction of emulsion drop size distributions with population balance equation models of multiple drop breakage. Colloid Surf. A-Physicochem. Eng. Asp., 361(1-3): 96-108.
Ramkrishna, D., 2000. Population balances, theory and applications to particulate systems in engineering. Academic Press, San Diego, CA, 355 pp.
Ribeiro, H.S., Ax, K. and Schubert, H., 2003. Stability of lycopene emulsions in food systems. J. Food Sci., 68(9): 2730-2734.
Ribeiro, L.M., Regueiras, P.F.R., Guimaraes, M.M.L., Madureira, C.M.N. and Cruzpinto, J.J.C., 1995. The dynamic behavior of liquid-liquid agitated dispersions: 1. The hydrodynamics. Comput. Chem. Eng., 19(3): 333-343.
Ribeiro, M.M., Regueiras, P.F., Guimaraes, M.M.L., Madureira, C.M.N. and Pinto, J., 2011. Optimization of breakage and coalescence model parameters in a steady-state batch agitated dispersion. Ind. Eng. Chem. Res., 50(4): 2182-2191.
Ribeiro, M.M.M., Guimaraes, M.M.L., Madureira, C.M.N. and Pinto, J.J.C.C., 2004. Non-invasive system and procedures for the characterization of liquid-liquid dispersions. Chem. Eng. J., 97(2-3): 173-182.
Richards, J.R. and Congalidis, J.P., 2006. Measurement and control of polymerization reactors. Comput. Chem. Eng., 30(10-12): 1447-1463.
Riebel, U. and Löffler, F., 1989. The fundamentals of particle-size analysis by means of ultrasonic spectrometry. Part. Part. Sys. Char., 6(4): 135-143.
Ritter, J. and Kraume, M., 2000. On-line measurement technique for drop size distributions in liquid/liquid systems at high dispersed phase fractions. Chem. Eng. Technol., 23(7): 579-582.
Rohn, N. and Keller, W., 2011, CFD - Lösungen für die Rührtechnik, oral presentation at: ProcessNet Jahrestreffen der Fachausschüsse Mischvorgänge und CFD, Dortmund, 21.-23.02., (in German).
Ross, S.L., Verhoff, F.H. and Curl, R.L., 1978. Droplet breakage and coalescence processes in an agitated dispersion: 2. Measurement and interpretation of mixing experiments. Ind. Eng. Chem. Fundam., 17(2): 101-108.
Ruiz, M.C. and Padilla, R., 2004. Analysis of breakage functions for liquid-liquid dispersions. Hydrometallurgy, 72(3-4): 245-258.
Sachweh, B., Heffels, C., Polke, R. and Rädle, M., 1998, Light scattering sensor for in-line measurements of mean particle sizes in suspensions, 7th European Symposium on Particle Characterization, Nuremberg, 635-644.
Sæther, O., 2001. Video-enhanced microscopy of emulsion droplets and size distribution. In: J. Sjöblom (Editor), Encyclopedic Handbook of Emulsion Technology. Marcel Dekker Inc., New York, pp. 349-360.
Saliakas, V., Kotoulas, C., Meimaroglou, D. and Kiparissides, C., 2008. Dynamic evolution of the particle size distribution in suspension polymerization reactors: A comparative study on Monte Carlo and sectional grid methods. Can. J. Chem. Eng., 86(5): 924-936.
Schäfer, M., 2001. Charakterisierung, Auslegung und Verbesserung des Makro- und Mirkomischens in gerührten Behältern. dissertation, Universität Erlangen-Nürnberg, pp. 180, (in German).
Scherze, I., Knofel, R. and Muschiolik, G., 2005. Automated image analysis as a control tool for multiple emulsions. Food Hydrocolloids, 19(3): 617-624.
Simmons, M.J.H., Zaidi, S.H. and Azzopardi, B.J., 2000. Comparison of laser-based drop-size measurement techniques and their application to dispersed liquid-liquid pipe flow. Opt. Eng., 39(2): 505-509.
Singh, K.K., Mahajani, S.M., Shenoy, K.T. and Ghosh, S.K., 2008. Representative drop sizes and drop size distributions in A/O dispersions in continuous flow stirred tank. Hydrometallurgy, 90(2-4): 121-136.
Singh, K.K., Mahajani, S.M., Shenoy, K.T. and Ghosh, S.K., 2009. Population balance modeling of liquid-liquid dispersions in homogeneous continuous-flow stirred tank. Ind. Eng. Chem. Res., 48(17): 8121-8133.
Srilatha, C., Mundada, T.P. and Patwardhan, A.W., 2010a. Scale-up of pump-mix mixers using CFD. Chem. Eng. Res. Des., 88(1): 10-22.

Srilatha, C., Morab, V., Mundada, T.P. and Patwardhan, A.W., 2010b. Relation between hydrodynamics and drop size distributions in pump-mix mixer. Chem. Eng. Sci., 65(11): 3409-3426.
Stone, H.A., 1994. Dynamics of drop deformation and breakup in viscous fluids. Annu. Rev. Fluid Mech., 26: 65-102.
Stoots, C.M. and Calabrese, R.V., 1995. Mean velocity-field relative to a Rushton turbine blade. AIChE J., 41(1): 1-11.
Taylor, G.I., 1934. The formation of emulsions in definable fields of flow. Proc. R. Soc. London, Ser. A, 146(858): 501-523.
Tcholakova, S., Vankova, N., Denkov, N.D. and Danner, T., 2007. Emulsification in turbulent flow: 3. Daughter drop-size distribution. J. Colloid Interface Sci., 310(2): 570-589.
Tsouris, C. and Tavlarides, L.L., 1994. Breakage and coalescence models for drops in turbulent dispersions. AIChE J., 40(3): 395-406.
Unadkat, H., Rielly, C.D., Hargrave, G.K. and Nagy, Z.K., 2009. Application of fluorescent PIV and digital image analysis to measure turbulence properties of solid-liquid stirred suspensions. Chem. Eng. Res. Des., 87(4A): 573-586.
Valentas, K.J. and Amundson, N.R., 1966. Breakage and coalescence in dispersed phase systems. Ind. Eng. Chem. Fundam., 5(4): 533-542.
Valentas, K.J., Bilous, O. and Amundson, N.R., 1966. Analysis of breakage in dispersed phase systems. Ind. Eng. Chem. Fundam., 5(2): 271-279.
van de Hulst, H.C., 1981. Light Scattering by Small Particles - Structure of Matter Series. Dover Publications, New York, 470 pp.
Van Gerven, T. and Stankiewicz, A., 2009. Structure, energy, synergy, time - the fundamentals of process intensification. Ind. Eng. Chem. Res., 48(5): 2465-2474.
Vankova, N., Tcholakova, S., Denkov, N.D., Ivanov, I.B., Vulchev, V.D. and Danner, T., 2007. Emulsification in turbulent flow: 1. Mean and maximum drop diameters in inertial and viscous regimes. J. Colloid Interface Sci., 312(2): 363-380.
Wachtel, R.E. and Lamer, V.K., 1962. The preparation and size distribution of some monodisperse emulsions. J. Colloid Sci., 17(6): 531-539.
Wang, T.F., Wang, J.F. and Jin, Y., 2003. A novel theoretical breakup kernel function for bubbles/droplets in a turbulent flow. Chem. Eng. Sci., 58(20): 4629-4637.
Wegener, M., Grünig, J., Stuber, J., Paschedag, A.R. and Kraume, M., 2007. Transient rise velocity and mass transfer of a single drop with interfacial instabilities - experimental investigations. Chem. Eng. Sci., 62(11): 2967-2978.
Wegener, M., 2009. Der Einfluss der konzentrationsinduzierten Marangonikonvektion auf den instationären Impuls- und Stofftransport an Einzeltropfen. dissertation, Technische Universität Berlin, pp. 231, (in German).
Wegener, M., Eppinger, T., Bäumler, K., Kraume, M., Paschedag, A.R. and Bänsch, E., 2009. Transient rise velocity and mass transfer of a single drop with interfacial instabilities-Numerical investigations. Chem. Eng. Sci., 64(23): 4835-4845.
Whewell, R.J., Hughes, M.A. and Hanson, C., 1975. Kinetics of Solvent-Extraction of Copper(II) with Lix Reagents:1. Single Drop Experiments. J. Inorg. Nucl. Chem., 37(11): 2303-2307.
Wichterle, K., 1995. Drop Breakup by Impellers. Chem. Eng. Sci., 50(22): 3581-3586.
Wille, M., Langer, G. and Werner, U., 2001. PDA measurement of drop size distribution for liquid-liquid dispersing in agitated tanks. Chem. Eng. Technol., 24(5): 475-479.
Wollny, S., Sperling, R., Heun, G. and Ritter, J., 2008, Numerische Untersuchungen von Partikelbeanspruchungen in turbulenten Strömungen mit Hilfe der strömungsabhängigen Gradienten, in proceedings of 10. Köthener Rührerkolloquium, Köthen, 17.06.2007, ISBN: 978-3-86011-015-7, pp. 13 (in German).
Wollny, S., 2010. Experimentelle und numerische Untersuchungen zur Partikelbeanspruchung in gerührten (Bio-)Reaktoren. dissertation, Technische Universität Berlin, pp. 177, (in German).
Worlitschek, J., Hocker, T. and Mazzotti, M., 2005. Restoration of PSD from chord length distribution data using the method of projections onto convex sets. Part. Part. Sys. Char., 22(2): 81-98.
Wulkow, M., Gerstlauer, A. and Nieken, U., 2001. Modeling and simulation of crystallization processes using parsival. Chem. Eng. Sci., 56(7): 2575-2588.
Yang, B., Takahashi, K. and Takeishi, M., 2000. Styrene drop size and size distribution in an aqueous solution of poly(vinyl alcohol). Ind. Eng. Chem. Res., 39(6): 2085-2090.
Yu, Z.Q., Chow, P.S. and Tan, R.B.H., 2008. Interpretation of Focused Beam Reflectance Measurement (FBRM) Data via Simulated Crystallization. Org. Process Res. Dev., 12(4): 646-654.
Yuan, H.G., Kalfas, G. and Ray, W.H., 1991. Suspension Polymerization. J. Macromol. Sci., Rev. Macromol. Chem. Phys., C31(2-3): 215-299.

Zadghaffari, R., Moghaddas, J.S. and Revstedt, J., 2010. Large-eddy simulation of turbulent flow in a stirred tank driven by a Rushton turbine. Comput. Fluids, 39(7): 1183-1190.
Zerfa, M. and Brooks, B.W., 1996. Prediction of vinyl chloride drop sizes in stabilised liquid-liquid agitated dispersion. Chem. Eng. Sci., 51(12): 3223-3233.
Zhou, G. and Kresta, S.M., 1998. Evolution of drop size distribution in liquid-liquid dispersions for various impellers. Chem. Eng. Sci., 53(11): 2099-2113.

Appendix A1 - Own publications and presentations

I. Peer reviewed Journals (full paper and abstracts)

[16] Maaß, S., Rojahn, J. Hänsch, R. and Kraume, M., **2011**. Automated drop detection using image analysis for online particle size monitoring in multiphase systems. Computers and Chemical Engineering (submitted): pp. 10.

[15] Maaß, S., Paul, N. and Kraume, M., **2011**. Influence of the dispersed phase fraction on experimental and predicted drop size distributions in breakage dominated systems. Chemical Engineering Science (submitted): pp. 12.

[14] Maaß, S., Buscher, S. and Kraume, M., **2011**. Analysis of particle strain in stirred bioreactors by drop breakage investigations. Biotechnology Journal (accepted): pp. 15.

[13] Maaß, S., Eppinger, T., Altwasser, S., Rehm, T. and Kraume, M., **2011**. Flow field analysis of stirred liquid-liquid systems in slim reactors. Chemical Engineering Technology (in press): pp. 15.

[12] Maaß, S. and Kraume, M., **2011**. Determination of breakage rates with single drop experiments. Chemical Engineering Science (submitted): pp. 20.

[11] Maaß, S., Rehm, T. and Kraume, M., **2011**. Prediction of drop sizes for liquid/liquid systems in stirred slim reactors - Part II: Multiple stage impellers. Chemical Engineering Journal, 168(2): 827–838.

[10] Maaß, S., Wollny, S., Voigt, A. and Kraume, M., **2011**. Experimental comparison of measurement techniques for drop size distributions in liquid/liquid dispersions. Experiments in Fluids, 50(2): 259-269.

[9] Hermann, S., Maaß, S., Walle, A., Schäfer, M. and Kraume, M., **2010**. Experimentelle und numerische Untersuchungen zu Ort und Art des Tropfenbruchs in gerührten Flüssig/flüssig-Systemen, Chemie Ingenieur Technik, 82(9): 1389-1389, (abstract).

[8] Maaß, S., Metz, F., Rehm, T. and Kraume, M., **2010**. Prediction of drop sizes for liquid-liquid systems in stirred slim reactors - Part I: Single stage impellers, Chemical Engineering Journal, 162(2): 792-801.

[7] Maaß, S., Grünig, J. and Kraume, M., **2009**. Techniki pomiarowe do rozkładu wielkości kropel w mieszanej cieczy - Measurement techniques for drop size distributions in stirred liquid/liquid systems., Chemical and Process Engineering, 30(4): 635-651.

[6] Maaß, S. and Kraume, M., **2009**. Experimentelle Untersuchungen zur Tropfenbeanspruchung in turbulenten Strömungen, Chemie Ingenieur Technik, 81(8): 1146-1147, (abstract).

[5] Maaß, S., Wollny, S., Sperling, R. and Kraume, M., **2009**. Numerical and experimental analysis of particle strain and breakage in turbulent dispersions, Chemical Engineering Research and Design, 87(4): 565–572.

[4] Maaß, S., Lutz, E., Metz, F., Rehm, T. and Kraume, M., **2008**. Experimentelle und numerische Untersuchungen von gerührten Flüssig/flüssig-Systemen für die PVC-Produktion mit mehrstufigen Rührern, Chemie Ingenieur Technik, 80(9): 1358, (abstract).

[3] Zaccone, A., Gäbler, A., Maaß, S., Marchisio, D. and Kraume, M., **2007**. Drop breakage in liquid-liquid stirred dispersions: Modelling of single drop breakage, Chemical Engineering Science, 62(22): 6297-6307.

[2] Maaß, S., Gäbler, A., Zaccone, A., Paschedag, A.R. and Kraume, M., **2007**. Experimental investigations and modelling of breakage phenomena in stirred liquid/liquid systems, Chemical Engineering Research and Design, 85(A5): 703-709.

[1] Maaß, S., Gäbler, A., Wegener, M., Zaccione, A., Paschedag, A. and Kraume, M., **2006**. Tropfenzerfall und Koaleszenz in gerührten Flüssig/flüssig-Systemen und deren Einfluss auf die Tropfengrößenverteilung, Chemie Ingenieur Technik, 78(9): 1347, (abstract).

II. Conference proceedings (full paper and abstracts)

[22] Maaß, S., Wallau, W., Hülagü, D., Hermann, S. and Kraume, M., **2011**, Overview of measurement techniques for sizing fluid particles in multi phase systems, 1st international symposium on Multiscale Multiphase Process Engineering, Kanazawa, Japan, 04.-07.10., pp. 6.

[21] Maaß, S. and Kraume, M., **2011**, Process intensification for coalescence hindered stirred liquid-liquid systems, 1st international symposium on Multiscale Multiphase Process Engineering, Kanazawa, Japan, 04.-07.10., pp. 6.
[20] Maaß, S., Hermann, S., Rojahn, J. and Kraume, M., **2011**, On-line monitoring of fluid particle size distributions using image analysis, 1st international symposium on Multiscale Multiphase Process Engineering, Kanazawa, Japan, 04.-07.10., pp. 6.
[19] Hermann, S., Maaß, S., Zedel, D., Walle, A., Schäfer, M. and Kraume, M., **2011**, Experimental and numerical investigations of drop breakage mechanism, 1st international symposium on Multiscale Multiphase Process Engineering, Kanazawa, Japan, 04.-07.10., pp. 6.
[18] Maaß, S. and Kraume, M., **2011**, Process intensification and monitoring of stirred liquid-liquid dispersions, International Symposium on Mixing in Industrial Processes VII, Beijing, China, 18.-22.09, pp. 2 (extended abstract).
[17] Hermann, S., Erdt, R., Maaß, S. and Kraume, M., **2011**, Untersuchungen zur Steuerung von Tropfengrößenverteilungen, 13. Köthener Rührerkolloquium, Köthen, 17.06.2010, ISBN: 978-3-86011-026-3, pp. 15.
[16] Hermann, S., Maaß, S., Kumar, S. and Kraume, M., **2010**, Modelling of coalescence in turbulent stirred liquid/liquid dispersions considering droplet charge, 4th International Conference on Population Balance Modelling, Berlin, 15.-17.09., pp. 15.
[15] Maaß, S., Hermann, S. and Kraume, M., **2010**, Determination of breakage rates with single drop experiments, 4th International Conference on Population Balance Modelling, Berlin, 15.-17.09., pp. 34.
[14] Rojahn, J., Maaß, S. and Kraume, M., **2010**, Measuring of particle size distributions in multi phase systems, HEFAT 2010, Antalya, 19.-21.07., pp. 6.
[13] Maaß, S. and Kraume, M., **2010**, Tropfenzerteilung in gerührten Dispersionen, 12. Köthener Rührer Kolloquium, Köthen, 17.-18.06.2009, ISBN: 978-3-86011-036-2, pp. 14.
[12] Maaß, S., Heldt, S., Hermann, S. and Kraume, M., **2010**, Influence of ionic strength on coalescence in liquid/liquid systems, WCPT VI, Nürnberg, 26.-29.04., pp. 4.
[11] Maaß, S., Rojahn, J. and Kraume, M., **2010**, Automated image processing for in-situ observation and control of multiphase dispersions occurring in chemical and process engineering, WCPT VI, Nürnberg, 26.-29.04., pp. 4.
[10] Maaß, S., Lutz, E., Metz, F., Rehm, T. and Kraume, M., **2009**, Analysis of stirred liquid/liquid systems for PVC-production in slim reactors with multi-stage stirrers, ACHEMA 2009, Frankfurt am Main, 11.-15.05, pp. 1 (abstract).
[9] Maaß, S., Wollny, S., Sperling, R. and Kraume, M., **2009**, Numerical and experimental analysis of particle strain and breakage in turbulent dispersions, 13th Conference on European Mixing, Kings College, London, 14.-17.04., pp. 8.
[8] Maaß, S., Grünig, J., Horn, S. and Kraume, M., **2008**, Measurement techniques for drop size distributions in stirred and fast coalescing liquid/liquid systems, 17th International Conference "Chemical Engineering and Chemical Apparatus Construction", Krakow, 07.-09.10., pp. 12.
[7] Maaß, S., Metz, F., Rehm, T. and Kraume, M., **2008**, Fundamental experimental and numerical analysis of stirred liquid/liquid systems for PVC-production in slim reactors with multi-stage stirrers, Sixth International Symposium on Mixing in Industrial Process Industries - ISMIP VI, Niagara on the Lake, Niagara Falls, Ontario, 17.-21.08., pp. 2 (extended abstract).
[6] Maaß, S., Paschedag, A.R. and Kraume, M., **2008**, Einfluss von Elektrolyten und Turbulenzparametern auf Tropfengrößenverteilungen in gerührten Flüssig/flüssig Systemen, 10. Köthener Rührerkolloquium, Köthen, 09.05.2007, ISBN: 978-3-86011-015-7, pp. 10.
[5] Maaß, S., Paschedag, A.R. and Kraume, M., **2007**, Influence of electrolytes and turbulence parameters on drop breakage and drop size distributions in Stirred Liquid/Liquid Dispersions, 6th International Conference on Multiphase Flow, Leipzig, 09.-13.07., pp. 6.
[4] Maaß, S., Gäbler, A., Zaccone, A., Paschedag, A. and Kraume, M., **2007**, Tropfenzerfall in gerührten Flüssig/flüssig-Systemen., 9. Köthener Rührer Kolloquium, Köthen, 14.06.2006, ISBN: 978-3-86011-012-6, pp. 8.
[3] Maaß, S., Wollny, S., Rojahn, J., Paschedag, A.R. and Kraume, M., **2007**, Comparison of measurement techniques for drop sizes in highly dispersed and fastly coalescing systems, PARTEC 2007, Nürnberg, 27.-29.03., pp. 4.
[2] Maaß, S., Paschedag, A.R. and Kraume, M., **2006**, Experimental and numerical investigations of coalescence and breakage phenomena in stirred liquid/liquid systems, 16th International Conference "Chemical Engineering and Plant Design", Berlin, 10.-11.10., pp. 8.

[1] Maaß, S., Gäbler, A., Wegener, M., Zaccone, A., Paschedag, A.R. and Kraume, M., **2006**, Drop breakage and daughter drop distribution in stirred liquid-liquid systems and their modelling within the population balance equation, 12th European Conference on Mixing, Bologna, 26.-30.06., pp. 8.

III. Oral and poster presentations (presenting author is underlined)

[47] Maaß, S. and Kraume, M., **2011**, Process intensification for coalescence hindered stirred liquid-liquid systems, 1st international symposium on Multiscale Multiphase Process Engineering, Kanazawa, Japan, 04.-07.10., (oral presentation).
[46] Maaß, S., Hermann, S., Rojahn, J. and Kraume, M., **2011**, On-line monitoring of fluid particle size distributions using image analysis, 1st international symposium on Multiscale Multiphase Process Engineering, Kanazawa, Japan, 04.-07.10., (oral presentation).
[45] Maaß, S., Wallau, W., Hülagü, D., Hermann, S. and Kraume, M., **2011**, Overview of meas-urement techniques for sizing fluid particles in multi phase systems, 1st international symposium on Multiscale Multiphase Process Engineering, Kanazawa, Japan, 04.-07.10., (poster presentation).
[44] Hermann, S., Maaß, S., Zedel, D., Walle, A., Schäfer, M. and Kraume, M., **2011**, Experimen-tal and numerical investigations of drop breakage mechanism, 1st international sym-posium on Multiscale Multiphase Process Engineering, Kanazawa, Japan, 04.-07.10., (oral presentation).
[43] Maaß, S. and Kraume, M., **2011**, Model based process intensification for stirred liquid-liquid systems, 8th European Congress of Chemical Engineering Berlin, Germany, 25.-29.09, (oral presentation).
[42] Maaß, S., Hermann, S., Rojahn, J. and Kraume, M., **2011**, On-line monitoring of drop size distributions in agitated vessels using image analysis, 8th European Congress of Chemical Engineering Berlin, Germany, 25.-29.09, (poster presentation).
[41] Maaß, S., Hermann, S. and Kraume, M., **2011**, Process intensification and monitoring of stirred liquid-liquid dispersions, International Symposium on Mixing in Industrial Processes VII, Beijing, China, 18.-22.09, (oral presentation).
[40] Maaß, S., Hermann, S. and Kraume, M., **2011**, Modellierung des Tropfenbruches in turbulenten Flüssig/flüssig-Dispersionen, ProcessNet Jahrestreffen der Fachausschüsse Extraktion, Fluidverfahrenstechnik, Mehrphasenströmungen und Phytoextrakte, Fulda, 03.-04.03., (poster presentation).
[39] Hermann, S., Maaß, S. and Kraume, M., **2011**, Untersuchungen zur Anzahl und Größenverteilung von Tochtertropfen in gerührten flüssig/flüssig-Systemen, ProcessNet Jahrestreffen der Fachausschüsse Extraktion, Fluidverfahrenstechnik, Mehrphasenströmungen und Phytoextrakte, Fulda, 03.-04.03., (poster presentation).
[38] Maaß, S., Rojahn, J., Hermann, S. and Kraume, M., **2011**, Automatisierte Tropfenerkennung durch Bildverarbeitung für die Tropfengrößenüberwachung und -steuerung., ProcessNet Jahrestreffen der Fachausschüsse Partikelmesstechnik und Grenzflächenbestimmte Systeme und Prozesse, Clausthal-Zellerfeld, 01.-02.03., (oral presentation).
[37] Maaß, S., Eppinger, T. and Kraume, M., **2011**, Ortsaufgelöste Untersuchung von Festbettreaktoren mit heterogener Reaktion, ProcessNet Jahrestreffen der Fachausschüsse Mischvorgänge und CFD, Dortmund, 21.-23.02., (oral presentation).
[36] Hermann, S., Maaß, S. and Kraume, M., **2011**, Einfluss des Stoffsystems und der Tropfengröße auf den Tropfenbruch, ProcessNet Jahrestreffen der Fachausschüsse Mischvorgänge und CFD, Dortmund, 21.-23.02., (oral presentation).
[35] Maaß, S. and Kraume, M., **2011**, Analyse von bruchdominierten, koaleszenzstabilisierten Systemen bei Variation des Dispersphasenanteils, ProcessNet Jahrestreffen der Fachausschüsse Mischvorgänge und CFD, Dortmund, 21.-23.02., (oral presentation).
[34] Hermann, S., Maaß, S., Walle, A., Schäfer, M. and Kraume, M., **2010**, Experimentelle und numerische Untersuchungen zu Ort und Art des Tropfenbruchs in gerührten Flüssig-flüssig-Systemen, ProcessNet Jahrestagung, Aachen, 21.09.-23.09., (poster presentation).
[33] Hermann, S., Maaß, S., Kumar, S. and Kraume, M., **2010**, Modelling of coalescence in turbulent stirred liquid/liquid dispersions considering droplet charge, 4th International Conference on Population Balance Modelling, Berlin, 15.-17.09., (poster presentation).
[32] Maaß, S., Hermann, S. and Kraume, M., **2010**, Determination of breakage rates with single drop experiments, 4th International Conference on Population Balance Modelling, Berlin, 15.-17.09., (oral presentation).

[31] Hermann, S., Maaß, S., A.Walle, M.Schäfer and Kraume, M., **2010**, Experimental and numerical investigations of drop size distributions in stirred liquid/liquid systems Mixing XXII - North American Mixing Forum, Victoria, BC Canada, 20.-25.06., (oral presentation).
[30] Maaß, S., Altwasser, S., Sperling, R., Rehm, T. and Kraume, M., **2010**, Experimental investigations of stirred liquid-liquid systems in slim reactors: Mixing time and minimum dispersion speed, Mixing XXII - North American Mixing Forum, Victoria, BC Canada, 20.-25.06., (poster presentation).
[29] Rojahn, J., Maaß, S. and Kraume, M., **2010**, Measuring of particle size distributions in multi phase systems, HEFAT 2010, Antalya, 19.-21.07., (oral presentation).
[28] Hermann, S., Erdt, R., Maaß, S. and Kraume, M., **2010**, Untersuchungen zur Steuerung von Tropfengrößenverteilungen, 13. Köthener Rührerkolloquium, Köthen, 17.06.2010, (oral presentation).
[27] Maaß, S., Grünig, J. and Kraume, M., **2010**, Measuring of particle size distributions in stirred tanks, International Conference on Multiphase Flow 2010, Tampa, Florida, 30.05.-04.06., (oral presentation).
[26] Maaß, S., Rojahn, J. and Kraume, M., **2010**, Automated image processing for in-situ observation and control of multiphase dispersions occurring in chemical and process engineering, WCPT6 2010, Nürnberg, 26.-29.04., (oral presentation).
[25] Maaß, S., Hermann, S. and Kraume, M., **2010**, Influence of ionic strength on coalescence in liquid/liquid systems, WCPT6 2010, Nürnberg, 26.-29.04., (poster presentation).
[24] Hermann, S., Vazquez, S., Maaß, S. and Kraume, M., **2010**, Transientes Verhalten von Tropfengrößenverteilungen in Abhängigkeit von unterschiedlichen Rührerdrehfrequenzfunktionen, ProcessNet Jahrestreffen des Fachausschusses "Extraktion", Kaiserslautern, 18.-19.03., (oral presentation).
[23] Hermann, S., Zillmer, M., Maaß, S. and Kraume, M., **2010**, Experimentelle Untersuchungen zum Einfluss des pH-Wertes auf den Tropfenbruch in Flüssig/flüssig-Systemen, ProcessNet Jahrestreffen der Fachausschüsse Agglomeration, Zerkleinern/Klassieren und Mischvorgänge, Fulda, 21.-23.02., (oral presentation).
[22] Maaß, S., Rojahn, J., Hermann, S. and Kraume, M., **2010**, Automatisierte Bildverarbeitung für Insitu Überwachung und Steuerung von Mehrphasen Systemen, ProcessNet Jahrestreffen der Fachausschüsse Agglomeration, Zerkleinern/Klassieren und Mischvorgänge, Fulda, 21.-23.02., (oral presentation).
[21] Maaß, S. and Kraume, M., **2009**, Analysis of particle strain in stirred bioreactors by drop breakage investigations., BioProScale Symposium, Berlin, 24.-27.11., (oral presentation).
[20] Maaß, S. and Kraume, M., **2009**, Experimentelle Untersuchungen zur Tropfenbeanspruchung in turbulenten Strömungen, ProcessNet Jahrestagung, Mannheim, 08.-10.09., (oral presentation).
[19] Maaß, S. and Kraume, M., **2009**, Tropfenzerteilung in gerührten Dispersionen, 12. Köthener Rührer Kolloquium, Köthen, 17.-18. Juni 2009, (oral presentation).
[18] Maaß, S., Lutz, E., Metz, F., Rehm, T. and Kraume, M., **2009**, Analysis of stirred liquid/liquid systems for PVC-production in slim reactors with multi-stage stirrers, ACHEMA 2009, Frankfurt am Main, 11.-15.05, (oral presentation).
[17] Maaß, S., Wollny, S., Sperling, R. and Kraume, M., **2009**, Numerical and experimental analysis of particle strain and breakage in turbulent dispersions, 13th Conference on European Mixing, Kings College, London, 14.-17.04., (oral presentation).
[16] Maaß, S., Wollny, S., Sperling, R., Heun, G. and Kraume, M., **2009**, Experimentelle und numerische Untersuchungen zur Tropfenbeanspruchung in turbulenten Strömungen, Jahrestreffen der Fachausschüsse Computational Fluid Dynamics, Mischvorgänge und Extraktion, Fulda, 29.-30.03, (oral presentation - tandem).
[15] Wollny, S., Sperling, R., Heun, G., Ritter, J., Maaß, S. and Kraume, M., **2008**, Bestimmung von Tropfengrößenverteilungen zur Charakterisierung von Rührorganen hinsichtlich der Partikelbeanspruchung, ProcessNet Jahrestreffen der Fachausschüsse Mehrphasenströmungen, Partikelmesstechnik und Zerkleinern/Klassieren, München, 10.-14.03., (poster presentation).
[14] Maaß, S., Lutz, E., Metz, F., Rehm, T. and Kraume, M., **2008**, Experimentelle und numerische Untersuchungen von gerührten Flüssig/Flüssig-Systemen für die PVC-Produktion mit mehrstufigen Rührern, ProcessNet Jahrestagung, Karlsruhe, 07.-09.10., (poster presentation).
[13] Maaß, S., Grünig, J., Horn, S. and Kraume, M., **2008**, Measurement techniques for drop size distributions in stirred and fast coalescing liquid/liquid systems., 17th International Conference "Chemical Engineering and Chemical Apparatus Construction", Krakow, 07.-09.10., (oral presentation).
[12] Maaß, S., Metz, F., Rehm, T. and Kraume, M., **2008**, Fundamental experimental and numerical analysis of stirred liquid/liquid systems for PVC-production in slim reactors with multi-stage stirrers, Sixth

International Symposium on Mixing in Industrial Process Industries- ISMIP VI, Niagara on the Lake, Niagara Falls, Ontario, 17.-21.08., (oral presentation).
[11] Maaß, S., Skale, T. and Kraume, M., **2008**, Bestimmung von Bruchraten zur Modellierung von Tropfengrößenverteilungen in gerührten Flüssig/flüssig-Dispersionen, ProcessNet Jahrestreffen des Fachausschusses Extraktion und des Arbeitskreises Phytoextrakte, Clausthal-Zellerfeld, 16.-18.04., (oral presentation).
[10] Maaß, S., Lutz, E., Metz, F., Rehm, T. and Kraume, M., **2008**, Experimentelle und numerische Untersuchungen von gerührten Flüssig/flüssig-Systemen für die PVC-Produktion mit mehrstufigen Rührsystemen, ProcessNet Jahrestreffen des Fachausschusses Mischvorgänge, Eisenach, 30.03.-01.04., (oral presentation).
[9] Maaß, S., Paschedag, A.R. and Kraume, M., **2007**, Influence of electrolytes and turbulence parameters on drop breakage and drop size distributions in stirred liquid/liquid dispersions, 6th International Conference on Multiphase Flow, Leipzig, 09.-13.07., (oral presentation).
[8] Maaß, S., Paschedag, A.R. and Kraume, M., **2007**, Einfluss von Elektrolyten und Turbulenzparametern auf Tropfengrößenverteilungen in gerührten Flüssig/flüssig Systemen, 10. Köthener Rührerkolloquium, Köthen, 09.05., (oral presentation).
[7] Maaß, S., Paschedag, A.R. and Kraume, M., **2007**, Analyse und Modellierung des Ladungseinflusses auf Tropfenzerfall und Tropfengrößenverteilungen in gerührten Flüssig/flüssig-Systemen, ProcessNet Jahrestreffen der Fachausschüsse Adsorption und Extraktion, Asselheim, 21.-23.03., (oral presentation).
[6] Maaß, S., Wollny, S., Rojahn, J., Paschedag, A.R. and Kraume, M., **2007**, Comparison of measurement techniques for drop sizes in highly dispersed and fastly coalescing systems, PARTEC 2007, Nürnberg, 27.-29.03., (oral presentation).
[5] Maaß, S., Paschedag, A.R. and Kraume, M., **2006**, Experimental and numerical investigations of coalescence and breakage phenomena in stirred liquid/liquid systems., 16th International Conference "Chemical Engineering and Plant Design", Berlin, 10.-11.10., (oral presentation).
[4] Maaß, S., Gäbler, A., Wegener, M., Zaccione, A., Paschedag, A. and Kraume, M., **2006**, Tropfenzerfall und Koaleszenz in gerührten Flüssig/Flüssig-Systemen und deren Einfluss auf die Tropfengrößenverteilung, ProcessNet Jahrestagung, Wiesbaden, 26.-28.09., (oral presentation).
[3] Maaß, S., Gäbler, A., Wegener, M., Zaccone, A., Paschedag, A.R. and Kraume, M., **2006**, Drop breakage and daughter drop distribution in stirred liquid-liquid systems and their modelling within the population balance equation, 12th European Conference on Mixing, Bologna, 26.-30.06., (poster presentation).
[2] Maaß, S., Gäbler, A., Zaccone, A., Paschedag, A. and Kraume, M., **2006**, Tropfenzerfall in gerührten Flüssig/flüssig-Systemen., 9. Köthener Rührer Kolloquium, Köthen, 14.06., (oral presentation).
[1] Maaß, S., Gäbler, A., Wegener, M., Zaccone, A., Paschedag, A. and Kraume, M., **2006**, Tropfenzerfall und Tochtertropfenverteilungen in gerührten Flüssig/flüssig-Systemen und deren Berücksichtigung in der Populationsbilanz., ProcessNet Jahrestreffen der Fachausschüsse Mischvorgänge und Wärme- und Stoffübertragung, Frankfurt am Main, 07.-08.03., (oral presentation).

Appendix A2 - Supervised projects and thesis

[23] Beseran Sauras, M., **2011**, Experimental analysis of breakage dominated, coalescence hindered liquid/liquid systems for various dispersed phase fractions in stirred vessels with aspect ratios larger 1.0, (diploma thesis).
[22] Buscher, S., **2011**, Einfluss der Tochtertropfenverteilung auf simulierte Tropfengrößen in bruchdominierten, koaleszenzstabilisierten Systemen, (student research report).
[21] Herden, J., **2011**, Automatische Analyse von Partikelgrößenverteilungen in Mehrphasensystemen mit Ziel der Echtzeitsteuerung, (bachelor thesis).
[20] Vazquez Pascual, B., **2011**, Computational analysis of breakage dominated, coalescence hindered liquid-liquid systems for various dispersed phase fractions in stirred vessels with aspect ratios larger 1.0, (diploma thesis).
[19] Aggrawal, R., **2010**, Simulating the influence of different operation parameters on drop sizes in agitated systems, (DAAD report).
[18] Brösigke, G., **2010**, Analyse des Strömungsfeldes in einstufigen schlanken Reaktoren zur Quantifizierung des Einflusses der Stromstörereintauchtiefe mit Hilfe von CFD Simulationen, (student research report).
[17] Dölchow, U., **2010**, Experimentelle Untersuchungen zum Einfluss des Phasenanteils in gerührten, bruchdomierten Flüssig/flüssig-Systemen, (bachelor thesis).
[16] Federowitz, S., **2010**, Experimentelle Analyse des Strömungsfeldes in schlanken Reaktoren zur Quantifizierung des Einflusses der Stromstörereintauchtiefe, (student research report).
[15] Kim, S.-J., **2010**, Analyse des Einflusses von Stromstörern auf Tropfengrößen in gerührten, schlanken Reaktoren, (student research report).
[14] Komaiko, J., **2010**, Experimental investigations on breaking single petroleum drops, (DAAD report).
[13] Paul, N., **2010**, Einfluss von oberflächenaktiven Substanzen beim Erzeugen von Emulsionen in ein- und mehrstufigen schlanken Rührkesseln, (diploma thesis).
[12] Rojahn, J., **2010**, Merkmalsextraktion und Formanalyse in der automatischen Bildanalyse am Beispiel der Quantifizierung von Tropfendurchmessern in Rührkesselreaktoren zur ergebnisabhängigen Ansteuerung entsprechender Rührmechanik, (diploma thesis).
[11] Schrempf, J., **2010**, Scale-Up beim Erzeugen von Emulsionen in mehrstufigen schlanken Rührkesseln, (diploma thesis).
[10] Zillmer, M., **2010**, Bestimmung experimenteller Bruchraten von Toluoltropfen in Wasser anhand von Einzeltropfenuntersuchungen, (diploma thesis).
[9] Ahmad, A., **2009**, Measurements of crystal size distributions with the endoscope technique, (DAAD report).
[8] Kumar, S., **2009**, Computational analysis of the influence of drop charge on drop sizes in stirred tanks (DAAD report).
[7] Guardiola, R.E., **2008**, Influence of the dispersed phase fraction on drop sizes in liquid/liquid systems - analyzing the model of Coulaloglou and Tavlarides (1977), (diploma thesis).
[6] Karr, J.-S., **2008**, Analyse und Simulation von Tropfengrößenverteilungen für die PVC-Produktion, (diploma thesis).
[5] Lutz, E., **2008**, Analyse von ein- und mehrstufigen Balkenrührwerken für die PVC-Produktion, (diploma thesis).
[4] Peszkowski, J., **2008**, Experimental investigations on single drops, (DAAD report).
[3] Skale, T., **2008**, Bestimmung von experimentellen Bruchraten Newtonscher Fluide unter der Variation von Strömungsparametern, (student research report).
[2] Metz, F., **2007**, Analyse von Rührwerken für die PVC-Produktion, (diploma thesis).
[1] Turner, S.T., **2007**, Experimental investigations and modeling of breakage phenomena in stirred liquid/liquid systems, (DAAD report).

Appendix A3 - Own publications used for the cumulative thesis (full text)

This thesis is based on the following publications. The order is chronological. Please note that the full text papers are only available via the publisher or via personal communication with the author.

I. Maaß, S., Gäbler, A., Zaccone, A., Paschedag, A.R. and Kraume, M., **2007**. Experimental investigations and modelling of breakage phenomena in stirred liquid/liquid systems. Chemical Engineering Research and Design, 85(A5): 703-709.

II. Zaccone, A., Gäbler, A., Maaß, S., Marchisio, D. and Kraume, M., **2007**. Drop breakage in liquid-liquid stirred dispersions: Modelling of single drop breakage. Chemical Engineering Science, 62(22): 6297-6307.

III. Maaß, S., Wollny, S., Sperling, R. and Kraume, M., **2009**. Numerical and experimental analysis of particle strain and breakage in turbulent dispersions. Chemical Engineering Research and Design, 87(4): 565–572.

IV. Maaß, S., Metz, F., Rehm, T. and Kraume, M., **2010**. Prediction of drop sizes for liquid-liquid systems in stirred slim reactors - Part I: Single stage impellers. Chemical Engineering Journal, 162(2): 792-801.

V. Maaß, S., Wollny, S., Voigt, A. and Kraume, M., **2011a**. Experimental comparison of measurement techniques for drop size distributions in liquid/liquid dispersions. Experiments in Fluids, 50(2): 259-269.

VI. Maaß, S., Rehm, T. and Kraume, M., **2011b**. Prediction of drop sizes for liquid-liquid systems in stirred slim reactors - Part II: Multiple stage impellers. Chemical Engineering Journal, 168(2): 827–838.

VII. Maaß, S. and Kraume, M., **2011**. Determination of breakage rates with single drop experiments. Chemical Engineering Science (DOI: 10.1016/j.ces.2011.08.027): pp. 20.

VIII. Maaß, S., Eppinger, T., Altwasser, S., Rehm, T. and Kraume, M., **2011c**. Flow field analysis of stirred liquid-liquid systems in slim reactors. Chemical Engineering Technology, 34(8): 1215–1227.

IX. Maaß, S., Buscher, S. and Kraume, M., **2011d**. Analysis of particle strain in stirred bioreactors by drop breakage investigations. Biotechnology Journal, 6(8): 979–992.

X. Maaß, S., Paul, N. and Kraume, M., **2011e**. Influence of the dispersed phase fraction on experimental and predicted drop size distributions in breakage dominated stirred liquid-liquid systems. Chemical Engineering Science (submitted): pp. 12.

XI. Maaß, S., Rojahn, J., Hänsch, R. and Kraume, M., **2011f**. Automated drop detection using image analysis for online particle size monitoring in multiphase systems. Computers and Chemical Engineering (submitted): pp. 10.